port No. FHWA-RD-73-52

ETECTION AND DEFINITION OF SUBSURFACE VOID PACES BY GROUND-BASED MICROWAVE RADIOMETERS

May 1972
Final Report

Prepared for
FEDERAL HIGHWAY ADMINISTRATION
Offices of Research & Development
Washington, D.C. 20590

NOTICE

This document is disseminated under the sponsorship of the Department of Transportation in the interest of information exchange. The United States Government assumes no liability for its contents or use thereof.

The contents of this report reflect the views of the contracting organization, which is responsible for the facts and the accuracy of the data presented herein. The contents do not necessarily reflect the official views or policy of the Department of Transportation. This report does not constitute a standard, specification, or regulation.

Technical Report Documentation Page

1. Report No.	2. Government Accession No.	3. Recipient's Cotolog No.
FHWA-RD-73-52		

4. Title and Subtitle
DETECTION AND DEFINITION OF SUBSURFACE VOID SPACES BY GROUND-BASED MICROWAVE RADIOMETERS,

5. Report Dote
May 1972

6. Performing Orgonizotion Code

7. Author(s)

8. Performing Orgonizotion Report No.
TR-1042-1

9. Performing Orgonizotion Nome ond Address
Resources Technology Corporation
1275 Space Park Drive, Suite 111
Houston, Texas 77058

10. Work Unit No. (TRAIS)
FCP 34E2-014

11. Contract or Grant No.
FH-11-7788

13. Type of Report ond Period Covered
Final Report
6/30/71 - 5/31/72

12. Sponsoring Agency Nome ond Address
U. S. Department of Transportation
Federal Highway Administration,
Offices of Research and Development
Washington, D. C. 20590

14. Sponsoring Agency Code
M-0068

15. Supplementory Notes
FHWA Contract Manager: H. T. Rib (HRS-21)

16. Abstroct

The results of an experimental program to detect and define subsurface voids using passive microwave radiometers is reported upon. A field measurements program was conducted at selected locations in Kansas by a team consisting of representatives of the Federal Highway Administration, Kansas State Highway Commission, Resources Technology Corporation and the Aerojet-General Corporation. A mobile field laboratory was used to gather measurements using radiometers operating at wavelengths of .8-21cm. Data were also obtained concerning ground truth parameters of soil moisture, temperature and density. Sensed electromagnetic data were correlated with ground truth data to determine the effects of soil parameters on microwave and infrared signals. The analysis identified significant anomalies worthy of further investigation.

17. Key Words	18. Distribution Stotement
Subsurface voids Microwave radiometers	No restrictions. This document is available through the National Technical Information Service, Springfield, Virginia 22151

19. Security Clossif. (of this report)	20. Security Clossif. (of this poge)	21. No. of Poges	22. Price
Unclassified	Unclassified	151	

Form DOT F 1700.7 (8-72) Reproduction of completed poge authorized

Table of Contents

Section Number	Title	Page
1.0	Introduction	1-1
2.0	Field Investigations	2-1
3.0	Analysis of Microwave Field Data	3-1
3.1	Microwave Emission Characteristics of Terrain	3-1
3.1.1	Microvariate Analysis of Physical Parameters	3-2
3.2	Scammon Line A	3-4
3.3	Scammon Line B	3-22
3.4	Galena Lines A and C'	3-29
3.5	Galena Line D	3-46
3.6	Galena Line E	3-53
3.7	Clay County Lines C and D	3-58
3.8	Kansas City Line A	3-66
3.9	Kansas City Line B	3-71
3.10	Kansas City Line C	3-71
4.0	Comparative Analysis of Microwave Data	4-1
4.1	Macrovariate Analysis of Physical Parameters	4-3
4.1.1	Temporal Redundancy	4-4
4.1.2	Spatial Redundancy	4-4
4.1.3	Signal Redundancy	4-4
4.1.4	Experimental Redundancy	4-11
4.2	Data Correlation	4-11
4.2.1	Correlation of Soil Moisture and Temperature	4-12
4.2.2	Correlation of Microwave Response and Ground Moisture	4-17
4.2.3	Correlation of Remotely Sensed Signals and Ground Temperature	4-21

Table of Contents
(Continued)

Section Number	Title	Page
5.0	Conclusions and Recommendations	5-1
5.1	Detailed Conclusions	5-1
5.2	Recommendations	5-2

List of Figures

Figure Number	Title	Page
1.1	Kansas Microwave Experimental Study Sites	1-2
2.1	AGC's Microwave Mobile Field Laboratory at the Topeka, Kansas Deck Site	2-2
2.2	Sketch of Radiometer Field-of-View for Various Antenna View Angles (Boom Height=20 Feet)	2-4
2.3	Typical Site Terrain a. Scammon Site Line A b. Galena Site Line A	2-6
3.1	Scammon Line A Ground Support Data	3-6
3.2a	Percent-Moisture Isolines at Scammon A, Northeast Perspective	3-9
3.2b	Percent-Moisture Isolines at Scammon A, Northwest Perspective	3-10
3.3a	Isotherms (°C) at Scammon A, Northeast Perspective	3-11
3.3b	Isotherms (°C) at Scammon A, Northwest Perspective	3-12
3.4	Correlation of Microwave and Infrared Data, Average Ground Moisture and Temperature Conditions at Scammon Line A	3-15
3.5	Correlation of Measurements-Scammon Line A	3-16
3.6	Scammon Line A Multifrequency Microwave Profile Data Taken at an Observational View Angle of 15°	3-18
3.7	Scammon Line A Multifrequency Microwave Profile Data Taken at an Observational View Angle of 30°	3-19
3.8	Scammon Line A Multifrequency Microwave Profile Data Taken at an Observational View Angle of 45°	3-20

List of Figures
(Continued)

Figure Number	Title	Page
3.9	Correlation of Measurements - Scammon B, Run 4	3-27
3.10	Microwave Profile - Scammon Line B	3-28
3.11	Galena Mining Field Showing Traverse Lines A and C'	3-31
3.12	Soil Moisture Sampling Grid Pattern Used For Galena Line C'	3-37
3.13	Correlation of Measurements Galena Line A, Run 1	3-39
3.14	Correlation of Measurements Galena Line A, Run 2	3-40
3.15	21 cm Microwave Profile Data for Galena Line A (Dash lines approximate microwave temperatures expected if foil were not present)	3-43
3.16	21 cm Microwave Profile Data for Galena Line C'	3-44
3.17	Correlation of Measurements, Galena D	3-50
3.18	Microwave Profile - Galena Line D	3-52
3.19	Correlation of Measurements - Galena Line E	3-56
3.20	Microwave Profile - Galena Line E	3-57
3.21	Correlation of Measurements - Clay County D	3-62
3.22	Correlation of Measurements - Clay County D	3-63
3.23	Microwave Profile - Clay County Line C	3-64

List of Figures
(Continued)

Figure Number	Title	Page
3.24	Microwave Profile - Clay County Line D	3-65
3.25	Microwave Profile - Kansas City Line A	3-67
3.26	Correlation of Measurements	3-68
3.27	Microwave Profile - Kansas City Line B	3-72
3.28	Correlation of Measurements Kansas City Line C	3-74
3.29	Microwave Profile - Kansas City Line C	3-75
4.1	Correlation of Vertical and Horizontal Polarizations of 21 cm Radiometer, Scammon Line A	4-5
4.2	Correlation of Vertical and Horizontal Polarizations of 6 cm Radiometer, Scammon Line A	4-6
4.3	Correlation of Vertical and Horizontal Polarizations of 2.2 cm Radiometer, Scammon Line A	4-7
4.4	Correlation of Vertical and Horizontal Polarization of 0.8 cm Rasiometer, Scammon Line A	4-8
4.5	Comparison of Vertical and Horizontal Polarizations for all Scammon A Microwave	4-10
4.6	Correlation Between Average Ground Temperature and Average Ground Moisture.	4-16

List of Figures
(Continued)

Figure Number	Title	Page
4.7	Correlation Between Average Ground Moisture for Five Levels and 21 cm Microwave Antenna Temperatures	4-18
4.8	Correlation Between Average Ground Moisture for Five Levles and 8.0 - 14.0μ Infrared Radiometric Temperatures	4-19
4.9	Correlation Between Average Moisture at 2 cm Depth and 8.0 - 14.0μ Infrared Radiometric Temperatures	4-20
4.10	Correlation Between Average Ground Temperature for Five Levels and 21 cm Microwave Antenna Temperatures	4-22
4.11	Correlation Between Average Ground Temperature For Five Levels and 8.0 - 14.0μ Infrared Radiometric Temperatures	4-23

List of Tables

Table Number	Title	Page
1-1	Summary of Kansas Investigations	1-3
3-1	Ground Truth Data Scammon Site Line B	3-23/25a
3-2	Ground Truth Data Galena Site Line A	2-32/34a
3-3	Ground Truth Data Galena Site Line C'	3-35/36
3-4	Ground Truth Data Galena Site Line D	3-47/49a
3-5	Ground Truth Data Galena Site Line E	3-54/55
3-6	Ground Truth Data Clay County K-82	3-59/61a
3-7	Ground Truth Data Kansas City Site Line A	3-69
3-8	Ground Truth Data Kansas City Site Line C	3-73a
4-1	Tabulation of M.W. Data by Station	4-13/15

1.0 INTRODUCTION

This final technical report presents the results of a study effort performed by RESOURCES TECHNOLOGY CORPORATION, Houston, Texas, and its major subcontractor the Microwave Division of Aerojet-General Corporation to "Determine the Accuracy of Ground-Band Microwave Radiometers for Determining the Presence and Limits of Subsurface Cavities." This work, performed under Contract DOT-FH-11-7788 with the Department of Transportation, Federal Highway Administration is primarily concerned with the feasibility of identifying subsidence-prone areas by means of passive microwave radiometry.

The specific tasks performed by RESOURCES TECHNOLOGY CORPORATION and its subcontractor included: (1) participation in pre-survey planning for the selection of test sites, definition with Federal Highway representatives; (2) direction and coordination of the field surveys using the mobile microwave laboratory and field personnel of the subcontractor; (3) reduction and correlation of microwave data with photographic information and ground measurements taken at the same time; (4) performing a detailed analysis of the microwave data for definition of subsurface cavities and their boundaries; (5) preparation of a final technical report.

Project planning meetings were conducted on location in Kansas in late July 1971. These meetings incorporated a visit at each test location to define survey lines and other requirements. Attendees included representatives of the Federal Highway Administration, the Kansas State Highway Commission, Resources Technology Corporation and Aerojet-General Corporation.

Five sites were selected for detailed survey with the microwave equipment. These included locations at Galena, Kansas; Scammon, Kansas; Kansas City, Kansas; Topeka, Kansas and Clay County, Kansas as shown in Figure 1.1. A summary of the specific objectives for each of the site locations is shown in Table 1-1. The five sites chosen afforded conventional access and favorable

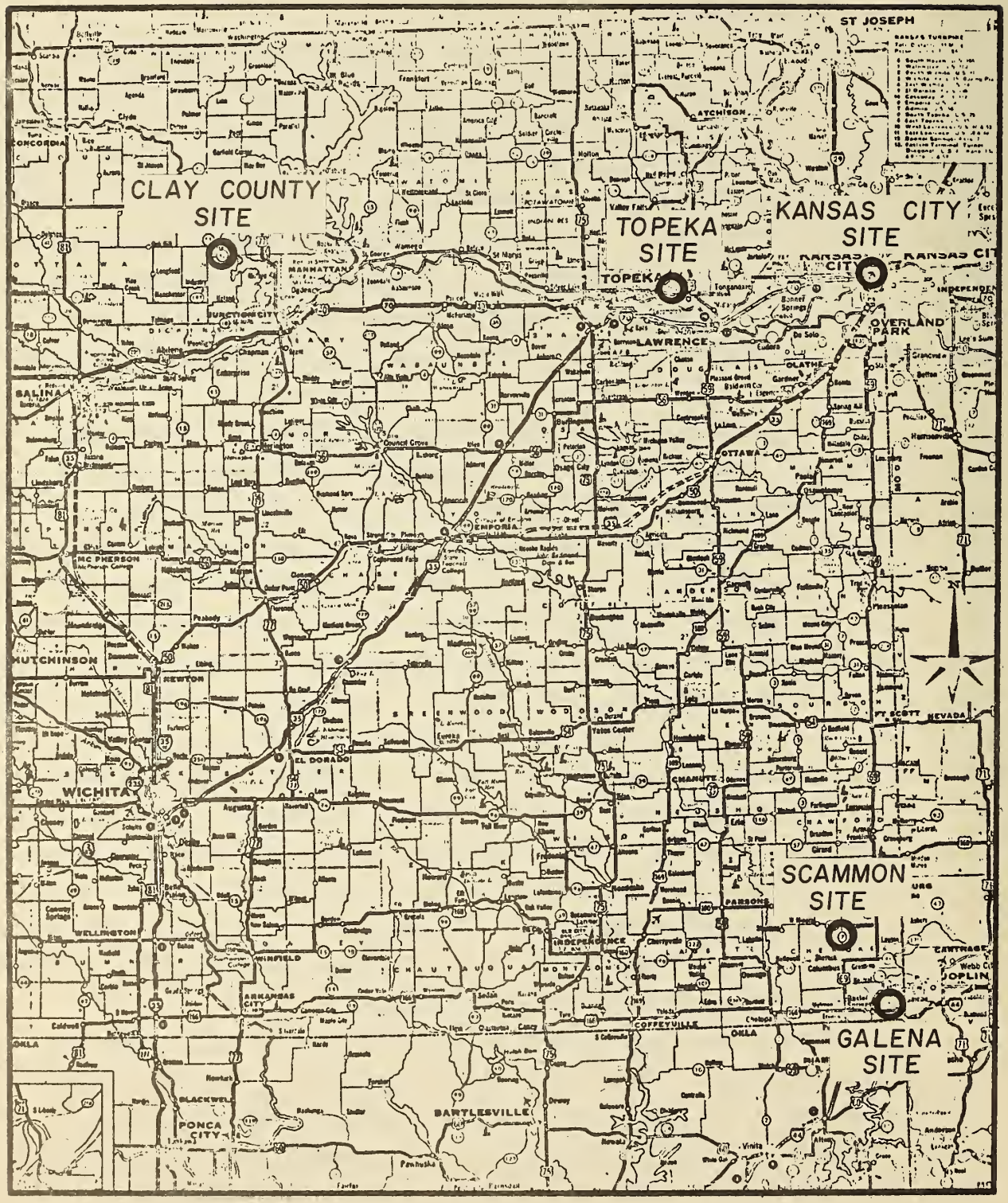

Figure 1.1 Kansas Microwave Experimental Study Sites

Table 1-1

Summary of Kansas Investigations

Site	Dates of Performance	Objective
Galena, Kansas	8/10/71 8/15/71	Microwave radiometric detection of subsurface voids and associated subsidence resulting from extensive lead and zinc mining activity
Scammon, Kansas	8/16/71 8/17/71	Microwave radiometric detection of subsurface voids and associated subsidence resulting from extensive shaft coal mining activity
Kansas City, Kan.	8/19/71	Microwave radiometric detection of subsurface voids and associated subsidence resulting from extensive limestone mining activity
Clay County, Kan.	8/21/71 8/22/71	Microwave radiometric detection of active subsidence associated with limestone solutioning
Topeka, Kansas	8/23/71	Microwave radiometric detection of voids contained within a freeway bridge deck.

conditions for conducting the microwave radiometric traverses. However, the area of each site was such that usually only a single traverse line could be established and the performance of microwave radiometric mapping operations (multiple laterally spaced traverses) was possible only at the Kansas City Site. For each site, continuous dual-polarized microwave profile data were obtained at observational wavelengths of 0.81, 2.2, 6.0 and 21cm. Ground data measurements of soil moisture content, soil thermometric temperature and soil density were collected by Kansas State Highway Commission personnel. Surface geology and other pertinent surface features of each site were noted and recorded by the investigators.

Following the field investigations all recorded data and field notes were collected for later reduction and analysis. The digitally recorded microwave data obtained during the field measurements were reduced to engineering units in the form of computer listings of brightness temperature for the vertical and horizontal polarization of each of the four microwave radiometers. The brightness temperature data were then plotted in the form of microwave profiles for each traverse line for subsequent analysis and interpretation in accordance with priorities established in joint conferences.

The data analysis and interpretation activities of the subcontractor were focused on data obtained from Line A of the Scammon site and Lines A and C' of the Galena sites while RESOURCES TECHNOLOGY CORPORATION investigators focused on the remaining sites. Data acquired at the Topeka site was not subjected to detailed analysis. The Scammon Line A analysis consisted of cross-correlation of the microwave radiometric profiles as a function of observational wavelength, view angle, and polarization. These data were also correlated with the available ground truth information. Unfortunately, subsurface control data concerning specific placement and structural detail of underground mines was lacking for this site and correlation of the microwave data to subsurface voids was not possible. With the exception of

Kansas City site, specific location data on known subsurface voids was generally not available to the point where precise correlation with the microwave data could be accomplished. Nonetheless, the Aerojet investigators felt that the subsurface control information which existed for the Galena Lines A and C was adequate for analysis. In this case they noted that the long wavelength (21cm) microwave data obtained while traversing these sites showed a close correspondence between the location of known subsurface activities and areas of anomalously low brightness temperature.

Section 2.0 of the report provides a description of the instrumentation and techniques used to obtain the microwave measurements. Section 3.0 details the analysis and interpretation of data from all project site locations with primary emphasis on the Galena and Scammon sites.

Section 4.0 of the report presents a comparative analysis of the microwave data in an attempt to delineate and evaluate the departures between the measured data and theoretical predictions. On this basis, conclusions and recommendations concerning the ability and accuracy of ground based microwave radiometers to detect subsurface cavities could be established. In Section 5.0 these conclusions, drawn from the study by RESOURCES TECHNOLOGY CORPORATION and its subcontractor, are presented as well as recommendations for additional analysis which could be performed to enhance the understanding of the data collected in this program.

Appendix A provides a review of the fundamentals of microwave radiometry and the emission characteristics of terrain. This appendix also describes the calibration and data reduction techniques used in conjunction with the Kansas investigations.

2.0 FIELD INVESTIGATIONS

During the Kansas microwave project dual-polarized radiometric traverses were performed at observational wavelengths of 21, 6.0, 2.2 and 0.81 cm with Microwave Division's Remote Sensing Field Laboratory. Figure 2.1 shows the field laboratory and the radiometric instrumentation while performing measurements on the Topeka, Kansas bridge deck site. The 6.0, 0.81, 2.2 and 21 cm radiometers are respectively mounted from left to right on the sensor platform. Details of the field laboratory, microwave instrumentation and fundamentals of microwave radiometry are contained in Appendix A of this document.

Continuous microwave measurements were taken as the field laboratory was driven along each traverse line. Aluminum foil strips, illustrated in Figure 2.1, were placed at discrete control stations to mark the radiometric data with respect to traverse position. The horizontally and vertically polarized brightness temperatures were digitally recorded at an integration time of 2.88 seconds on the digital data acquisition system contained in the field laboratory. The 21 and 6.0 cm data were also recorded on two dual-channel analog strip chart recorders for real-time examination. Appendix A gives details concerning the reduction of the digitally recorded data along with the description of the techniques used to calibrate the microwave sensors.

Microwave profiles were obtained at 15°, 30° and 45° above nadir for each traverse line, in order to determine observational viewing angles best suited for the analysis of the Kansas data. The field laboratory performed each traverse in the forward and reverse directions. Consequently, the radiometers were pointed in the same direction for each viewing angle. During the study it was found that most of the controlling

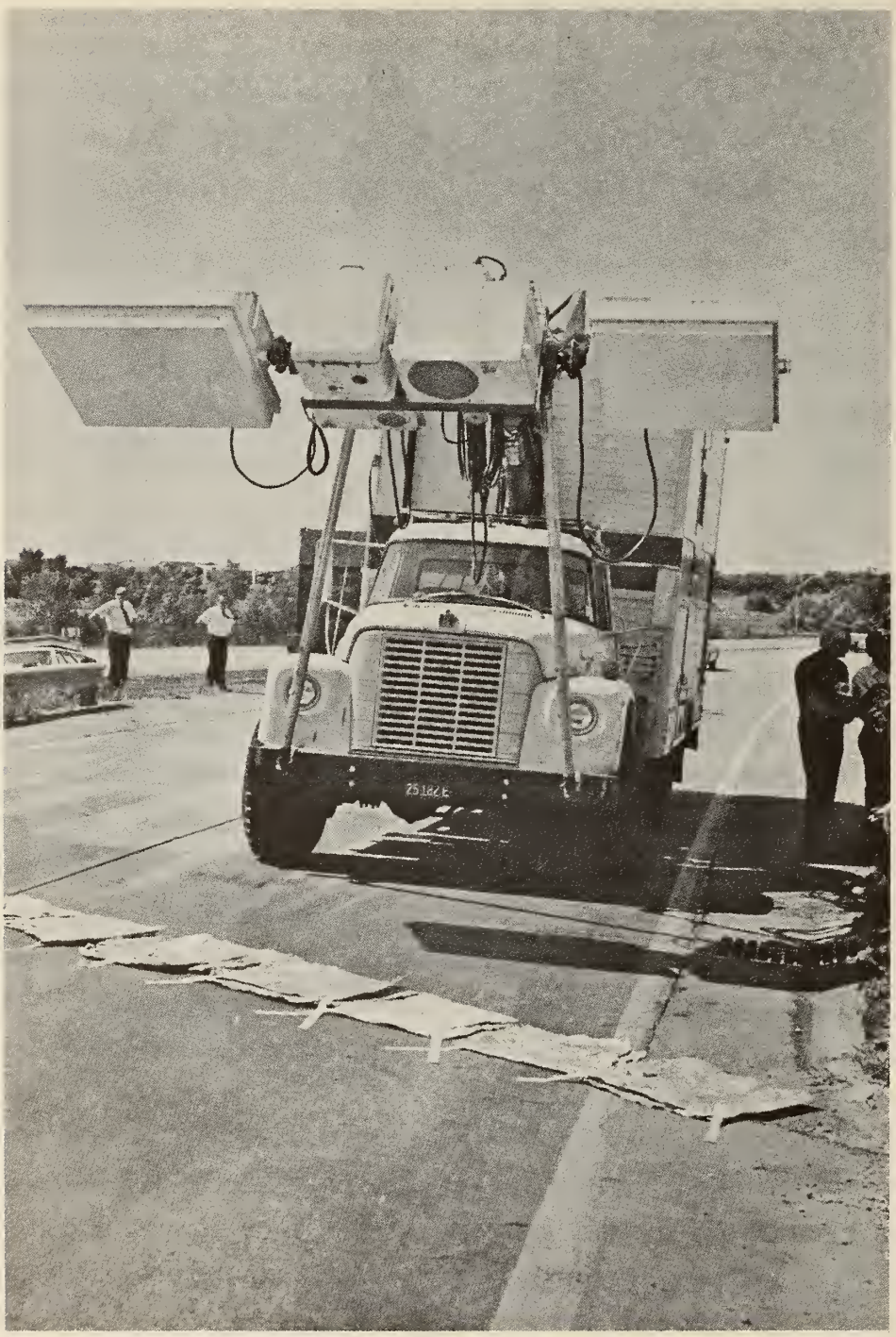

Figure 2.1 AGC's Microwave Mobile Field Laboratory at the Topeka, Kansas Bridge Deck Site

microwave emission parameters (i.e., areas of high moisture content) were localized in small areas and more pronounced anomalies were obtained at 15° and 30° viewing angles where the sensor field-of-view was smallest. This comment is particularly applicable to the 21 cm sensor which utilizes a 15° field of view. The various radiometric sensor fields of view and their dependence on antenna viewing angle are illustrated in Figure 2.2. This figure also illustrates the physical separation of the beam prints that occur due to the orientation of the microwave radiometers when mounted on the field laboratory's sensor platform. Note that 21 and 6.0 cm radiometers measure emission from different portions of the terrain surface.

Ground support measurements were taken by personnel from the Kansas State Highway Commission and were usually performed immediately following completion of the microwave traverses. Support measurements were taken at 100-foot intervals along the traverse lines and included (1) collection of integrated soil samples for determination of moisture content, (2) thermistor determination of the vertical thermometric temperature profiles, and (3) nuclear densitormetric determinations of material density. Surface temperatures were also monitored with a Barnes PRT-5 (8-14μ) infrared radiometer mounted on the field laboratory sensor platform. Also, to provide documentation concerning terrain surface characteristics, continuous 35mm photographs along with descriptive voice recordings were taken for each traverse line. The support measurements were very time-consuming and consequently, the number of measurements available for analysis of the microwave data are limited and, in most cases, the ground truth information is insufficient for a direct point-to-point correlation of the physical data and brightness temperature anomalies that occurred during the survey.

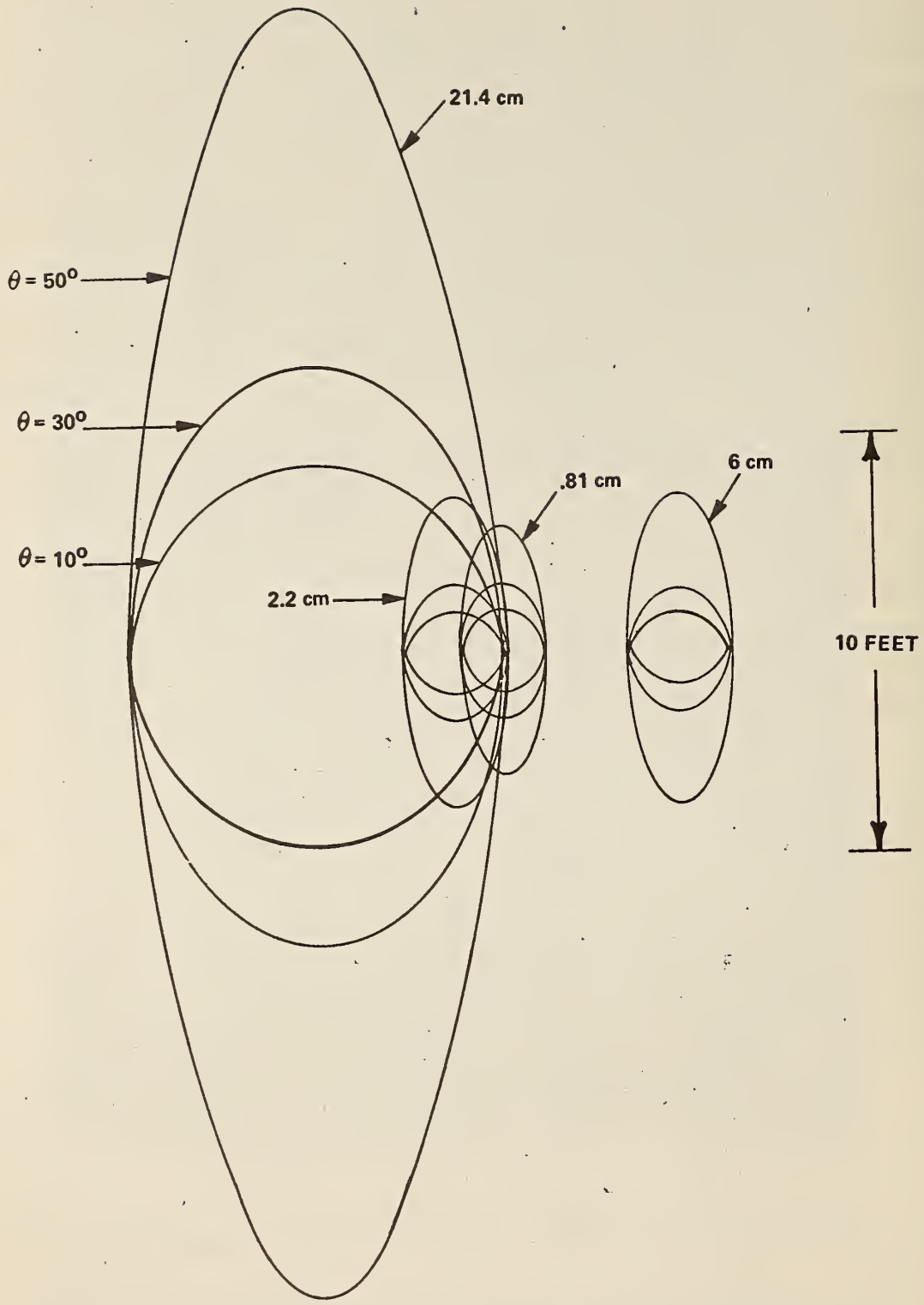

Figure 2.2 Sketch of Radiometer Field-of-View for Various Antenna View Angles (Boom Height = 20 Feet)

Prior to the actual field survey, investigators spent a week on the Scammon and Galena sites locating the traverse lines in each site. The criteria in making these locations were (1) accessibility, (2) surface conditions, (3) known locations of underground voids and subsidence prone areas and (4) bearing strength of the surface to be traversed. Since the Field Laboratory is mounted on a large truck weighing approximately six tons locations were limited to terrain which was level or of fairly shallow slopes. Bearing strengths in the Galena area was extremely important in that the weight of the van precluded those areas where there was a danger of collapse of the mine roof. In fact, on one line which was selected, Galena Line B, the van did sink in mine tailings and had to be towed out.

Very little detailed information was available about actual depths to void spaces, at Scammon or Galena. Much of this information was gathered from farmers in the area, the local library and the office of the Kansas Bureau of Mines who furnished old maps of the mines within the Galena area. Additionally, some areas which appeared to meet the conditions necessary for traversing were privately owned land and permission could not be obtained for access from the landowners.

Ideally the ground surface of each line should be free of vegetation and level, to permit a homogeneous surface to be viewed simultaneously by all radiometers and to maintain constant viewing angles. The investigators were able to select all lines in the Scammon, Clay County and Kansas City sites and Galena Lines C', D and E to very nearly meet this criteria. Line A of the Galena Site was just barely accessible to the van. Figure 2.3 a and b are pictures of the Scammon Site, Line A and the Galena Site, Line A.

a. Scammon Site Line A

b. Galena Site Line A

Figure 2.3 Typical Site Terrain

3.0 ANALYSIS OF MICROWAVE FIELD DATA

This segment of the report describes (1) phenomena influencing microwave emission by geologic materials, (2) results concerning data collected on Scammon Line A, and Galena Lines A and C' as interpreted by the Aerojet-General personnel and (3) results of data collected on Scammon Lines B and C, Galena Lines D and E, Clay County Lines C and D and Kansas City Lines A, B and C.

3.1 Microwave Emission Characteristics of Terrain

This section provides a brief description of the surface characteristics and bulk material properties considered important in the interpretation of the Kansas microwave profile data. These include (1) soil or overburden moisture content, (2) material density, (3) vegetal cover, and (4) terrain surface roughness.

The microwave brightness temperature of soils and overburden varies inversely with moisture content. A moisture increase of one percent (dry weight basis) results in a corresponding brightness temperature decrease of about 4°K for typical near-specular soils. The penetration or effective depth of investigation by microwave radiometry also decreases with increasing moisture content. For an observational wavelength of 21 cm, the effective depth of investigation can vary from several feet to a few inches, depending on moisture content. Specific examples of the effect of moisture content on microwave emission are cited in Appendix A.

The microwave brightness temperature of geologic material also decreases with increasing material density. Studies performed on volcanic rocks of varying densities indicate brightness temperature changes of about 15°K for density variations ranging from 1.3 to 2.3 g/cm^3. Appendix A cites relevant examples.

3.1.1 Microvariate Analysis of Physical Parameters

The interaction between incoming solar radiation and the earth's surface causes a unique and extremely narrow boundary layer to be formed between the freely circulating air and the bedrock or soil parent material below the uppermost layers of soil. Ideally, the first few feet of soils may be stratified into three horizons consisting of a dark colored surface layer (A-horizon) composed of decaying vegetal matter, a mid-layer (B-horizon) which collects the fine organic and nonorganic particles leached from above, and low layer (C-horizon) consisting of the parent material. Together the A and B horizons are termed the solum.

Horizontal variations in the solum over short distances occur primarily as a function of variations in surface topography, vegetal assemblages, subsurface geology (ie, parent material), and artificially induced changes by man. Under normal conditions, the interaction of water, solar radiation (manifested primarily in heat fluctuations), air, and plants cause a complex sequence of physical events to occur which result in rather unique conditions of temperature and moisture in the horizontal plane and which vary over a broad range in the vertical plane and through time. Although pedalogists successfully classify soils over broad areas of the United States, no soils can be considered homogeneous at the scale employed in this study. As will be demonstrated below, the microvariations in soil conditions over distance of several hundred feet induce large variance in the microwave signal. Because the 21 cm radiometer has soil penetrability no greater then several feet under the best of conditions, the resulting profiles measure fluctuations in the solum in general and the A horizon in particular.

It is the solum precisely which exhibits the largest fluctuations in moisture and temperature, normally on a diurnal basis. Diurnal variations in the physical conditions of solum are superposed on the second, third or higher harmonics. These

correspond with annual or longer cyclic variations which in themselves were not considered in this study. (It cannot be determined from these data whether or not detection of subsurface voids would be more effective during one season than during another.)

Previous experimental work in microwave radiometry has led investigators to believe that with the exception of vegetation the surficial factors generally have significantly less effect on the 21 cm radiometer response than soil moisture and soil temperature. One of the objectives of the RESOURCES TECHNOLOGY CORPORATION analytical approach is to test the degree to which soil moisture content and temperature affect the data. In this study vegetal effects were purposely minimized during the data collection phase in order to reduce the complexity of the problem. (No microwave mathematical model currently exists which accounts for vegetal effects. These therefore must be evaluated qualitatively by photography and field observation).

The magnitude of the moisture content in a soil per unit volume is a function of the total input of water plus the antecedent moisture. Antecedent moisture consists of gravitational water, that is water percolating with some downward vector toward the ground table; capillary water, moving with some upward vector or water held in place in the interstices of the soil particles by water surface tension forces; and water molecules chemically bonded by electromagentic forces to inorganic or organic soil particles.

In practice it is difficult to differentiate the water types in the field. Water infiltrates into a dry soil in response to both gravitational and capillary forces but the average hydraulic conductivity is strongly influenced by soil and vegetal types and total amount of initial input.

Vegetal cover and terrain surface roughness (relative to the sensor wavelength) cause scattering of microwave energy

which tends to mask the effects of bulk material properties such as moisture content and density. Scattering by foliage and the terrain surface is more severe at shorter wavelengths. The effect of scattering due to both foliage and terrain surface roughness is to increase microwave brightness temperatures. Vegetation on the study sites described in this section was generally sparse and patchy and exhibited no pronounced influence on the 21 cm radiometric response. The effects due to terrain surface roughness were relatively unimportant at 21 and 6.0 cm observational wavelengths while the effects were, at times, significant at the shorter wavelengths.

Other considerations that were of minor to negligible consequence in analyzing the radiometric data include (1) variations in incident sky radiation (negligible at λ = 21 cm), (2) variations in the effective antenna incidence angle resulting from topographic relief and/or vehicle orientation, (3) nonuniform soil thermometric temperature distribution and (4) possible interference phenomena due to subsurface layering within the overburden (there was no evidence of the occurrence of interference phenomena during the Kansas measurements).

3.2 Scammon Line A

On 16 August 1971, a series of N-S trending microwave traverses were performed along a 650-foot section of highway right-of-way directly west of Kansas State Route 7. The microwave traverses were initiated at 1600 hours and terminated at 1730 hours. Sky conditions were clear, the thermometric air temperature was 308°K and the relative humidity was approximately 70 percent.

The traverse line, situated approximately 2.5 miles north of Columbus, Kansas is contained in an area characterized by shaft coal mines having a clay-shale overburden less than 75 feet. Unfortunately, subsurface control data concerning

specific placement and depth of overburden of the underground mine shafts are lacking and direct correlation of the microwave data to geophysical features associated with subsurface voids is not possible for this site. Consequently, the analysis concerning this site is restricted to a comparison of the microwave data and the ground support measurements taken during the study. Also, localized thunder showers occurred in the area two days prior to the initiation of these measurements. The distribution of moisture (and therefore microwave brightness temperatures) in a uniform overburden is primarily determined by the local topography immediately following precipitation, whereas, in the absence of recent precipitation, the moisture distribution is determined primarily by subsurface characteristics. Due to the occurrence of recent precipitation, the investigators believe the former to be prevalent for this site.

Ground support measurements were performed immediately following completion of the microwave traverses and are illustrated in Figure 3.1. These measurements were taken at 100 foot intervals along the traverse line and include (1) collection of soil samples for moisture determination at depth intervals corresponding to 0-2, 0-4, 0-8, 0-16, and 0-32 cm; (2) determination of the vertical thermometric temperature profiles to a depth of 32 cm; and (3) integrated density measurements to a depth of 30 cm. The above measurements were performed both 5 feet east and 5 feet west of the center of the traverse line. As can be seen, the sampled soil moisture contents generally increase with depth at each station. Notable exceptions occur at stations 149+50 west and stations 152+50 east and west. The low and high 0-32 cm moisture values are 9 and 22 percent at station 149+50 west and east, respectively. All other 0-32 cm moisture contents lie within the range of these values. The

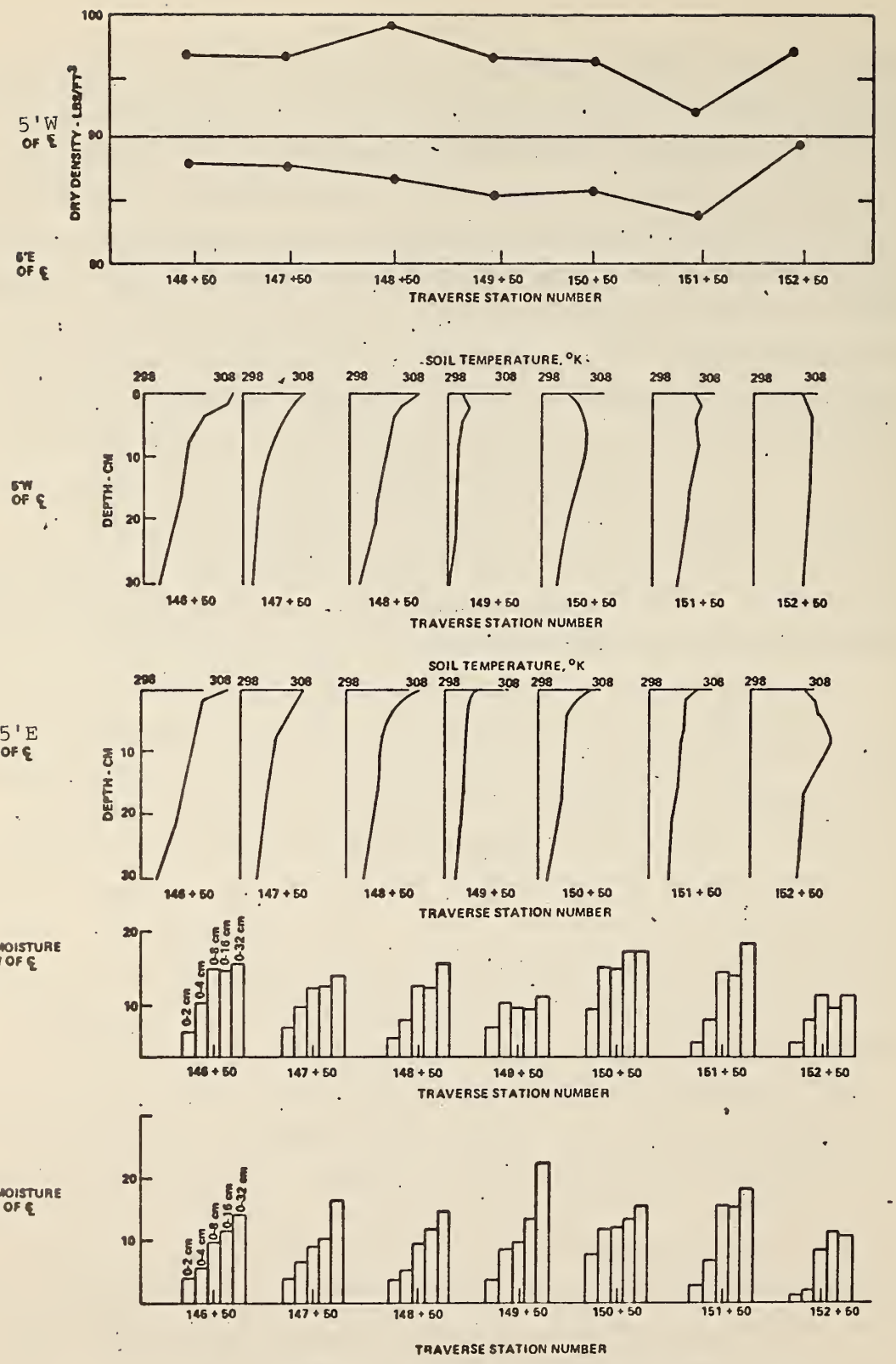

Figure 3.1 Scammon Line A Ground Support Data

0-2 cm values are generally uniform throughout the traverse line. The 0-4, 0-8 and 0-16 values exhibit moisture content ranges of 2-14, 7.8-15.5 and 7.5-16.5 percent, respectively. It is interesting to note that similar minimum moisture values at the 0-8, 0-16 and 0-32 cm depth intervals all occur at station 149+50 west.

The thermometric temperatures of the soil generally decrease with increasing depth and percent moisture content. Notable exceptions occur at stations 149+50 and 150+50 west, and at station 152+50 east. At station 149+50 west the low temperatures of the profile indicate an area of comparatively high moisture content, however, the mositure data for this station also exhibits comparatively low values. The opposite occurs at stations 150+50 west and 152+50 east. At these stations, the temperature profiles increase significantly from the surface to a depth of 8 cm. (Note that the corresponding moisture contents also increase.) These inconsistencies are probably attributable to measurement errors encountered while the samples were being obtained. With the exception of the above-mentioned stations, no significant point-to-point variations of thermometric temperatures were noted at a given depth throughout the traverse line and consequently, these data are considered to have minor importance in the analysis of the microwave data.

The vegetal cover in the beam of the 6.0 and 21 cm radiometers ranged intermittently from negligible amounts to a solid 6 inch grass cover throughout the traverse line. The 2.2 and 0.81 cm radiometers were viewing a clear surface except between stations 146+50 and 148+00 where the vegetal cover ranged from a 3-6 inch high, 5 to 25 percent grass cover. Throughout the traverse line, brightness temperature contribution due to vegetal cover is negligible. Also, as can be seen in Figure 3.1, point-to-point density variations were slight and are considered to be unimportant in the analysis of the microwave data.

While reading the following discussion concerning the results of the microwave survey for this site, the reader is reminded that although the above mentioned ground truth data offer general correlative information, the quantity is insufficient, and a detailed point-to-point correlation of the geophysical data (particularly soil moisture values) to the data obtained with the microwave sensors is not possible. To illustrate the complexity of the actual variations in temperature and moisture along the line, the diagrams in Figures 3.2a, 3.2b, 3.3a and 3.3b were constructed. In Figure A in both cases views the rectangular block from the northeast and Figure B views the same rectangle from the northwest providing a relatively easy comparison of spatial variations. The prime distortion in the figures occurs in the vertical scale which is exaggerated at a ratio of about 145:1 to the horizontal scale. This of course greatly exaggerates the perturbations along the line in there vertical plane.

Figure 3.2 illustrates the 3-dimensional aspect of moisture variations. Whereas the lines of equal moisture nearly parallel the surface and form a nearly regular pattern of isoline spacing for most of the profile in Figure 3.2a, an entirely different perspective is gained only ten feet to the west in Figure 3.2b where isolines exhibit greater fluctuation in the vertical plane and are generally irregularly spaced. Because of the pronounced upwelling of moisture on the south side of the line (and in general on the west side of the line) the surface expression of lines of equal moisture are normal to the direction of the profile. Thus, one would expect that if moisture induces a dominant effect on microwave temperature then it would be readily apparent along this particular profile.

Similarly, Figure 3.3 illustrates the response of the expected microwave antenna temperature and shows that the effect

Figure 3.2a Percent-moisture Isolines at Scammon A, Northeast Perspective

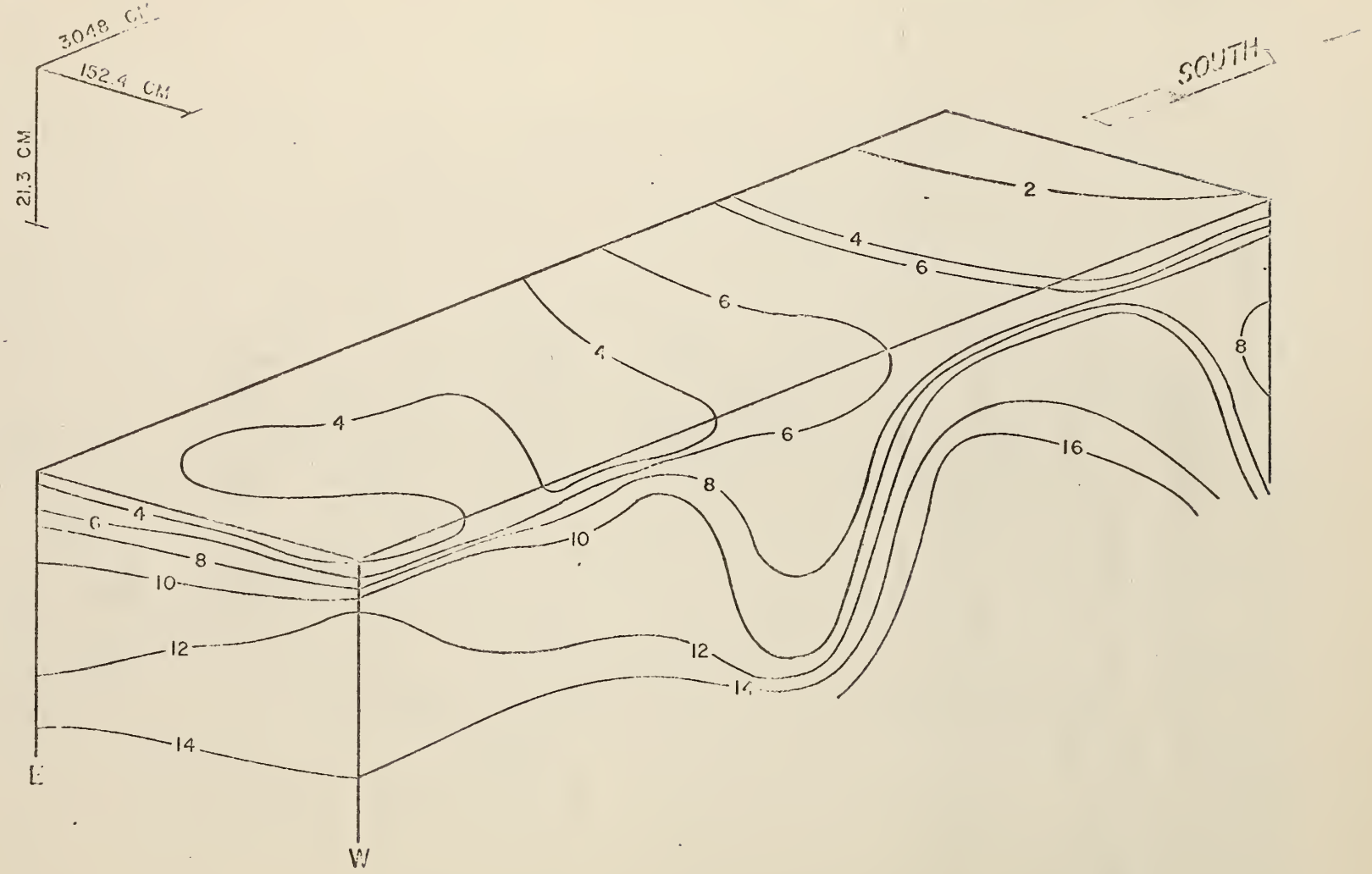

Figure 3.2b Percent-Moisture Isolines at Scammon A Site, Northwest Perspective

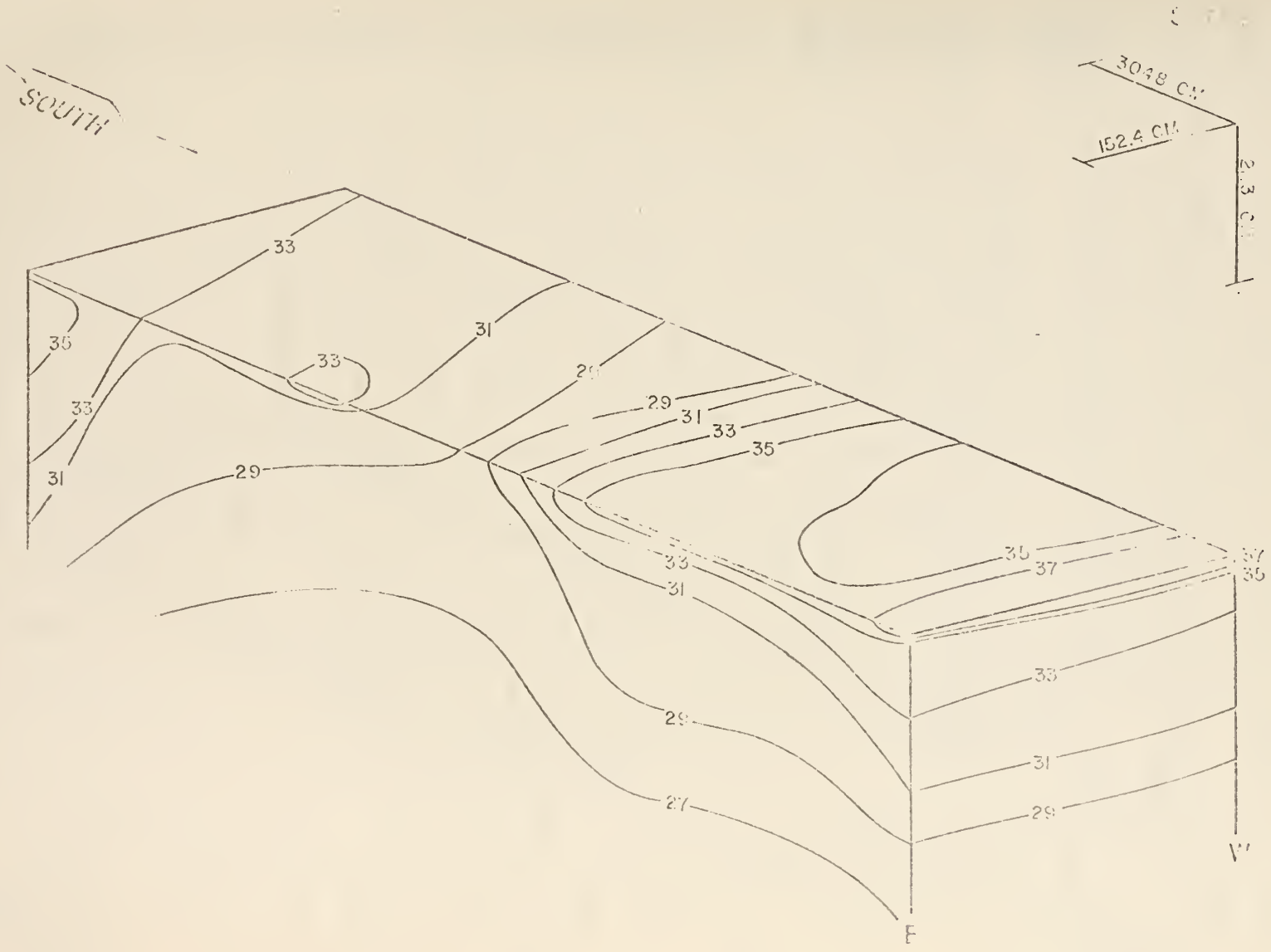

Figure 3.3a Isotherms (°C) at Scammon Line A, Northeast Perspective

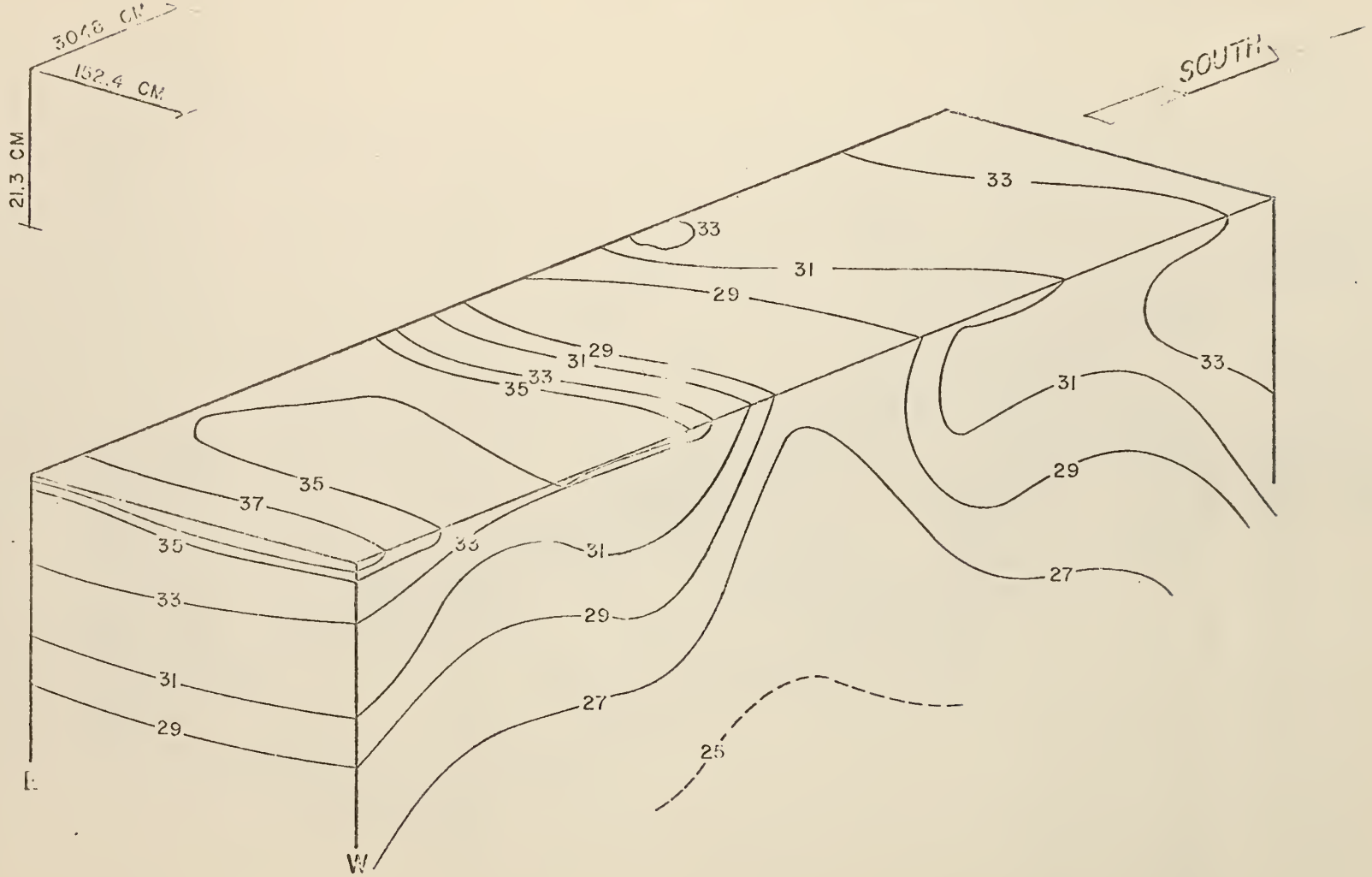

Figure 3.3b Isotherms (°C) at Scammon Line A, Northwest Perspective

induced by ground temperature on microwave temperature would be nearly identical to that of the soil moisture. Furthermore, the subsurface temperature distribution is not unlike subsurface moisture distribution in overall fluctuations. When the isotherms are superposed on the moisture at the Scammon Site, a generally inverse relationship between soil and temperature becomes apparent.

The essential traits in the preceeding illustrations are the lack of areal homogeneity which characterizes those factors which most profoundly effect the microwave response, and the obvious interaction between moisture and ground temperature. It is reasonable to presume that the former trait is partially induced by a lack of homogeneity in the soil.

The determination of the heat flux density near and at the surface, that is the average heat flow in and out of the soil, requires knowledge of two factors, the termal conductivity and the volumetric heat capacity, both of which fluctuate as functions of the soil/air/water mixture. Vacillation of both factors is considerable in the uppermost portions of the solum and attenuates with depth. Examples derived from many geographic locations suggest that fluctuations in sand and sandy loam soils generally exceed those of clay soils and that below approximately 20 centimeters the annual fluctuation rather than diurnal fluctuations become predominant. It should be noted at this juncture that Figure 3.2 and 3.3 in the main illustrate a rather ephemeral diurnal condition. Isolines in both cases no doubt, will be rapidly altered in the upper soil stratum. The diurnal fluctuations near the surface probably have strong effect on the microwave signal causing major vacillations which contribute considerable "noise" to the signal. Separation of the diurual effects from the higher order harmonic effects, as well as separation of geographically local effects from regional effects emerge as the major data reduction objectives of microwave survey precedures.

To avoid unnecessary complications in subsequent analysis, the various components of stations were averaged (in this case, the east and west values of temperature and moisture) and the reduced estimates utilized to separate the various effects.

Figure 3.4 shows a point-to-point correlation between the horizontal and vertical polarized 21 cm (30° look angle) radiometer, the Barnes PRT-5 infrared measurement and the isolines of the averaged moisture and temperature conditions at the Scammon A Site. In a relative sense a comparison of the microwave signal with the moisture fluctuations suggests essentially no correlation. That is, the lowest microwave temperature in both polarizations corresponds with a point to the left of the most prominent upward perturbation in the moisture isolines. Indeed, microwave temperatures continue to rise as the radiometer passes to the right over the "wettest" soil. However, when viewing the line as a unit, microwave temperatures to the right of 149+50 are, on an average, lower than those temperatures to the left of the same point, and perhaps partially reflect the wet soils.

In contrast, the microwave temperatures correspond closely with the ground temperatures. Point 149+50 lies directly above the lowest ground temperatures and as a unit, ground temperatures to the left of that point exceed those to the right of that point. Oddly, infrared temperatures tend to reflect ground temperatures. Reasons for this response were not apparent in the data.

To visually test the correlation between the spatial variance in microwave and infrared temperatures, and the spatial variance in moisture and temperature, the latter were plotted for each station as a function of the magnitude of the parameter at each depth (Figure 3.5). The point-to-point correlations reveal that the overall distribution in microwave temperatures weakly reflect ground temperatures and an inverse relationship

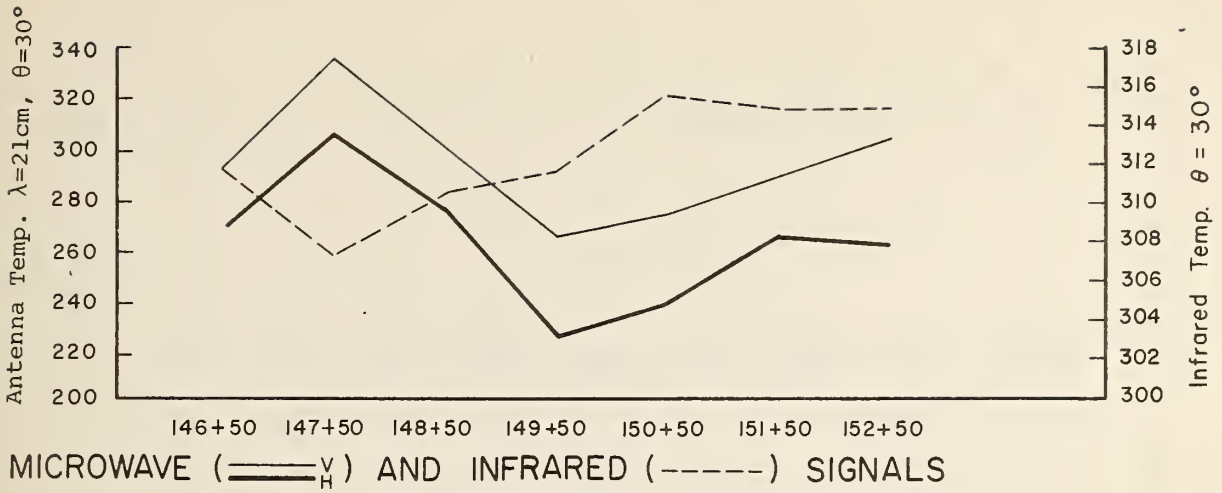

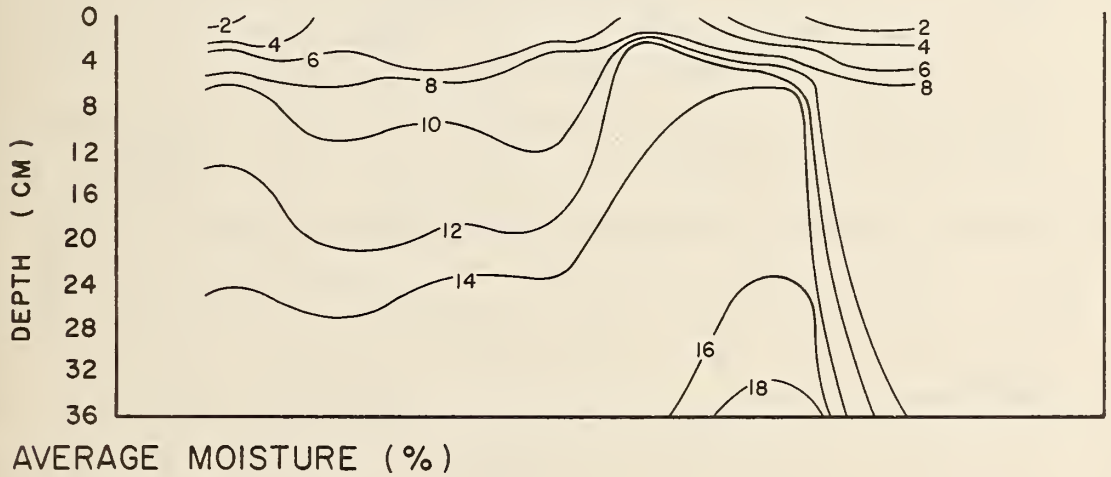

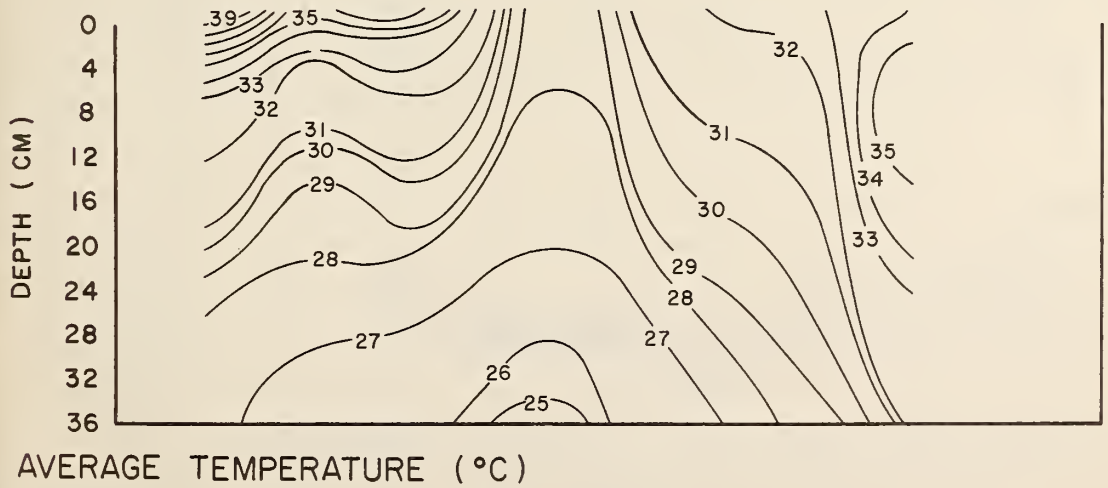

Figure 3.4 Correlation of Microwave and Infrared Data, Average Ground Moisture and Temperature Conditions at Scammon Line A

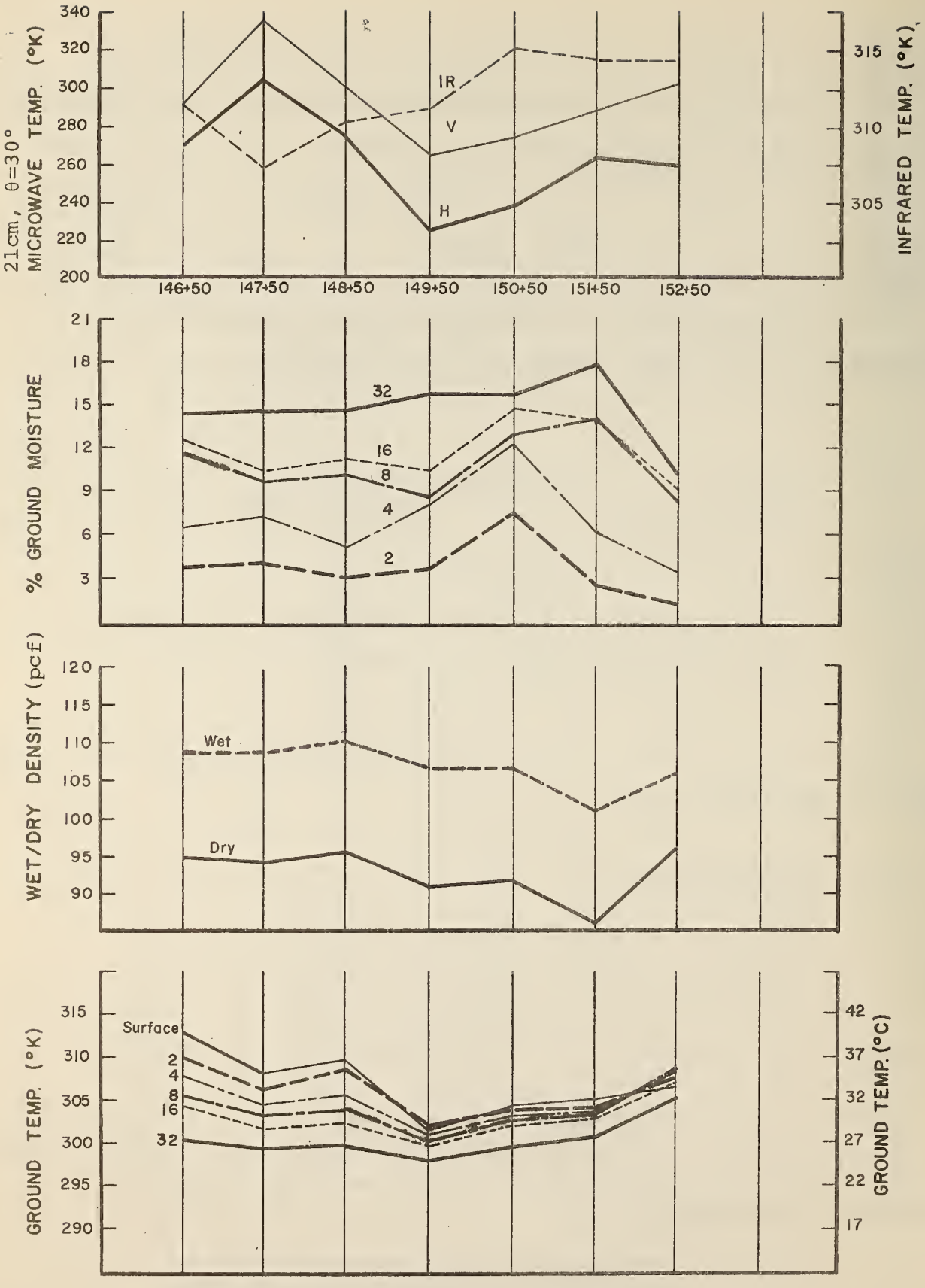

Figure 3.5 Correlation of Measurements - Scammon Line A

with moisture. The sensitivity of the radiometer to either factor, however, appears to be less than the excursions noted in either factor.

To better integrate the measured ground conditions through depth at the Scammon A Site averages were calculated for the following data sets: 2 cm and 4 cm; 2 cm, 4 cm, and 8 cm; 2 cm, 4 cm, 8 cm, and 16 cm; and 2 cm, 4 cm, 8 cm, 16 cm, and 32 cm. Using the averaged value for each set it was determined that no one set appeared better or substantially changed the spatial correlations. Consequently the five level average was utilized for further comparative purposes to data collected from the other sites.

Microwave data taken at the four observational wavelengths for respective view angles of 15°, 30° and 45° are shown in Figures 3.6, 3.7 and 3.8. Note that the 0.81 cm brightness temperatures are consistently warmer and less polarized than the corresponding longer wavelength temperatures, and that there is apparently little correlation between measured moisture conditions and microwave emission at 0.81 cm. The limited correlation with moisture observed at this wavelength is due to non-specular scattering associated with surface roughness. In general, larger brightness temperature anomalies were observed as the observational wavelength increased. This is especially evident between stations 148+50 and 150+00 where the brightness temperatures at wavelengths of 6.0 and 21 cm exhibit pronounced cool anomalies for the 15° and 30° viewing angles. The less pronounced anomalies at 45° are attributed to less areal resolution (i.e., non-beam-filling conditions) associated with increasingly large radiometric beamprints that are encountered as the observational viewing angles are increased from nadir (refer to Section 2.0).

An additional point of interest occurs between stations 150+00 and 151+00. A slight topographic low (resulting from draingage) exists in this area of the traverse line. This fact

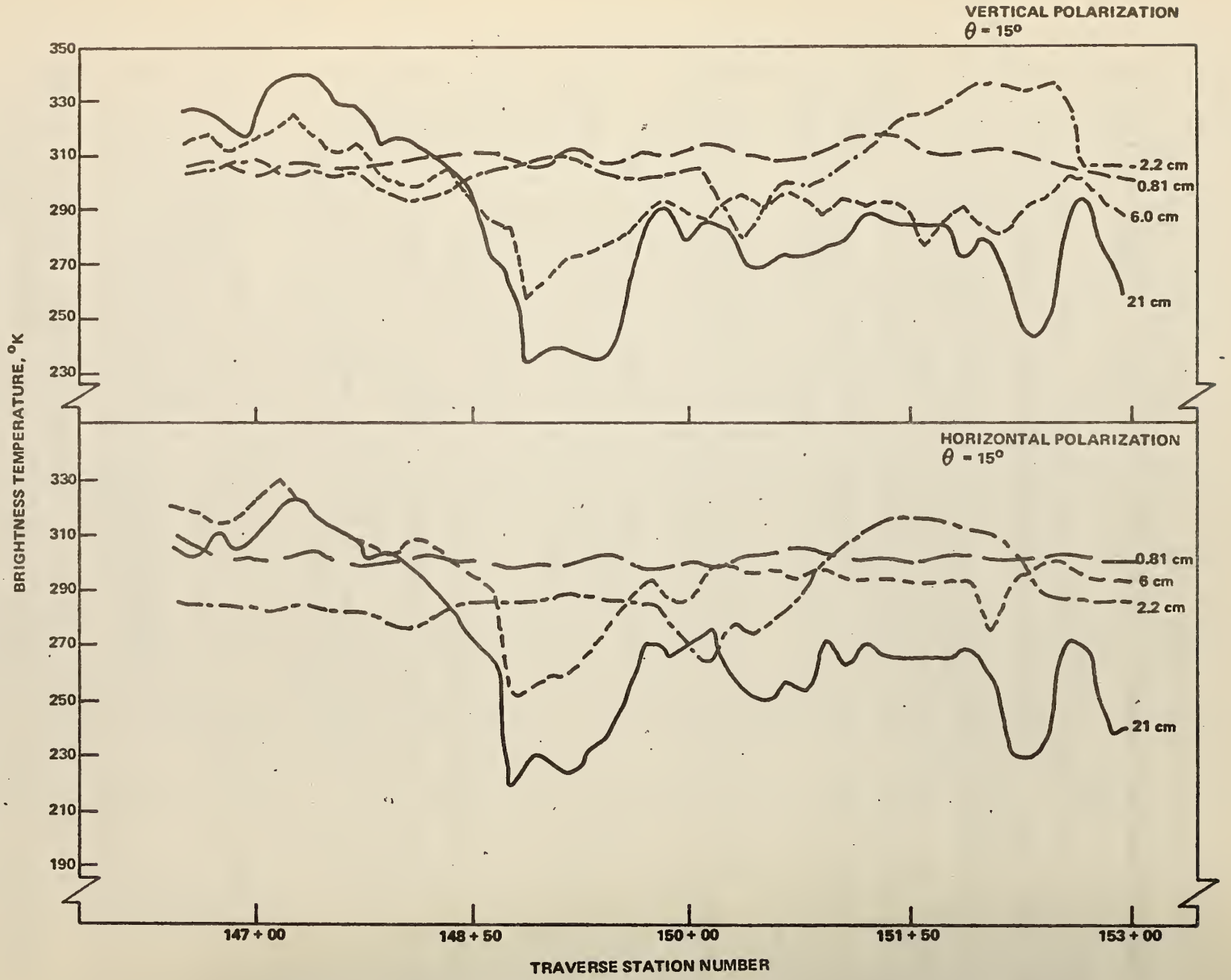

Figure 3.6 Scammon Line A Multifrequency Microwave Profile Data Taken at an Observational View Angle of 15°

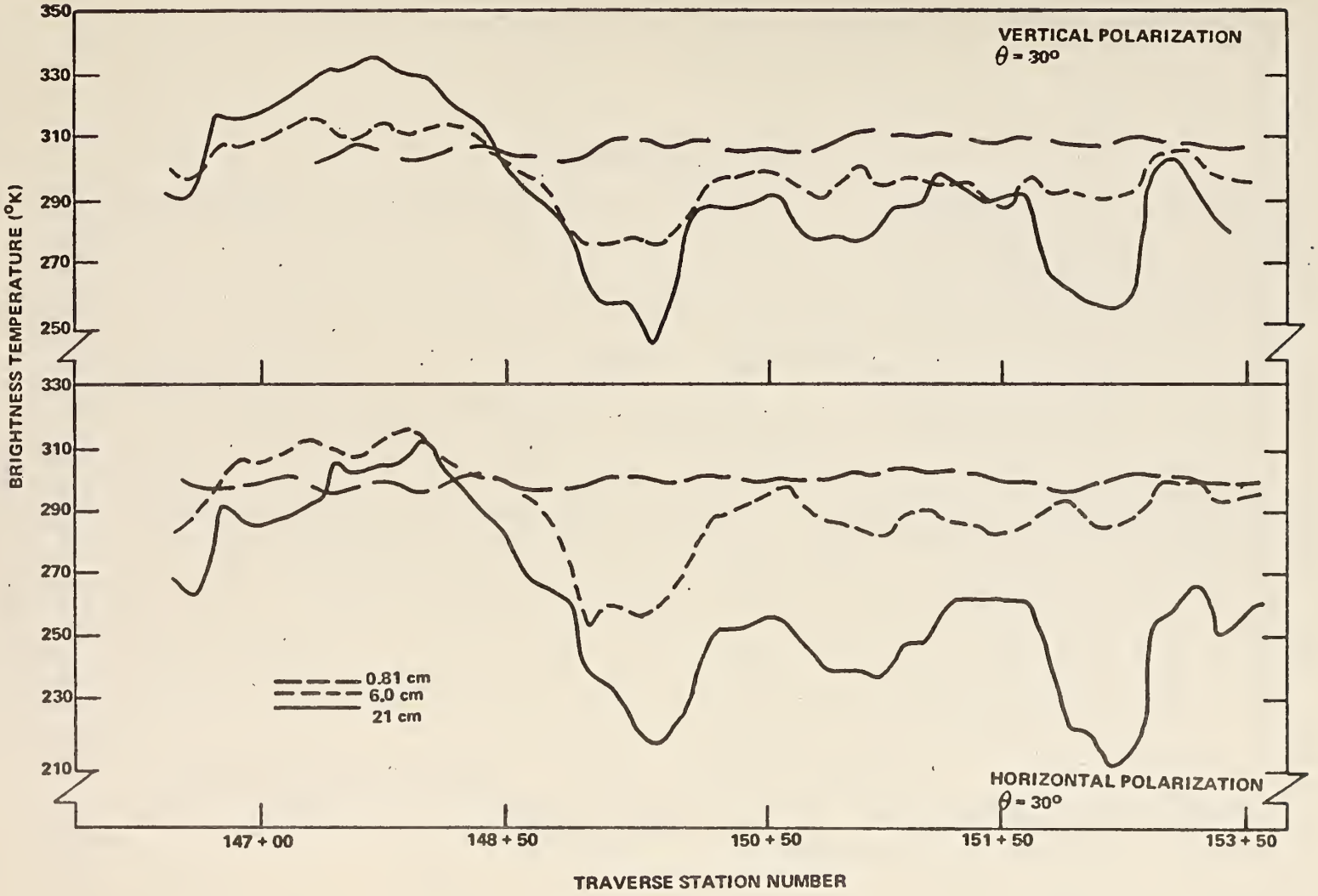

Figure 3.7 Scammon Line A Multifrequency Microwave Profile Data Taken at an Observational View Angle of 30°

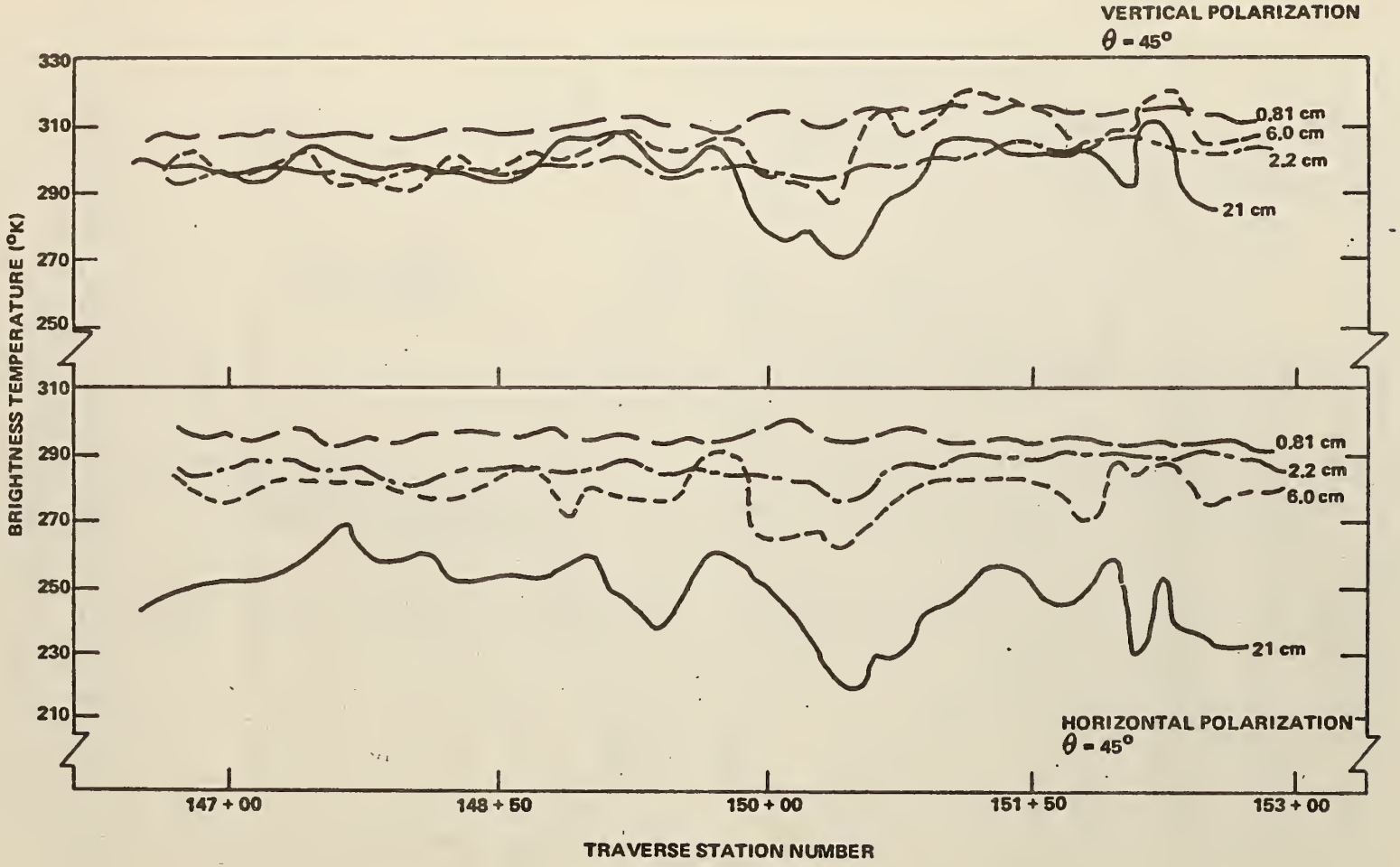

Figure 3.8 Scammon Line A Multifrequency Microwave Profile Data Taken at an Observational View Angle of 45°

combined with the recent occurrence of precipitation, implies an area of increased moisture content. This implication is verified by the cool horizontally polarized 21 cm brightness temperature differentials of approximately 16°, 27° and 33°K for the 15°, 30° and 45° viewing angles, respectively (21 cm beam-filling conditions were achieved at the 45° view angle for this anomaly). Note the general lack of response exhibited by the 6.0 cm data. The 21 and 6.0 cm data indicate (1) that the area of increased moisture content was primarily localized in the field of view of the 21 cm radiometer and that a lateral east to west decreasing vertical soil moisture gradient was in existence across the traverse line (the respective orientation of the 21 and 6.0 cm radiometers was east to west), or (2) that the increased moisture content was too deep for the 6.0 cm sensor to measure. Since the topographic low extended uniformly across the traverse line, the investigators believe the latter to be true.

The above interpretation is further substantiated by the presence of an additional topographic low that also extended uniformly across the traverse line at station 152+25. Note the pronounced anomalies that are occurring at 21 cm along with the general lack of response exhibited by the 6.0 cm data. The less pronounced 21 cm anomaly occurring at the 45° viewing angle is again attributed to high areal beam averaging associated with increasingly large nadir viewing angles.

The excessively warm 21 and 6.0 cm brightness temperatures encountered (especially evident between stations 147+00 and 148+50 at the 15° and 30° viewing angles) throughout the traverse line are attributed to the utilization of incorrect antenna loss terms when these data were reduced. However, it should be emphasized that no short-term radiometric gain fluctuations were encountered for these sensors while the traverses

were being performed, and the relative brightness temperature anomalies that occurred are valid. Pronounced short term drift problems were encountered for the 2.2 cm radiometer at the 30° viewing angle (partially indicated between stations 149+75 and 152+50, Figure 3.6) and consequently, these data were not utilized for this analysis.

In summary, there appears to be adequate correlation between soil moisture and the microwave emission at 6.0 and 21 cm. The 21 cm horizontally polarized brightness temperatures are the most sensitive with the radiometric responses decreasing as a function of decreasing observational wavelength. The predominant parameter at 2.2 and 0.81 cm appears to be non-specular scattering associated with surface roughness. For beam-filling conditions, an observational view angle of 45° appears to be optimum at 21 cm. However, most of the high moisture concentrations were localized in small areas and more pronounced anomalies were obtained with the higher areal resolution achieved at 15° and 30° viewing angles. At these longer wavelengths, the effects of soil moisture is the primary factor controlling the microwave emission with surface roughness being secondary. The point-to-point variations of thermometric temperature and density were slight, and the investigators consider these parameters to be of least correlative importance for this site.

3.3 Scammon Line B

Scammon Line B data were obtained on August 17, 1971 between 13:65 and 14:23. The line was 900 feet long with aluminum foil strips located 200 feet apart. The weather was clear although recent rains raised percentage of ground moisture in the upper strata considerable above normal conditions. Ground truth sampling shortly followed collection of microwave data. These are given in Table 3-1.

TABLE 3-1 GROUND TRUTH DATA SCAMMON SITE LINE B

Station	Dist. ℄ Truck	Sample Number	Depth (Cm.)	Percent Moisture	Average Temp.	Wet Density (pcf)	% Moisture @ 32 (Cm.)	Dry Density (pcf)
				Surface	31.0			
343+50	5'E	EA-42	2	23.9	22.6	95.5	20.3	79.4
		EB-42	4	24.6	22.6			
		EC-42	8	24.2	22.6			
		ED-42	16	21.7	23.3			
		EE-42	32	20.3	23.7			
				Surface	32.7			
343+50	5'W	WA-42	2	10.8	24.5	95.75	9.6	87.4
		WB-42	4	10.1	25.0			
		WC-42	8	10.4	25.0			
		WD-42	16	9.7	24.0			
		WE-42	32	9.6	24.8			
				Surface	34.5			
344+50	5'E	EA-43	2	13.5	23.2	107.5	17.6	91.4
		EB-43	4	12.5	22.5			
		EC-43	8	13.0	22.3			
		ED-43	16	16.1	23.0			
		EE-43	32	17.6	23.4			
				Surface	31.5			
344+50	5'W	WA-43	2	11.6	26.9	100.75	16.3	86.6
		WB-43	4	11.8	26.7			
		WC-43	8	13.9	26.0			
		WD-43	16	14.8	23.2			
		WE-43	32	16.3	23.6			
				Surface	34.7			
345+50	5'E	EA-44	2	13.4	24.2	113.0	16.9	96.7
		EB-44	4	12.0	23.9			
		EC-44	8	10.3	23.5			
		ED-44	16	11.6	23.3			
		EE-44	32	16.9	23.4			

TABLE 3-1 GROUND TRUTH DATA SCAMMON SITE LINE B
(Continued)

Station	Dist. ℄ Truck	Sample Number	Depth (Cm.)	Percent Moisture	Average Temp.	Wet Density (pcf)	% Moisture @ 32 (Cm.)	Dry Density (pcf)
				Surface	33.6			
345+50	5'W	WA-44	2	15.1	24.5	106.75	17.6	90.8
		WB-44	4	14.2	23.7			
		WC-44	8	16.7	23.2			
		WD-44	16	17.3	23.1			
		WE-44	32	17.6	22.8			
				Surface	38.6			
346+50	5'E	EA-45	2	11.4	25.5	96.5	13.1	85.3
		EB-45	4	11.0	23.6			
		EC-45	8	11.0	23.3			
		ED-45	16	9.2	23.2			
		EE-45	32	13.1	23.5			
				Surface	36.7			
346+50	5'W	WA-45	2	5.6	30.9	89.5	9.2	82.0
		WB-45	4	4.9	29.3			
		WC-45	8	7.0	27.7			
		WD-45	16	7.4	24.3			
		WE-45	32	9.2	24.2			
				Surface	41.8			
347+50	5'E	EA-46	2	10.1	24.1	92.0	14.1	80.6
		EB-46	4	11.9	23.7			
		EC-46	8	11.7	24.0			
		ED-46	16	14.5	23.5			
		EE-46	32	14.1	23.2			
				Surface	39.7			
347+50	5'W	WA-46	2	7.9	27.1	95.75	7.4	89.2
		WB-46	4	6.9	25.9			
		WC-46	8	7.5	25.9			
		WD-46	16	6.4	24.1			
		WE-46	32	7.4	----			

TABLE 3-1 GROUND TRUTH DATA SCAMMON SITE LINE B
(Continued)

Station	Dist. ℄ Truck	Sample Number	Depth (Cm.)	Percent Moisture	Average Temp.	Wet Density (pcf)	% Moisture @ 32 (Cm.)	Dry Density (pcf)
					Surface 44.1			
348+50	5'E	EA-47	2	15.2	24.2	102.2	16.2	88.0
		EB-47	4	14.1	24.4			
		EC-47	8	13.3	24.0			
		ED-47	16	14.7	23.2			
		EE-47	32	16.2	23.5			
					Surface 37.7			
348+50	5'W	WA-47	2	9.4	27.8	108.5	10.4	98.3
		WB-47	4	12.6	26.9			
		WC-47	8	9.0	25.5			
		WD-47	16	8.5	24.5			
		WE-47	32	10.4	24.4			
					Surface 46.8			
349+50	5'E	EA-48	2	20.8	29.0	96.5	16.9	82.9
		EB-48	4	14.5	25.4			
		EC-48	8	15.5	24.6			
		ED-48	16	15.8	23.7			
		EE-48	32	16.9	22.8			
					Surface 43.1			
349+50	5'W	WA-48	2	10.6	29.4	94.5	14.5	82.5
		WB-48	4	12.8	26.5			
		WC-48	8	13.9	25.8			
		WD-48	16	10.8	24.6			
		WE-48	32	14.5	23.7			
					Surface 47.6			
350+50	5'E	EA-49	2	15.1	29.3	99.25	15.3	86.1
		EB-49	4	11.3	27.6			
		EC-49	8	10.4	26.6			
		ED-49	16	9.8	25.4			
		EE-49	32	15.3	24.4			

TABLE 3-1 GROUND TRUTH DATA SCAMMON SITE LINE B
(Continued)

Station	Dist. ℄ Truck	Sample Number	Depth (Cm.)	Percent Moisture	Average Temp.	Wet Density (pcf)	% Moisture @ 32 (Cm.)	Dry Density (pcf)
				Surface	43.5			
350+50	5'W	WA-49	2	7.4	27.9	99.5	12.9	38.1
		WB-49	4	11.0	26.7			
		WC-49	8	12.9	25.7			
		WD-49	16	11.2	24.2			
		WE-49	32	12.9	23.3			
				Surface	45.4			
351+50	5'E	EA-50	2	4.3	33.1	107.5	13.5	94.7
		EB-50	4	8.4	30.8			
		EC-50	8	11.1	29.3			
		ED-50	16	13.5	26.8			
		EE-50	32	13.5	25.5			
				Surface	45.9			
351+50	5'W	WA-50	2	11.3	28.0	107.5	14.2	94.1
		WB-50	4	10.6	28.2			
		WC-50	8	14.6	26.6			
		WD-50	16	12.9	28.1			
		WE-50	32	14.2	24.8			
				Surface	48.6			
352+50	5'E	EA-51	2	12.9	32.0	91.5	12.0	81.7
		EB-51	4	11.7	31.2			
		EC-51	8	12.8	30.2			
		ED-51	16	14.6	30.4			
		EE-51	32	12.0	26.1			
				Surface	43.0			
352+50	5'W	WA-51	2	6.0	36.0	96.5	14.3	84.4
		WB-51	4	8.3	34.2			
		WC-51	8	9.2	32.5			
		WD-51	16	10.1	30.5			
		WE-51	32	14.3	25.5			

NOTE: Temperatures on this project are centigrade.
All densities are taken with a nuclear densitometer (12" Probe).

In comparison with other sites, the correlation plot of moisture for Scammon Line B (Figure 3.9) does not exhibit the typical increase in moisture with depth, no doubt reflecting differences in soil permeability along the profile as well as recent rainfall at the surface. Percentages of moisture are high for all depths without large perturbations across the length of the line with the exception of Stations 346+50 and 351+50 where average moisture deviates negatively from the overall average. A very slight drop in average moisture corresponding with an equally slight rise in average ground temperature occurs across the profile.

With the exception of surface temperatures, temperatures for all depths are relatively constant. Prominent perturbations occur at Stations 348+50 at the surface, and at 351+50 and 346+50 at 2 cm. Whereas the rise in temperatures at the latter two stations correspond with a decrease in soil moisture, the decrease in ground temperature at the surface at Station 348+50 no doubt corresponds with some very localized surface anomaly (not obvious on hand held photographs) and does not reflect a deep seated effect.

Unlike many other lines in the study area which are characterized by relatively consistant wet and dry density values, Scammon Line B is distinguished by large swings in density values from station to station reflecting microvariations in soil conditions along the profile.

Fluctuations of about 20°K in both polarizations of the microwave profile are similar in general and in detail (Figure 3.10). Antenna temperatures indicate low emissions at the beginning of the line (Station 343+50) with a gradual rise reaching a "peak" around 348+00, followed by a drop (Stations 349+50 and 350+50) and a second rise (351+50).

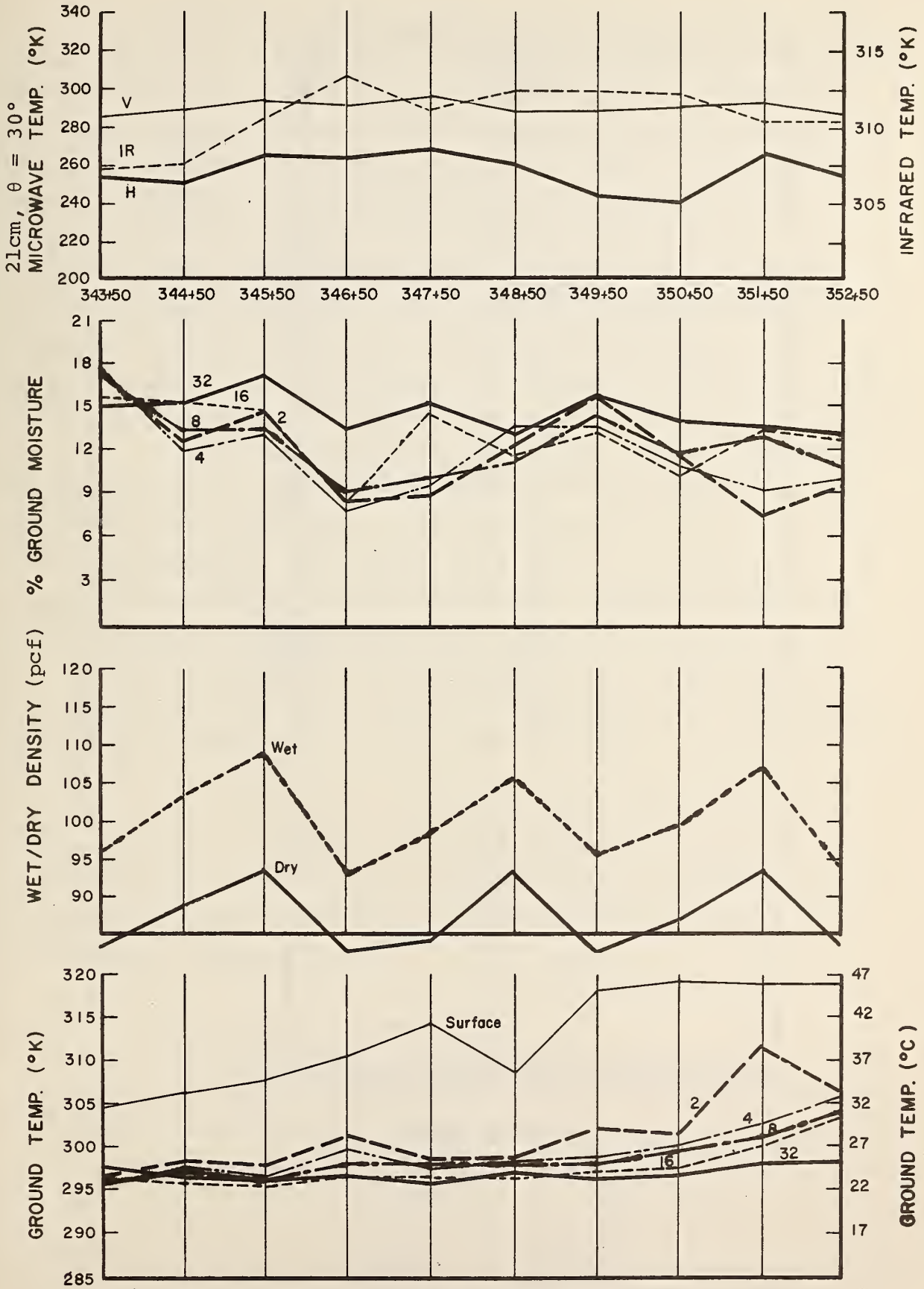

Figure 3.9 Correlation of Measurements Scammon B, Run 4

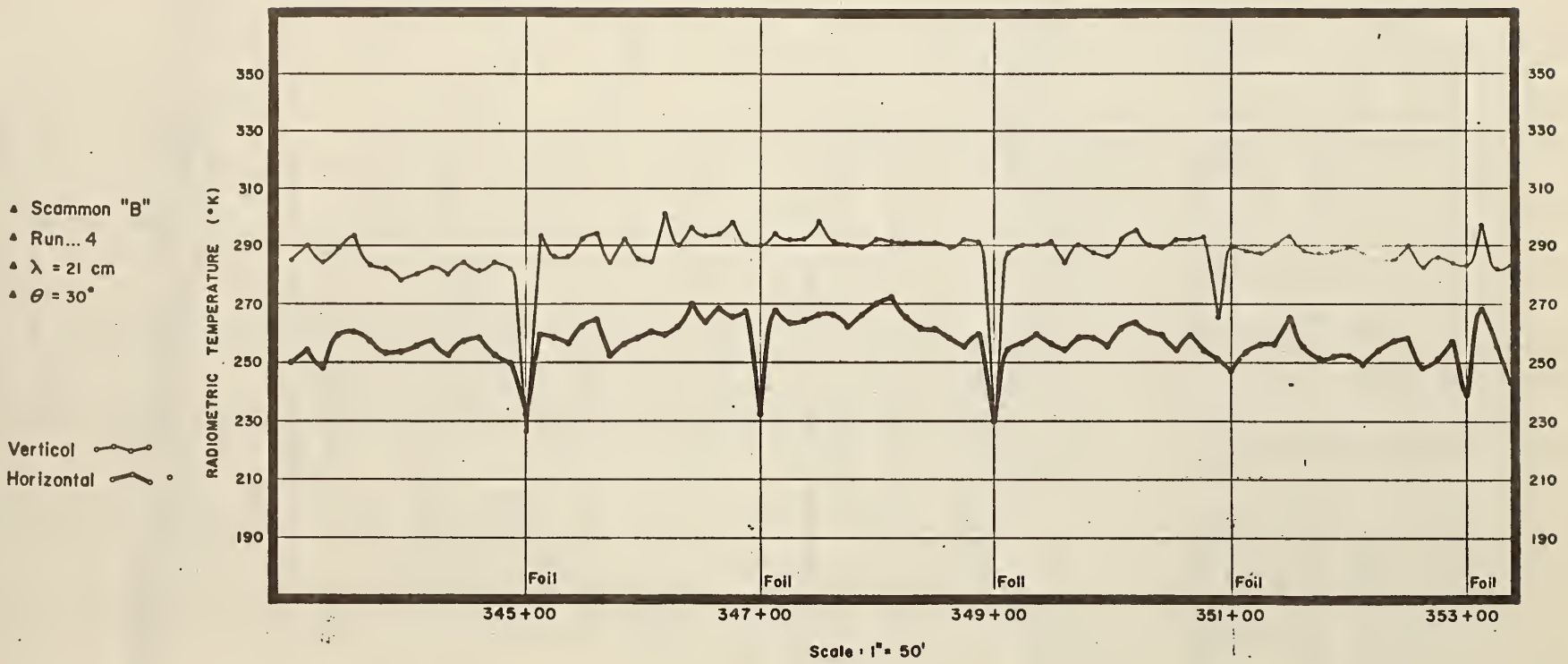

Figure 3.10 Microwave Profile - Scammon Line B

Although point-to-point correlations indicate prominent deviations in the high moisture-low microwave temperature relationship, this line tends to suggest such a correlation. MW energy sensed by the L Band radiometer along this profile however, appears to be emitted from the upper 8 centimeters. This is evident in the general trend in parameters shown in Figure 3.9 and in detail on the same figure at 351+50 where surface moisture drops and ground and antenna temperatures show a corresponding rise. In contrast, a similar drop in moisture content and rise in ground temperatures occurring at Station 346+50 is not sensed by radiometer. Indeed, the microwave signal shows a slight drop where a slight rise is expected.

No obvious correspondence exists between the wet/dry densities and the microwave signals, or the infrared signals and any ground parameter. One cannot help but note, however, the correspondence in overall trend of the infrared signal between 343+50 and 350+50 and the surface ground temperatures. Whereas ground temperatures show a rise at 347+50 and a drop at 348+50, IR temperatures indicate a rise at 346+50 and a corresponding drop at 347+50. It is feasible that the offset occurred in the data reduction process rather than in space at the Scammon B site.

In summary, the L Band microwave radiometer shows no correspondence with wet or dry bulk densities, and only poor correspondence with ground moisture. Slightly better correspondence is seen in the relationship of the microwave signal and ground temperature.

3.4 Galena Lines A and C'

On August 11-13, 1971, the microwave traverses were performed in Galena, Kansas mining field. The mining field is situated in the southeast corner of Kansas and is representative

of the "Tri-State" area where extensive lead and zinc mining has taken place. Two N-S trending traverse lines of 950 (Line A) and 400 (Line C') feet in length were established in an area characterized by fill and tailings composed of crushed chert mixed with silt. Unlike Scammon Line A, comparatively good subsurface control exists for this site. Figure 3.11 shows the two traverse lines superimposed on a map of the mining field. Although the map is old and sketchy, it does at least provide general information concerning placement of the mined out areas. Also, adjacent to the traverse lines numerous sink holes and shallow shaft openings were present making the free water surface of the water table readily visible. No precipitation had occurred in the area since August 1 and the investigators feel reasonably certain that overburden soil moisture equilibrium conditions were achieved.

The Line A traverses were performed between 1100 and 1200 hours on August 11. Sky conditions consisted of a high thick scattered cloud cover and the air temperature was about 303°K. On August 13 the Line C' traverses were performed at approximately 1600 hours. At this time, the sky conditions consisted of a high thick broken overcast and the air temperature was 306°K.

Correlative surface control measurements for Line A were performed in similar fashion to the Scammon site and are compiled in Table 3-2. Surface control measurements for Line C', Table 3-3, were concentrated in areas of anomalous microwave emission at stations 12+30, 12+50 and 14+30. Figure 3.12 illustrates the sampling locations used at each of these locations. At each sampling location, measurements were performed to determine (1) percent soil moisture content for depth intervals corresponding to 0-2, 0-4, 0-16, 0-32 and approximately 0-56 cm; and (2) integrated density values to a depth of 30 cm. Thermometric temperature profiles were not determined for this line.

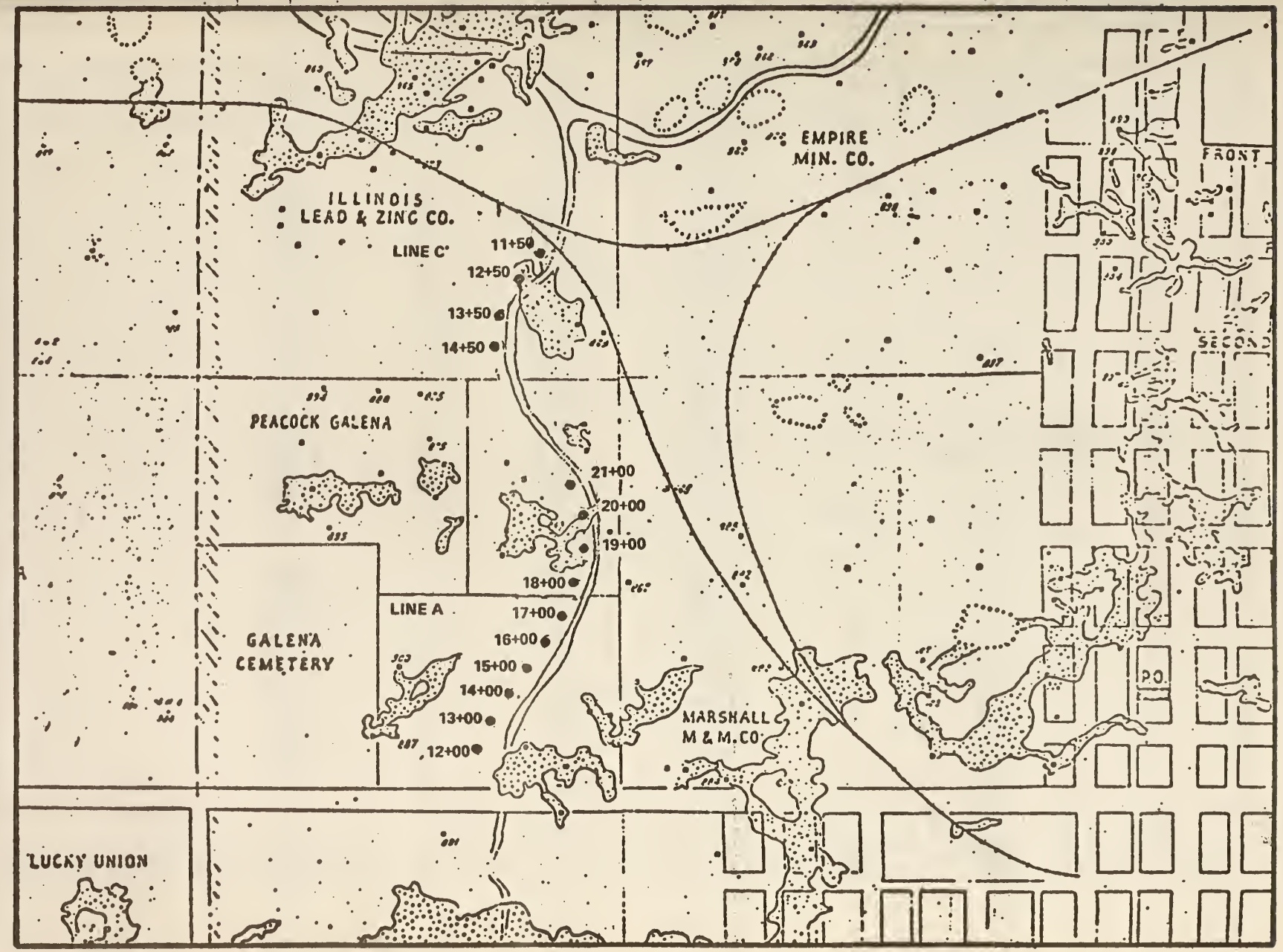

Figure 3.11 Galena Mining Field Showing Traverse Lines A and C'

TABLE 3-2 GALENA SITE LINE A

Station	Dist. ℄ Truck	Sample Number	Depth (Cm.)	Percent Moisture	Average Temp.	Wet Density (pcf)	% Moisture @ 32 (Cm.)	Dry Density (pcf)
				Surface	311.1			
12+00	10'E	EA-1	2	4.1	308.0	111.0	6.2	104.6
		EA-1A	2	1.9	308.0			
		EB-1	4	3.5	307.0			
		EB-1A	4	5.8	307.8			
		EC-1	8	5.3	307.0			
		EC-1A	8	3.7	307.0			
		ED-1	16	6.0	306.6			
		ED-1A	16	9.0	306.6			
		EE-1	32	6.2	303.4			
		EE-1A	32	7.2	303.4			
				Surface	318.9			
13+00	10'E	EA-2	2	2.7	309.1	98.0	17.1	83.7
		EA-2A	2	5.0	309.1			
		EB-2	4	12.3	307.9			
		EB-2A	4	2.3	307.9			
		EC-2	8	9.8	305.3			
		EC-2A	8	5.0	305.3			
		ED-2	16	13.0	303.7			
		ED-2A	16	11.6	303.7			
		EE-2	32	17.1	300.7			
		EE-2A	32	13.7				
				Surface	316.2			
14+00	12'E	EA-3	2	1.3	313.9	103.0	6.6	96.6
		EB-3	4	1.3	310.7			
		EC-3	8	4.1	306.9			
		ED-3	16	5.4	304.5			
		EE-3	32	6.6	303.8			
				Surface	321.1			
14+00	12'W	WA-3	2	.4	314.4	86.75	6.3	81.6
		WB-3	4	.9	311.8			
		WC-3	8	5.2	306.4			
		WD-3	16	6.4	305.1			
		WE-3	32	6.3	302.3			

TABLE 3-2 GALENA SITE LINE A
(Continued)

Station	Dist. ℄ Truck	Sample Number	Depth (Cm.)	Percent Moisture	Average Temp.	Wet Density (pcf)	% Moisture @ 32 (Cm.)	Dry Density (pcf)
					Surface 319.1			
15+00	9'W	WA-4	2	.9	316.3	102.25	5.4	97.0
		WA-4A	2	0.0	316.3			
		WB-4	4	0.0	313.0			
		WB-4A	4	.8	313.0			
		WC-4	8	3.3	306.7			
		WC-4A	8	4.3	306.7			
		WD-4	16	4.2	305.3			
		WD-4A	16	3.1	305.3			
		WE-4	32	5.4	301.9			
		WE-4A	32	5.3	301.9			
					Surface 320.5			
16+00	13'E	EA-5	2	.4	317.0	92.75	6.2	87.3
		EB-5	4	.5	312.5			
		EC-5	8	2.2	309.7			
		ED-5	16	5.6	305.6			
		EE-5	32	6.2	302.6			
					Surface 326.6			
16+00	10'W	WA-5	2	.4	319.3	88.25	6.1	83.1
		WB-5	4	.9	309.7			
		WC-5	8	2.0	308.8			
		WD-5	16	3.8	303.7			
		WE-5	32	6.1	300.7			
					Surface 322.1			
17+00	6'E	EA-6	2	.4	313.6	98.5	4.9	93.9
		EB-6	4	.6	316.2			
		EC-6	8	2.1	308.9			
		ED-6	16	3.7	305.5			
		EE-6	32	4.9	302.4			
					Surface 317.7			
17+00	6'W	WA-6	2	.4	317.7	94.0	5.0	89.5
		WB-6	4	.4	313.6			
		WC-6	8	1.8	308.9			
		WD-6	16	4.4	305.9			
		WE-6	32	5.0	303.0			

TABLE 3-2 GALENA SITE LINE A
(Continued)

Station	Dist. ℄ Truck	Sample Number	Depth (Cm.)	Percent Moisture	Average Temp.	Wet Density (pcf)	% Moisture @ 32 (Cm.)	Dry Density (pcf)
				Surface	320.3			
18+00	6'E	EA-7	2	.5	314.8	106.0	5.3	100.6
		EB-7	4	.9	308.1			
		EC-7	8	1.7	306.8			
		ED-7	16	4.7	304.4			
		EE-7	32	5.3	301.9			
				Surface	320.0			
18+00	6'W	WA-7	2	.5	314.4	92.25	5.4	87.5
		WB-7	4	.9	310.2			
		WC-7	8	2.6	308.2			
		WD-7	16	5.0	305.5			
		WE-7	32	5.4	302.3			
				Surface	322.4			
19+00	9'E	EA-8	2	1.5	312.8	99.25	8.7	91.3
		EB-8	4	1.5	308.6			
		EC-8	8	1.4	307.6			
		ED-8	16	3.4	305.4			
		EE-8	32	8.7	303.2			
				Surface	320.6			
19+00	6'W	WA-8	2	.4	315.1	93.75	5.4	88.9
		WB-8	4	.4	309.5			
		WC-8	8	2.4	306.8			
		WD-8	16	3.5	304.8			
		WE-8	32	5.4	302.0			
				Surface	319.4			
20+00	6'E	EA-9	2	.4	315.7	110.5	5.0	105.2
		EB-9	4	.9	310.4			
		EC-9	8	1.9	308.1			
		ED-9	16	2.4	306.1			
		EE-9	32	5.0	303.7			

TABLE 3-2 GALENA SITE LINE A
(Continued)

Station	Dist. ℄ Truck	Sample Number	Depth (Cm.)	Percent Moisture	Average Temp.	Wet Density (pcf)	% Moisture @ 32 (Cm.)	Dry Density (pcf)
					Surface 318.3			
20+00	6'W	WA-9	2	0.0	311.3	121.0	4.7	115.6
		WB-9	4	.8	309.6			
		WC-9	8	2.3	308.5			
		WD-9	16	4.1	306.8			
		WE-9	32	4.7	304.2			
					Surface 315.5			
21+00	6'E	EA-10	2	.4	311.5	104.0	4.6	99.4
		EA-10A	2	.4	311.5	105.0	8.5	96.8
		EB-10	4	2.1	310.9			
		EB-10A	4	1.7	310.9			
		EC-10	8	3.9	308.9			
		EC-10A	8	4.4	308.9			
		ED-10	16	7.0	307.5			
		ED-10A	16	6.1	307.5			
		EE-10	32	4.6	305.1			
		EE-10A	32	8.5	305.1			

NOTE: Temperatures on this site are kelvin.

All densities are taken with a nuclear densitometer (12"Probe).

TABLE 3-3 GALENA SITE LINE C'

Station	Dist. ℄ Truck	Sample Number	Depth (Cm.)	Percent Moisture	Average Temp.	Wet Density (pcf)	% Moisture @ 32 (Cm.)	Dry Density (pcf)
12+30	29'E	EA-18	4	.4	No Temp.	93.0	5.5	88.1
	of Sta.	SA-18	4	.4		89.0	5.6	84.3
		WA-18	4	.4		98.25	6.2	92.5
	14'W	NA-18	4	.4		93.0	5.4	88.2
	of Conc.	CA-18	4	.9		89.0	5.3	84.5
	Wall	EB-18	16	.4				
		SB-18	16	.4				
		WB-18	16	9.7				
		CB-18	16	5.3				
		EC-18	32	5.5				
		SC-18	32	5.6				
		WC-18	32	6.2				
		NC-18	32	5.4				
		CC-18	32	5.3				
		ED-18	21"	6.2				
		SD-18	19"	6.8				
		WD-18	23"	5.4				
		ND-18	21"	6.3				
		CD-18	22"	4.7				
12+50	28'E	EA-19	4	.8	No Temp.	84.25	6.6	79.0
	of Sta.	SA-19	4	.4		97.5	4.8	93.0
		WA-19	4	.8		103.25	4.9	98.4
	11'W	NA-19	4	1.1		90.5	4.1	86.9
	of Conc.	CA-19	4	1.2		99.0	6.6	92.9
	Wall	EB-19	16	3.1				
		SB-19	16	5.2				
		WB-19	16	3.8				
		NB-19	16	3.7				
		CB-19	16	5.5				
		EC-19	32	6.6				
		SC-19	32	4.8				
		WC-19	32	4.9				
		NC-19	32	4.1				
		CC-19	32	6.6				
		ED-19	19"	6.6				

TABLE 3-3 GALENA SITE LINE C'
(Continued)

Station	Dist. ℄ Truck	Sample Number	Depth (Cm.)	Percent Moisture	Average Temp.	Wet Density (pcf)	% Moisture @ 32 (Cm.)	Dry Density (pcf)
		SD-19	21"	5.7				
		WD-19	24"	5.1				
		ND-19	23"	6.3				
		CD-19	22"	5.7				
14+30	25'E	EA-20	4	.8	No Temp.	90.5	3.6	87.3
	of Sta.	SA-20	4	0.0		101.5	5.0	96.7
		WA-20	4	2.8		91.25	5.4	87.5
	25'W	NA-20	4	2.1		88.0	3.6	84.9
	of Conc.	CA-20	4	.9		98.25	3.9	94.6
	Wall	EB-20	16	3.1				
		SB-20	16	5.2				
		WB-20	16	5.4				
		NB-20	16	2.9				
		CB-20	16	3.6				
		EC-20	32	3.6				
		SC-20	32	5.0				
		WC-20	32	5.4				
		NC-20	32	3.6				
		CC-20	32	3.9				
		ED-20	19"	4.5				
		SD-20	22"	4.5				
		WD-20	23"	4.9				
		ND-20	24"	5.6				
		CD-20	23"	4.4				

NOTE: All densities are taken with a nuclear densitometer (12" Probe).

The D Samples are measured in inches, not centimeters.

Densities are computed from the moisture content at 32 Cm.

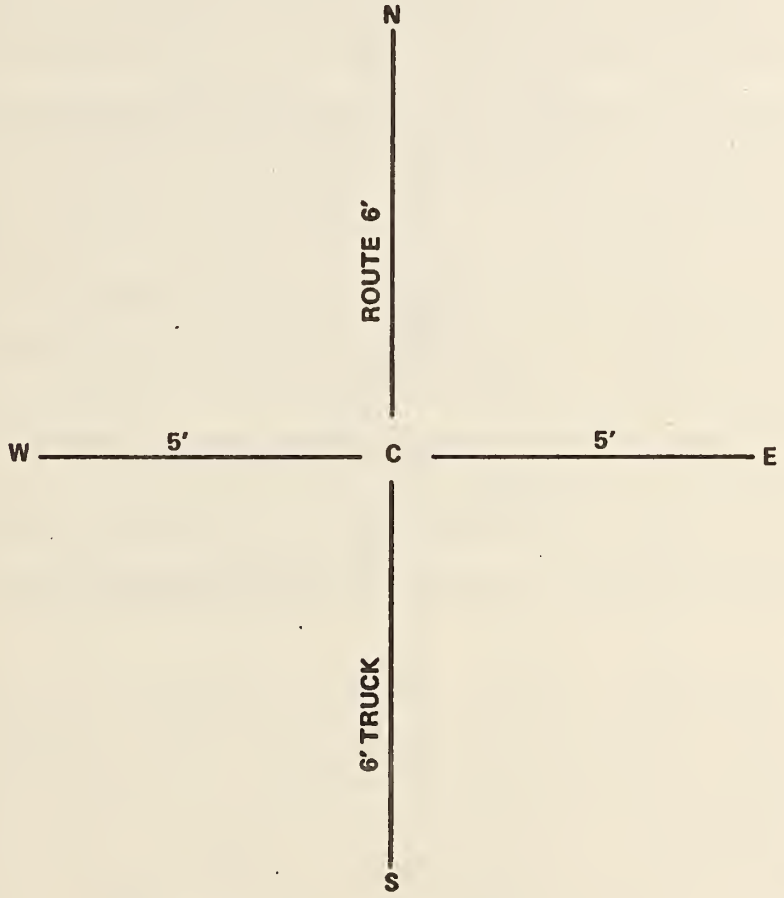

Figure 3.12 Soil Moisture Sampling Grid Pattern Used For Galena Line C'

The ground moisture percentages recorded at the Scammon A Site range betwen about 3 and 19 percent and ground temperatures range between 300°K and 313°K. A short time prior to field measurements at Scammon, the site received a rainfall which resulted in rather high percentages of moisture in the solum. Nonetheless the magnitude of the soil mositre and temperatures recorded at Scammon is not unlike those recorded at the other sites with the exception of Galena A where the soil moisture levels were low (0.4 to 7 percent) and the temperatures high (320°K to 322°K). Under the dry soil Galena conditions it was hypothesized that the 21 cm microwave penetration would exceed that of the wetter soils at the other sites. In order to evaluate the effect of these conditions an analysis of the Galena A site data was conducted which paralleled that of the Scammon site.

Figure 3.13 and 3.14 show the spatial correlation between the ground conditions and the remotely sensed temperatures.

Like the Scammon A Site, antenna temperatures in detail show little correlations with either moisture or temperature. At microwave wavelengths, the horizontal polarization does drop several degrees at station 13+00 (Figure 3.13) where soil moisture percentages increase, but vertical polarization shows, enigmatically, a rise in microwave temperature. It was noted that, vertical and horizontal polarizations in this study area normally tend to vary in a like manner. Additionally, Station 18+00 in Figure 3.14 shows a prominant 30° drop in antenna temperatue which does not correlate well with either percentage moisture or ground temperatures.

Infrared temperatures in Figure 3.13 correspond weakly with ground moisture conditions as they did at the Scammon A Site. Correspondence is even less noticable however, in Figure 3.14. In each case the expected high positive correlation

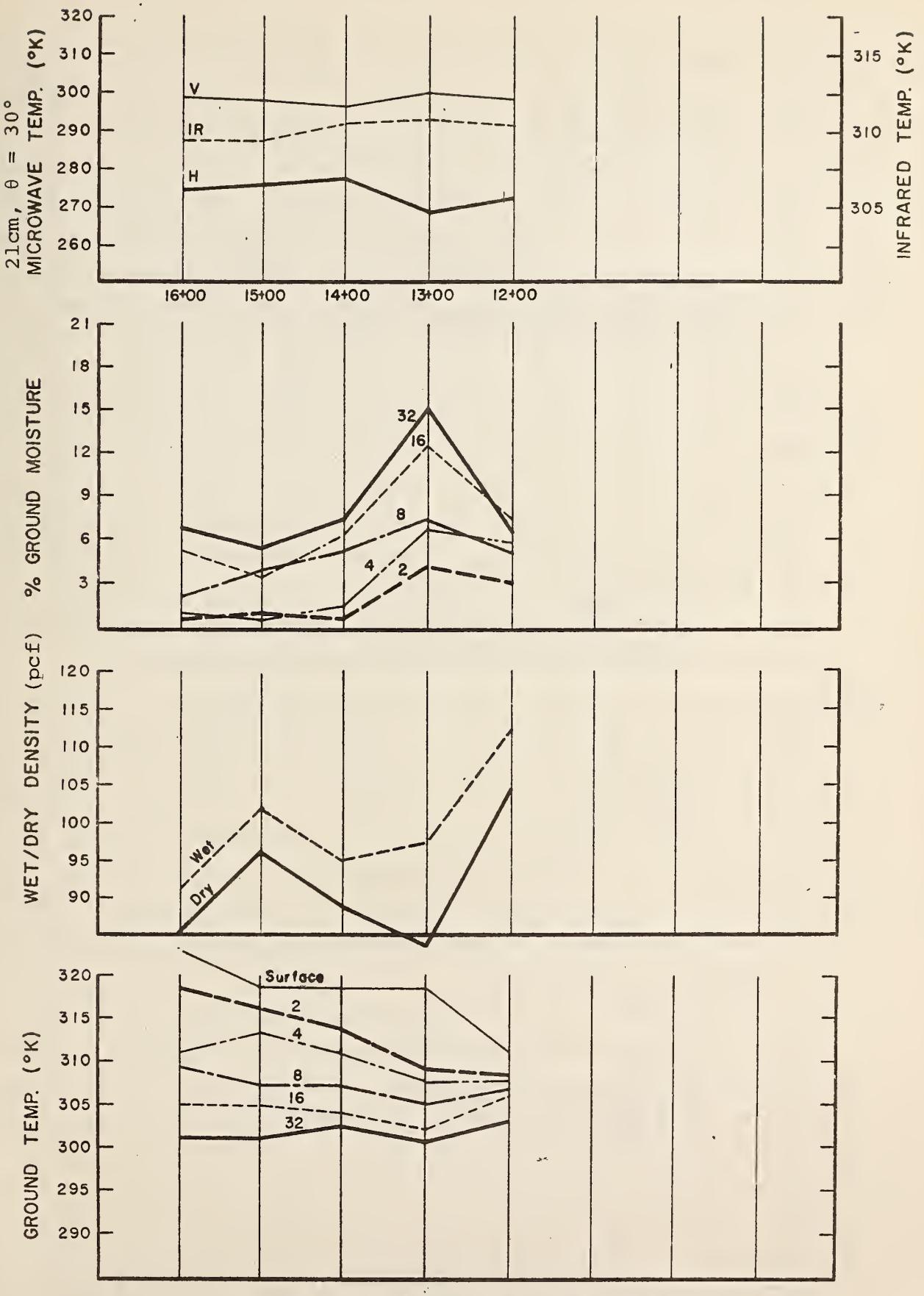

Figure 3.13 Correlation of Measurements Galena Line A, Run 1

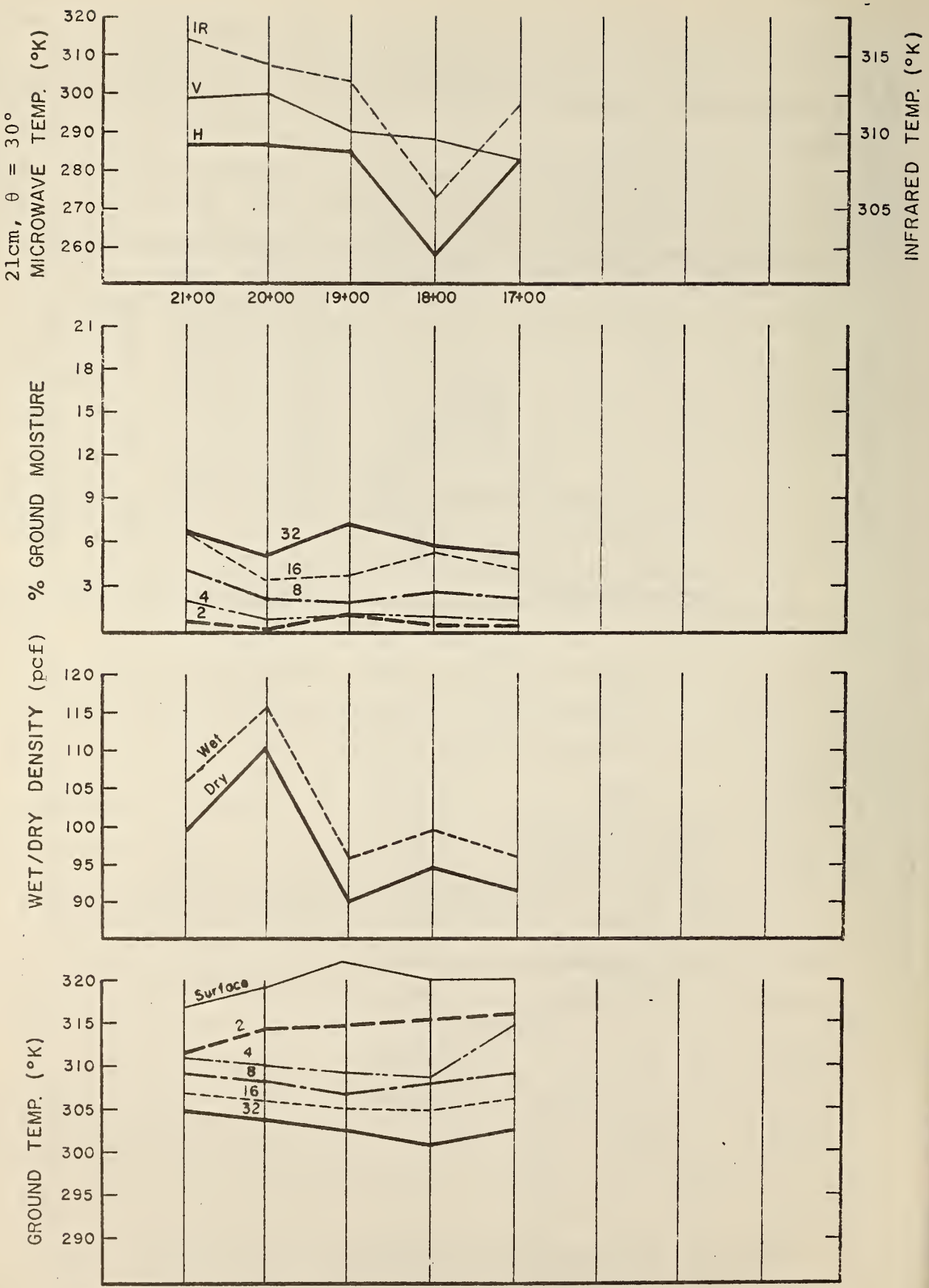

Figure 3.14 Correlation of Measurements Galena Line A, Run 2

between ground surface temperatures and infrared temperatures does not occur.

With the exception of 13+00 no significant point-to-point soil moisture variations were encountered for the depth intervals measured throughout Line A. Percent moisture content (dry weight basis) varies only from 4.7 to 6.7 at the 0-32 cm depth interval. At station 13+100 a narrow area of comparatively wet clay, probably deposited by an old drainage channel, existed and accounts for the 15.4 percent as an "average" moisture content measured at the 0-32 cm depth interval. Like Line A, both 0-32 and 0-56 cm moisture data collected on Line C' range from 4.4 to 6.8 percent and exhibit no significant point-to-point variations. Where data are available, thermometric temperatures generally decrease as a function of increasing soil moisture content on a point-to-point basis. Variations in the measured dry density values are slight and provide little correlative importance for this site.

Microwave profile data for Lines A and C' are given in Figures 3.15 and 3.16 respectively. These data were obtained at an observational wavelength of 21 cm and a viewing angle 30° from nadir. Note the pronounced cool brightness temperature anomalies that occur at stations 11+80, and between stations 12+25 and 12+60 for Line C'. These anomalies far exceed contributions attributable to the data provided by the surface control measurements. It is known that for soil moisture contents of about 7.5 percent (by volume) the soil penetration of the 21 cm radiometer can exceed its own free-space wavelength by at least an order of magnitude (Poe, et al, 1971, 1972). Thus, for most moisture conditions encountered at the Galena site, the 21 cm radiometer was probably penetrating approximately a factor of four deeper than the deepest moisture samples taken.

The above-mentioned anomalies provide a point-to-point correlation to the mined out areas illustrated on Figure 3.11. The distribution of moisture (and therefore microwave brightness temperatures) in an overburden that is in a state of moisture equilibrium is primarily determined by subsurface structure. As previously stated, the free water surface of the water table was visible in the shallow shaft openings adjacent to the traverse lines. Since no lateral shafts were also visible, the investigators assume that the shaft ceilings were at least as deep as the free surface of the water table. If this assumption is correct, and also if fracturing of the ceiling rock of the shafts has occurred, a higher moisture concentration would be created in the overlying overburden due to capillary rise of moisture from the water-filled shafts. Due to the extreme localization of these anomalies combined with their comparatively large polarization differences, the investigators feel that the above assumptions are true and that the 21 cm radiometer is responding to an overburden soil moisture distribution that is directly associated with the presence of water-filled subsurface voids.

A less pronounced 21 cm cool brightness temperature anomaly occurs at station 19+75 on Line A. Note that it also exhibits a point-to-point correlation to a mined out area illustrated on Figure 3.11. However, when compared to the before mentioned Line C' anomalies, both its amplitude and degree of polarization are less pronounced. Also note that its absolute magnitude is similar to the comparatively uniform data obtained between stations 12+00 and 16+00. Correlative ground truth information is insufficient to adequately describe the microwave emission occurring in these areas and the investigators are reluctant to attribute the station 19+75 anomaly to the presence of the mined out area. Rather, the 21 cm radiometer

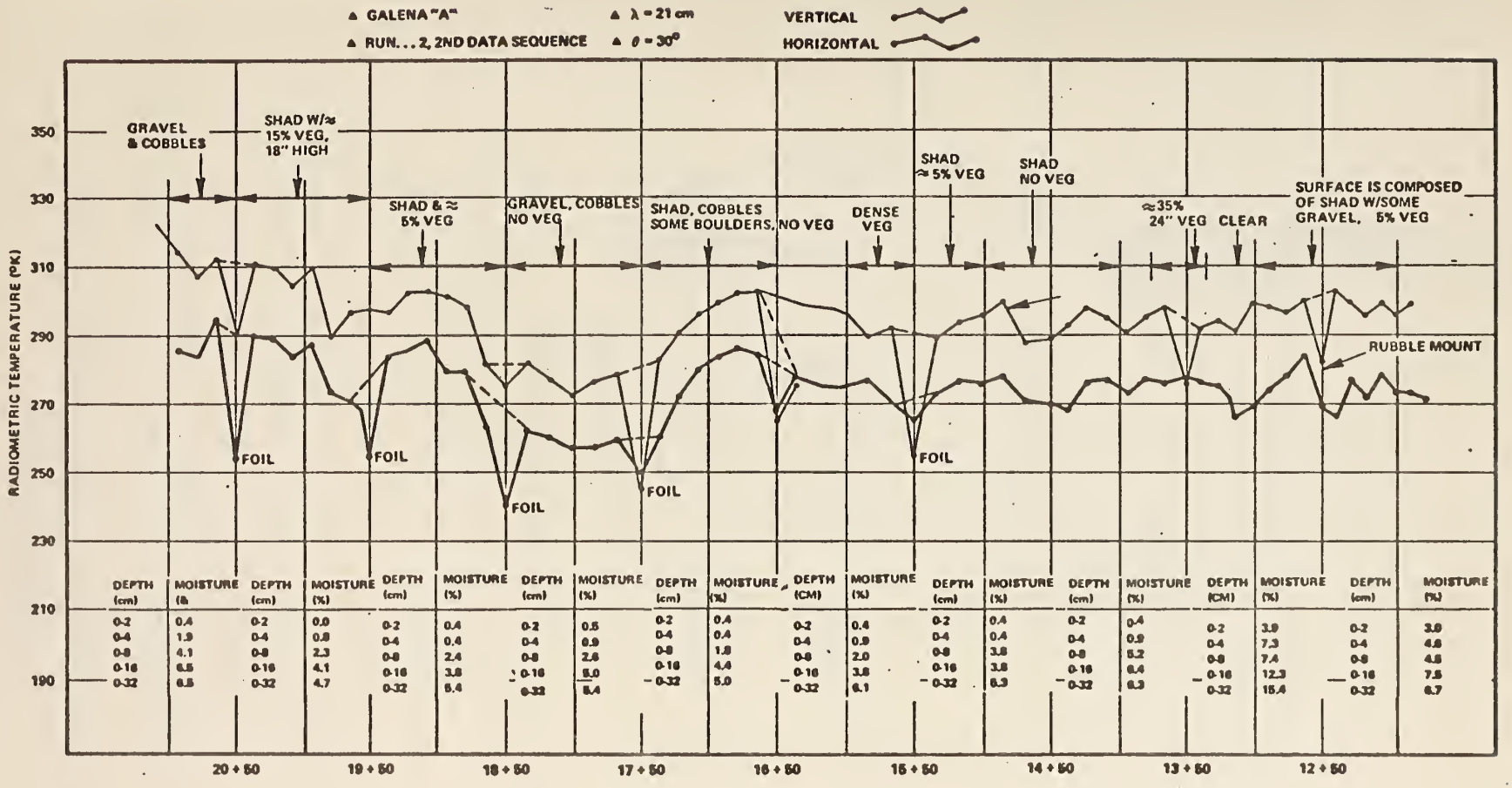

Figure 3.15 21cm Microwave Profile Data for Galena Line A (Dash lines approximate microwave temperatures expected if foil were not present)

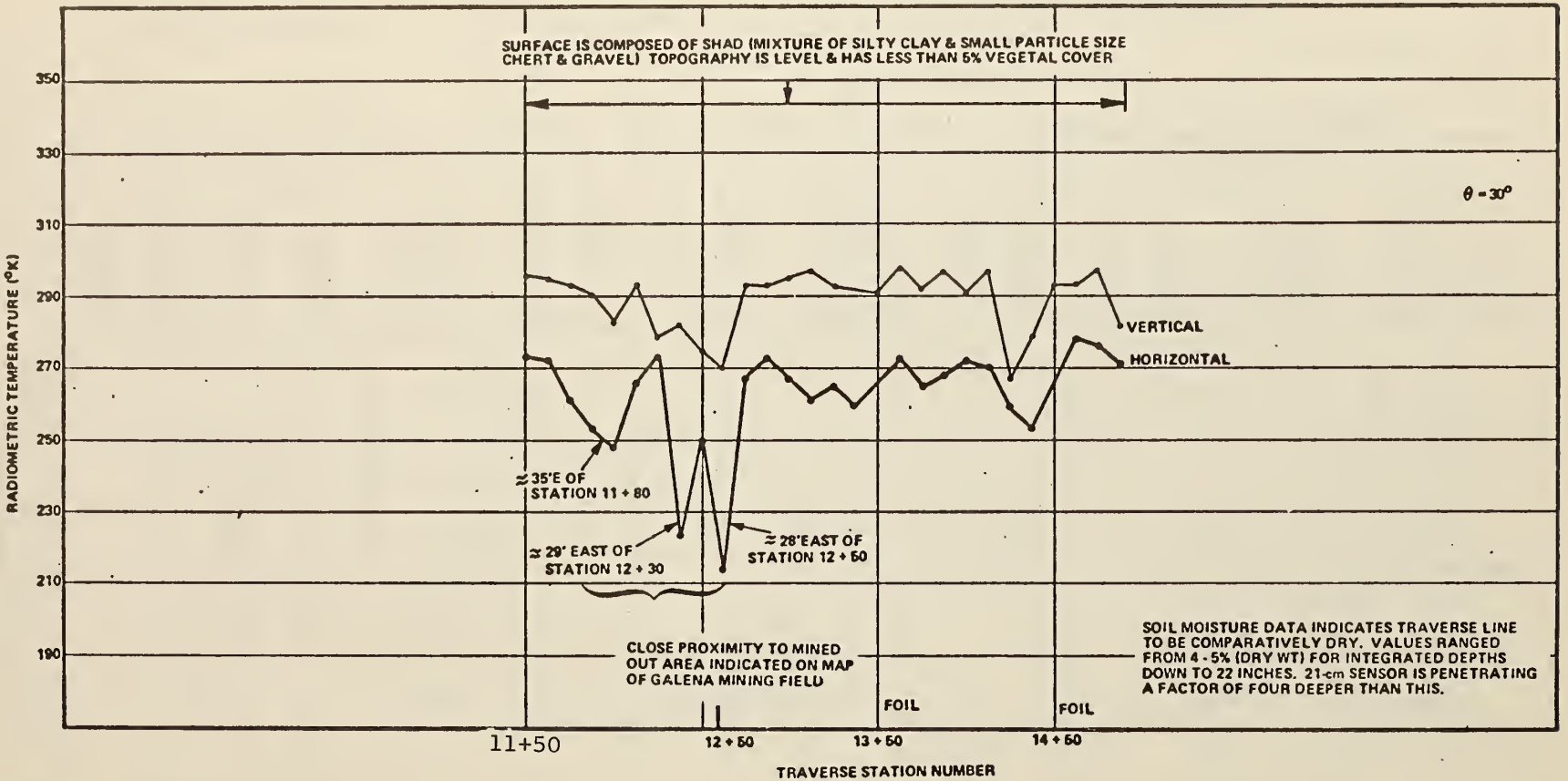

Figure 3.16 21cm Microwave Profile Data for Galena Line C'

is probably responding to a localized area at station 19+75 that exhibits similar bulk physical properties to those contained between stations 12+00 and 16+00.

Additional cool brightness temperature anomalies occur from station 17+00 to station 18+75 on Line A, and at station 14+30 on Line C'. Note the decreased polarization differences exhibited by both anomalies. These radiometric lows indicate (1) a sharp increase in material density with increasing depth, (2) the possible presence of a metallic ore body, or (3) a combination of these two effects. Due to the decrease in polarization, these anomalies do not indicate pronounced increases in soil moisture content.

The highest degree of vegetal cover encountered for both traverse lines existed between stations 13+40 and 13+60 on Line A. Here a 35 percent, 24-inch-hidh grass cover prevailed. Comparing the microwave data corresponding to this area with data obtained from adjacent areas of low vegetal cover, it can be seen that vegetal effects at 21 cm are unimportant for this site. The fact that the 21 cm radiometer did not respond to the high 0-32 cm moisture content at Line A, station 13+00 is attributed to beam smear encountered when viewing narrow features with the 15° field of view of this sensor.

In summary, the large 21 cm microwave anomalies that occur at stations 11+80, and between stations 12+25 and 12+60 for Line C' were the only features indicative of potential subsidence situations for this site. The anomalies exhibit direct point-to-point correlation to known areas of underground mining activity and are believed to result from subtle changes in the overburden moisture properties due to the presence of water-filled subsur-ace voids. This interpretation can be substantiated by (1) subsequent failure of the terrain surface in the indicated areas, or (2) by drilling core holes in the vicinity

of the anomalous 21 cm responses. The analysis concerning this site was based mostly on the diagnostic character exhibited by the microwave profile data. Unfortunately, like the Scammon site, the available ground truth information concerning this site is not representative of the brightness temperature anomalies that occurred and consequently, a direct point-to-point correlation of the physical data to the radiometric responses could not be made.

3.5 Galena Line D

The Galena site Line D data were collected on August 15, 1971 under clear skys between 14:05 and 14:42. Approximately 800 feet of data were collected with aluminum foil markers every 100 feet. Ground moisture down to 8 centimeters were low, and ground temperatures relatively high. Similar to the other sites, ground truth was obtained shortly after collection of remotely sensed data. These are given in Table 3-4.

Moisture and temperature characteristics of the soil (Figure 3.17) are stratified nicely. Percentages of moisture remain nearly constant in the upper 8 centimeters but fluctuate broadly at 16 and 32 centimeters. Although the inverse relationship between soil moisture and ground temperature generally holds (moisture increases with depth, temperature decreases with depth) exceptions occur in three stations.

Stations 14+50 and 17+50 are characterized by large perturbations in moisture profile at 32 centimeters, but a nearly constant temperature. The expected increase in ground temperature does not occur. At station 15+50, temperatures drop at the 2 centimeter level with no corresponding rise in soil moisture.

Wet and dry bulk densities show a prominent perturbation downward at Station 16+50 and no obvious correlation with either ground temperature or percentage moisture.

TABLE 3-4 GROUND TRUTH DATA GALENA SITE LINE D

Station	Dist. ℄ Truck	Sample Number	Depth (Cm.)	Percent Moisture	Average Temp.	Wet Density (pcf)	% Moisture @ 32 (Cm.)	Dry Density (pcf)
					Surface 313.4			
19+50	5'N	NA-25	2	1.8	310.9	* 112.0	* 13.3	98.8
		NB-25	4	7.2	309.7			
		NC-25	8	5.5	306.7			
		ND-25	16	13.3	304.4			
		NE-25	32	----	301.6			
					Surface 319.1			
19+50	5'S	SA-25	2	3.0	310.7	105.0	13.1	92.8
		SB-25	4	4.9	308.1			
		SC-25	8	8.0	306.0			
		SD-25	16	10.6	304.4			
		SE-25	32	13.1	302.4			
18+50	5'N	NA-26	2	1.4	36.0	* 111.5	* 8.3	102.9
		NB-26	4	3.0	33.8			
		NC-26	8	6.6	32.8			
		ND-26	16	8.3	31.5			
					Surface 321.2			
18+50	5'S	SA-26	2	.8	315.1	116.0	12.9	102.7
		SB-26	4	1.6	312.3			
		SC-26	8	5.6	309.2			
		SD-26	16	7.4	306.3			
		SE-26	32	12.9	301.9			
17+50	5'N	NA-27	2	1.2	36.5	* 119.5	* 10.1	108.5
		NB-27	4	4.9	36.5			
		NC-27	8	5.4	36.1			
		ND-27	16	10.1	31.7			
					Surface 320.6			
17+50	5'S	SA-27	2	.8	318.2	106.5	7.0	99.5
		SB-27	4	1.2	315.3			
		SC-27	8	1.4	309.3			
		SD-27	16	6.5	306.2			
		SE-27	32	7.0	302.7			

TABLE 3-4 GROUND TRUTH DATA GALENA SITE LINE D
(Continued)

Station	Dist. ℄ Truck	Sample Number	Depth (Cm.)	Percent Moisture	Average Temp.	Wet Density (pcf)	% Moisture @ 32 (Cm.)	Dry Density (pcf)
16+50	5'N	NA-28	2	2.1	36.8	* 93.75	* 10.2	85.1
		NB-28	4	2.0	35.4			
		NC-28	8	4.9	33.2			
		ND-28	16	10.2	29.9			
				Surface	44.4			
16+50	5'S	SA-28	2	1.4	36.0	94.0	12.3	83.7
		SB-28	4	3.0	34.1			
		SC-28	8	4.5	32.4			
		SD-28	16	7.9	29.9			
		SE-28	32	12.3	26.8			
15+50	5'N	NA-29	2	1.6	29.8	*112.0	* 4.7	107.0
		NB-29	4	3.2	29.8			
		NC-29	8	2.7	28.9			
		ND-29	16	4.7	28.1			
				Surface	40.0			
15+50	5'S	SA-29	2	2.7	29.4	106.75	14.1	93.6
		SB-29	4	3.6	27.6			
		SC-29	8	7.1	26.3			
		SD-29	16	6.3	26.0			
		SE-29	32	14.1	24.7			
14+50	5'N	NA-30	2	2.9	34.8	* 88.5	* 5.4	83.7
		NB-30	4	4.1	33.9			
		NC-30	8	4.8	32.8			
		ND-30	16	5.4	29.0			
				Surface	39.0			
14+50	5'S	SA-30	2	4.9	35.9	113.5	5.9	107.2
		SB-30	4	4.9	34.2			
		SC-30	8	6.1	31.5			
		SD-30	16	5.4	29.3			
		SE-30	32	5.9	26.4			

TABLE 3-4 GROUND TRUTH DATA GALENA SITE LINE D
(Continued)

Station	Dist. ℄ Truck	Sample Number	Depth (Cm.)	Percent Moisture	Average Temp.	Wet Density (pcf)	% Moisture @ 32 (Cm.)	Dry Density (pcf)
13+50	5'N	NA-31	2	1.7	35.6	*92.75	* 9.1	8[illegible].0
		NB-31	4	1.5	34.5			
		NC-31	8	7.1	33.4			
		ND-31	16	9.1	29.8			
				Surface	40.4			
13+50	5'S	SA-31	2	4.1	36.0	106.5	17.1	90.9
		SB-31	4	11.6	33.8			
		SC-31	8	11.7	32.2			
		SD-31	16	15.1	30.5			
		SE-31	32	17.1	26.9			
12+50	5'N	NA-32	2	4.3	34.0	*107.5	* 7.9	99.6
		NB-32	4	4.0	33.4			
		NC-32	8	5.9	30.1			
		ND-32	16	7.9	28.1			
				Surface	42.7			
12+50	5'S	SA-32	2	2.6	35.7	97.5	13.9	85.4
		SB-32	4	3.6	34.6			
		SC-32	8	8.1	31.6			
		SD-32	16	10.3	29.5			
		SE-32	32	13.9	26.4			
11+50	5'N	NA-33	2	.9	37.4	*108.0	* 3.2	104.7
		NB-32	4	2.2	36.5			
		NC-32	8	2.1	34.4			
		ND-32	16	3.2	33.1			
				Surface	41.4			
11+50	5'S	SA-33	2	1.8	36.1	90.75	7.7	84.3
		SB-33	4	2.5	35.2			
		SC-33	8	2.7	33.4			
		SD-33	16	6.3	32.0			
		SE-33	32	7.7	28.4			

TABLE 3-4 GROUND TRUTH DATA GALENA SITE LINE D
(Continued)

Station	Dist. ℄ Truck	Sample Number	Depth (Cm.)	Percent Moisture	Average Temp.	Wet Density (pcf)	% Moisture @ 32 (Cm.)	Dry Density (pcf)
10+50	5'N	NA-34	2	.5	No Temp.	* 108.0	* 3.6	104.2
		NB-34	4	.4				
		NC-34	8	.9				
		ND-34	16	3.6				
10+50	5'S	SA-34	2	1.4	33.6	103.25	8.4	95.2
		SB-34	4	2.2	32.7			
		SC-34	8	1.6	30.3			
		SD-34	16	4.3	28.2			
		SE-34	32	8.4	26.6			

NOTES: *These densities are computed from the moisture content at 16 Cm..

Temperatures at 19+50, 18+50S, 17+50S are kelvin, all others are centigrade

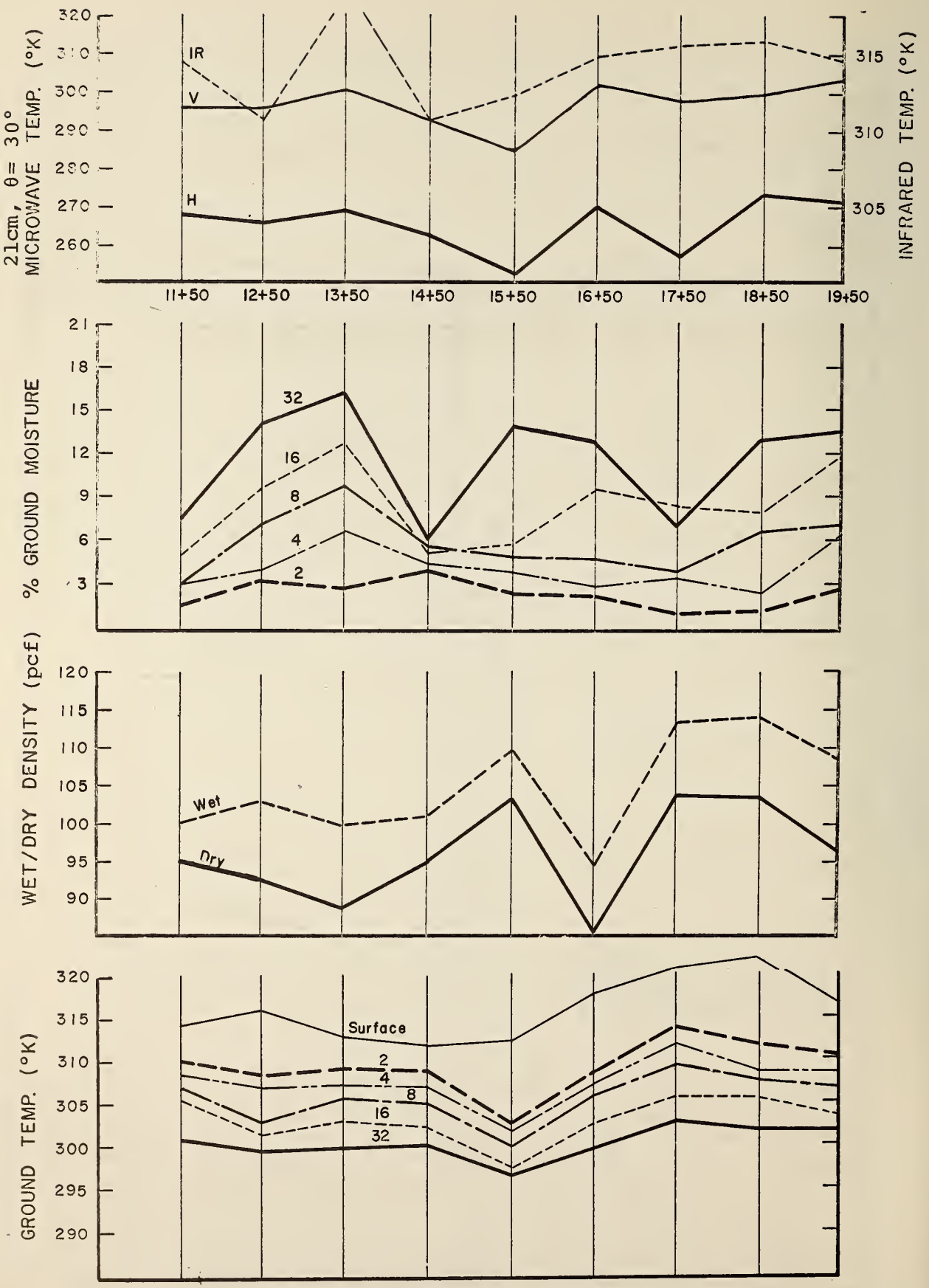

Figure 3.11 Correlation of Measurements
Galena D

The L Band microwave response along Galena Line D (Figure 3.18) does not possess the consistency characterized by moisture in the upper strata of the line nor the fluctuation occurring at depth. Because the upper soil strata are relatively dry the assumption apparently holds that emissions from greater depths are sensed, however, at 32 centimeters percentage soil moistures nearly equal those of Scammon Line A. Thus, the expected drop in antenna temperatures over "wet" spots does not occur.

Unlike correspondence with moisture, visual correspondence with ground temperatures (particularly 2 cm depth) is high. The single exception occurs at Station 17+50 where antenna temperatures drop in the horizontal polarization.

The reason for the exception is not apparent on the data, however, the drop at 17+50 is part of a downward trend which reaches a low 230°K at about 18+00 (Figure 3.18). An anomaly of this magnitude normally corresponds with an aluminum foil but as is obvious on Figure 3.18, the foil is placed at Station 18+50 and the anomaly at 18+00 corresponds with some unrecognized natural or man induced phenomenon.

Between Station 14+50 and 19+50, relatively good correlation in IR temperature with surface ground temperatures occurs, however, parameters other than soil moisture, temperature or density apparently perturb the IR signal between 11+50 and 14+50 where no correspondence is evident.

As in most other lines in the study area, only tenuous correspondence between the remotely sensed signals and soil density is indicated in the data. At best along Galena Line D correspondence occurs between near surface ground temperatures and the remotely sensed signals. No reflection of soil moisture conditions in the microwave signal is obvious.

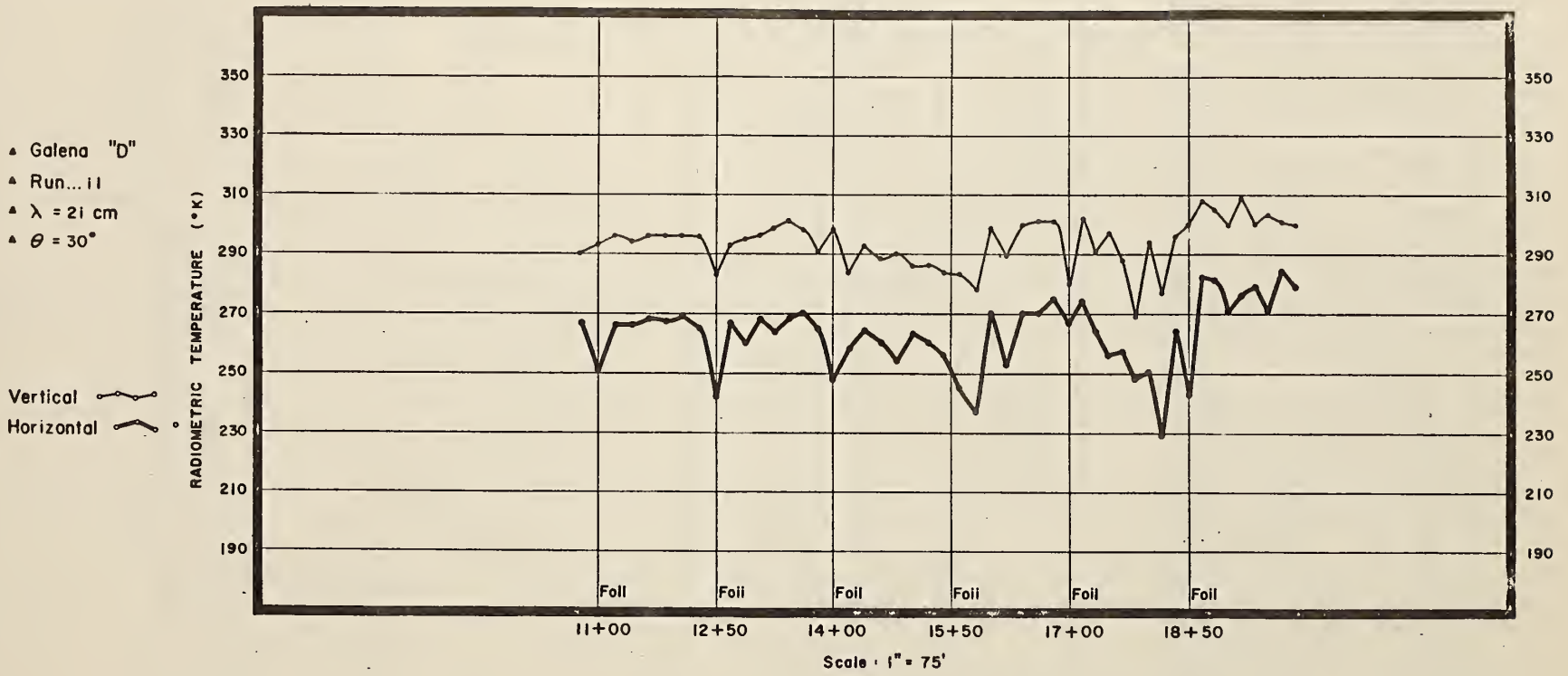

Figure 3.18 Microwave Profile - Galena Line D

3.6 Galena Line E

Galena Line E consists of approximately 350 feet with four ground truth stations spaced 100 feet apart. The 21 cm, 30° look angle data were captured between 12:31 and 12:52 on Sugust 15, 1971. Table 3-5 details the ground measurements data.

General correspondence with previous lines exists in the inverse relationship between ground moisture and ground temperature (Figure 3.19). The relationship is especially strong in the upper few centimeters and like Galena Line D, the relationship breaks down at the greater depths.

Perturbations in the microwave signal cause a range in antenna temperatures of about 20°K (Figure 3.20). Correspondence between antenna temperatures and soil moisture and ground temperatures follows expected trends for the four ground truth stations. Where soil moisture decreases, antenna temperatures increase. Whether or not this relationship is related casually or happened by chance cannot be determined from the four stations above. It is apparent from other lines, however, that this strong a M.W. response to moisture is not typical.

For reasons which are not apparent in the ground truth, the IR temperatures show a decrease where ground temperatures at the surface and at 2 cm increase (Station 12+50) and conversely an increase in temperature where soil moisture increases. This IR response is not entirely compatible with the results of previous studies and does not agree with basic physical theory.

Finally, rough correspondence at Stations 13+50 -- 11+50 occurs between the microwave signal and the dry bulk density which increases at Station 12+50, however, the correspondence of three points is insufficient to draw any definitive conclusions.

TABLE 3-5 GROUND TRUTH DATA GALENA SITE LINE E

Station	Dist. ℄ Truck	Sample Number	Depth (Cm.)	Percent Moisture	Average Temp.	Wet Density (pcf)	% Moisture @ 32 (Cm.)	Dry Density (pcf)
					Surface 317.5	103.5	6.8	96.9
10+50	5'E	EA-21	2	1.2	312.4			
		EB-21	4	4.8	307.7			
		EC-21	8	7.7	305.7			
		ED-21	16	8.1	303.8			
		EE-21	32	6.8	302.0			
					Surface 319.9			
10+50	5'W	WA-21	2	.9	311.7	116.0	9.9	105.6
		WB-21	4	2.0	309.0			
		WC-21	8	6.0	305.3			
		WD-21	16	9.4	303.0			
		WE-21	32	9.9	301.1			
					Surface 325.8			
11+50	5'E	EA-22	2	1.8	314.7	113.5	14.1	99.4
		EB-22	4	2.5	311.0			
		EC-22	8	3.9	306.5			
		ED-22	16	4.2	302.3			
		EE-22	32	14.1	300.5			
					Surface 329.2			
11+50	5'W	WA-22	2	3.2	308.2	118.5	10.3	107.4
		WB-22	4	2.9	304.4			
		WC-22	8	5.4	303.4			
		WD-22	16	6.0	301.2			
		WE-22	32	10.3	300.1			
					Surface 328.8			
12+50	5'E	EA-23	2	1.1	310.0	115.5	7.5	107.4
		EB-23	4	2.8	307.1			
		EC-23	8	4.7	306.1			
		ED-23	16	4.7	303.8			
		EE-23	32	7.5	301.7			

TABLE 3-5 GROUND TRUTH DATA GALENA SITE LINE E
(Continued)

Station	Dist. ℄ Truck	Sample Number	Depth (Cm.)	Percent Moisture	Average Temp.	Wet Density (pcf)	% Moisture @ 32 (Cm.)	Dry Density (pcf)
					Surface 327.1			
12+50	5'W	WA-23	2	1.5	316.4	110.0	7.1	102.7
		WB-23	4	2.1	312.9			
		WC-23	8	4.6	307.5			
		WD-23	16	7.2	303.0			
		WE-23	32	7.1	300.1			
					Surface 318.4			
13+50	5'E	EA-24	2	4.1	309.8	118.5	12.4	105.4
		EB-24	4	3.8	307.8			
		EC-24	8	7.8	303.6			
		ED-24	16	8.4	301.3			
		EE-24	32	12.4	300.7			
					Surface 314.9			
13+50	5'W	WA-24	2	1.9	314.1	107.5	10.4	97.3
		WB-24	4	2.2	311.3			
		WC-24	8	4.5	308.8			
		WD-24	16	7.8	303.9			
		WE-24	32	10.4	301.1			

NOTES: Temperatures on this project are kelvin.

All densities are taken with a nuclear densitometer (12" Probe).

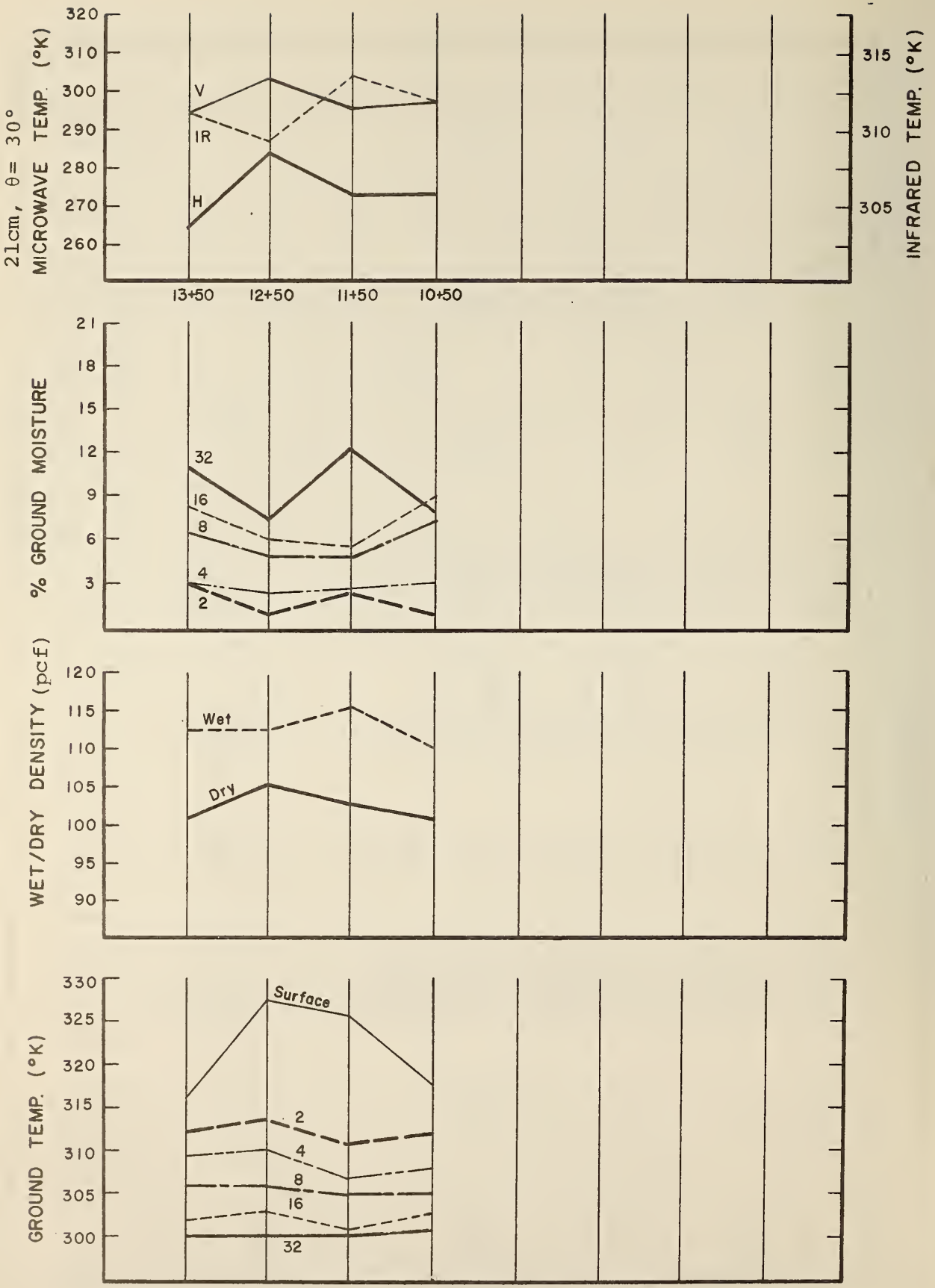

Figure 3.19 Correlation of Measurements Galena Line E

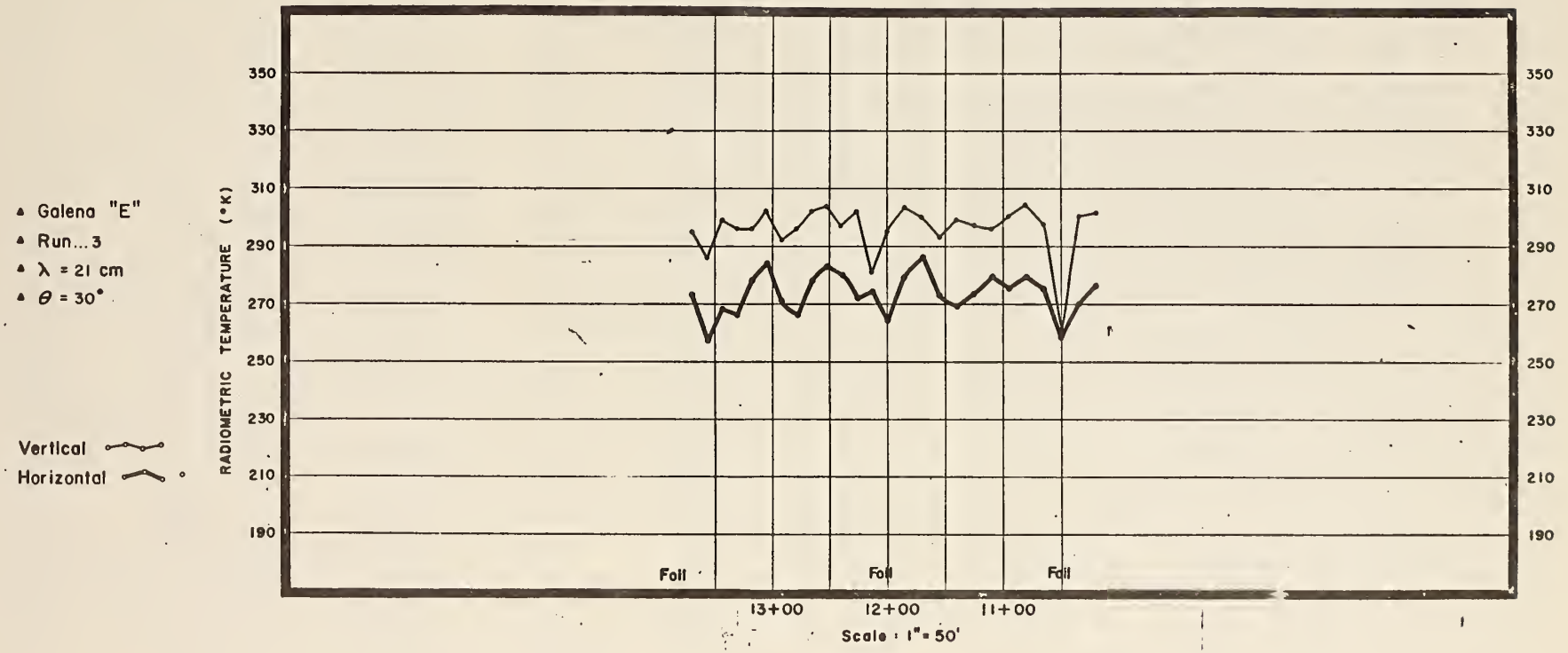

Figure 3.20 Microwave Profile - Galena Line E

3.7 Clay County Lines C and D

L Band radiometer data at 30° look angle for Clay County Lines C & D were collected between 15:98 and 16:25, and 16:87 and 17:11 respectively on August 22, 1971. The sky was clear and all radiometers were functioning properly. Although most ground truth data were collected shortly after sensing was completed, ground temperature for the surface 2 cm, 4 cm, and 8 cm depths were not collected. These data are compiled in Table 3-6. Clay County Line C has 3 ground truth stations and Line D has 4 ground truth stations. In both cases the stations are irregularly spaced (Figure 3.21 and Figure 3.22).

Relationships between ground parameters at the Clay County Sites are not unlike those depicted at the Scammon and Galena sites. The inverse soil temperature/soil moisture relationship is indicated although heat stratification of percentage moisture occurring at other lines appears somewhat distorted at Stations 188+50, 190+00, 195+00, 210+40.

Fluctuations in the radiometric signal at Line C range approximately 20°K, (Figure 3.23) much like previously noted sites, however, that range at Line D is on the order of 40°K (Figure 3.24). Further, whereas the trend in antenna temperature between 186+00 and 192+00 shows a slight increase (1.5°K per 100') the trend between 207+00 and 213+00 shows a dramatic rise of 4°K per 100 feet.

Referring to the trends in antenna temperatures to soil conditions, Line C shows a prominent upward perturbation at about 188+25 followed by a downward trend to Station 189+00. This roughly corresponds in space to the decrease in moisture at 188+80 and the rise at 190+00 thus suggesting a slight spatial offset in the microwave signal. The trend in soil moisture which can be deduced from the 4 stations in C however shows no steady decrease as would be expected if soil moisture had a

TABLE 3-6 GROUND TRUTH DATA CLAY COUNTY K-82

Station	Dist. ℄ Truck	Sample Number	Depth (Cm.)	Percent Moisture	Average Temp.	Wet Density (pcf)	% Moisture @ 32 (Cm.)	Dry Density (pcf)
115+00	℄	CA-97	2	8.0		110	15.6	95.1
		CB-97	4	10.8				
		CC-97	8	10.2				
		CD-97	16	13.3	28.5			
		CE-97	32	15.6	26.1			
116+80	℄	CA-100	2	3.2		104.5	14.2	91.5
		CB-100	4	9.1				
		CC-100	8	9.8				
		CD-100	16	13.5	30.9			
		CE-100	32	14.2	27.5			
120+00	℄	CA-96	2	4.2		98.25	15.6	85.0
		CB-96	4	7.5				
		CC-96	8	10.0				
		CD-96	16	11.0	30.6			
		CE-96	32	15.6	27.5			
125+00	℄	CA-95	2	6.5		98.5	15.7	85.1
		CB-95	4	10.4				
		CC-95	8	12.0				
		CD-95	16	13.8	26.2			
		CE-95	32	15.7	24.8			
130+00	℄	CA-94	2	7.3		102.25	14.2	89.5
		CB-94	4	9.6				
		CC-94	8	9.7				
		CD-94	16	11.5	26.2			
		CE-94	32	14.2	25.0			
140+00	℄	CA-92	2	10.8		93.75	15.5	81.2
		CB-92	4	11.6				
		CC-92	8	12.5				
		CD-92	16	13.9	24.5			
		CE-92	32	15.5	23.5			

TABLE 3-6 GROUND TRUTH DATA CLAY COUNTY K-82
(Continued)

Station	Dist. & Truck	Sample Number	Depth (Cm.)	Percent Moisture	Average Temp.	Wet Density (pcf)	% Moisture @ 32 (Cm.)	Dry Density (pcf)
145+00	&	CA-91	2	8.8		103.0	16.0	88.8
		CB-91	4	9.1				
		CC-91	8	10.3				
		CD-91	16	12.7	27.5			
		CE-91	32	16.0	25.1			
150+00	&	CA-90	2	4.8		103.0	10.2	93.5
		CB-90	4	9.6				
		CC-90	8	11.5				
		DC-90	16	12.9	27.2			
		CE-90	32	10.2	25.5			
155+00	&	CA-89	2	6.1		91.0	13.8	80.0
		CB-89	4	8.1				
		CC-89	8	9.5				
		CD-89	16	12.5	26.5			
		CE-89	32	13.8	24.7			
160+00	&	CA-88	2	7.3		99.5	14.2	87.1
		CB-88	4	9.3				
		CC-88	8	10.6				
		CD-88	16	13.8	28.6			
		CE-88	32	14.2	26.1			
165+00	&	CA-87	2	7.2		106.75	12.6	94.8
		CB-87	4	9.6				
		CC-87	8	10.2				
		CD-87	16	12.6	28.4			
		CE-87	32	12.6	26.0			
170+00	&	CA-86	2	3.2		102.25	11.0	92.1
		CB-86	4	5.5				
		CC-86	8	4.5				
		CD-86	16	9.4	27.5			
		CE-86	32	11.0	26.4			

TABLE 3-6 GROUND TRUTH DATA CLAY COUNTY K-82
(Continued)

Station	Dist. ℄ Truck	Sample Number	Depth (Cm.)	Percent Moisture	Average Temp.	Wet Density (pcf)	% Moisture @ 32 (Cm.)	Dry Density (pcf)
175+00	℄	CA-85	2	3.5		101.0	12.8	89.5
		CB-85	4	5.1				
		CC-85	8	7.4				
		CD-85	16	9.4	28.5			
		CE-85	32	12.8	26.5			
180+00	℄	CA-84	2	3.7		105.0	12.0	93.8
		CB-84	4	5.7				
		CC-84	8	7.4				
		CD-84	16	10.6	28.7			
		CE-84	32	12.0	26.5			
185.00	℄	CA-83	2	6.7		110.5	14.0	96.9
		CB-83	4	11.3				
		CC-83	8	11.1				
		CD-83	16	13.3	28.0			
		CE-83	32	14.0	26.2			
188+80	℄	CA-99	2	1.7		108.0	12.5	96.0
		CB-99	4	7.4				
		CC-99	8	9.4				
		CD-99	16	12.1	31.6			
		CE-99	32	12.5	28.3			
190+00	℄	CA-82	2	9.2		107.0	14.8	93.2
		CB-82	4	13.5				
		CC-82	8	11.2				
		CD-82	16	12.7	27.0			
		CE-82	32	14.8	25.8			
195+00	℄	CA-81	2	5.7		100.75	13.7	88.6
		CB-81	4	6.8				
		CC-81	8	8.7				
		CD-81	16	14.2	28.0			
		CE-81	32	13.7	27.1			

TABLE 3-6 GROUND TRUTH DATA CLAY COUNTY K-82
(Continued)

Station	Dist. ℄ Truck	Sample Number	Depth (Cm.)	Percent Moisture	Average Temp.	Wet Density (pcf)	% Moisture @ 32 (Cm.)	Dry Density (pcf)
200+00	℄	CA-80	2	8.2		96.5	12.1	86.1
		CB-80	4	10.1				
		CC-80	8	10.4				
		CD-80	16	12.5	29.0			
		CE-80	32	12.1	27.0			
205+00	℄	CA-79	2	5.5		109.5	12.4	97.4
		CB-79	4	5.7				
		CC-79	8	7.1				
		CD-79	16	9.1	27.4			
		CE-79	32	12.4	26.3			
210+00	℄	CA-78	2	6.0		101.5	11.8	90.8
		CB-78	4	4.7				
		CC-78	8	8.5				
		CD-78	16	11.9	28.0			
		CE-78	32	11.8	26.8			
210+40	℄	CA-98	2	5.2		100.5	14.9	87.5
		CB-98	4	6.8				
		CC-98	8	7.6				
		CD-98	16	10.2	29.7			
		CE-98	32	14.9	26.5			

NOTES: Temperatures on this project are centigrade (not averaged).

All test sites are approximately 20' Lt. of ℄ K-82.

All densities are taken with a nuclear densitometer (12" Probe).

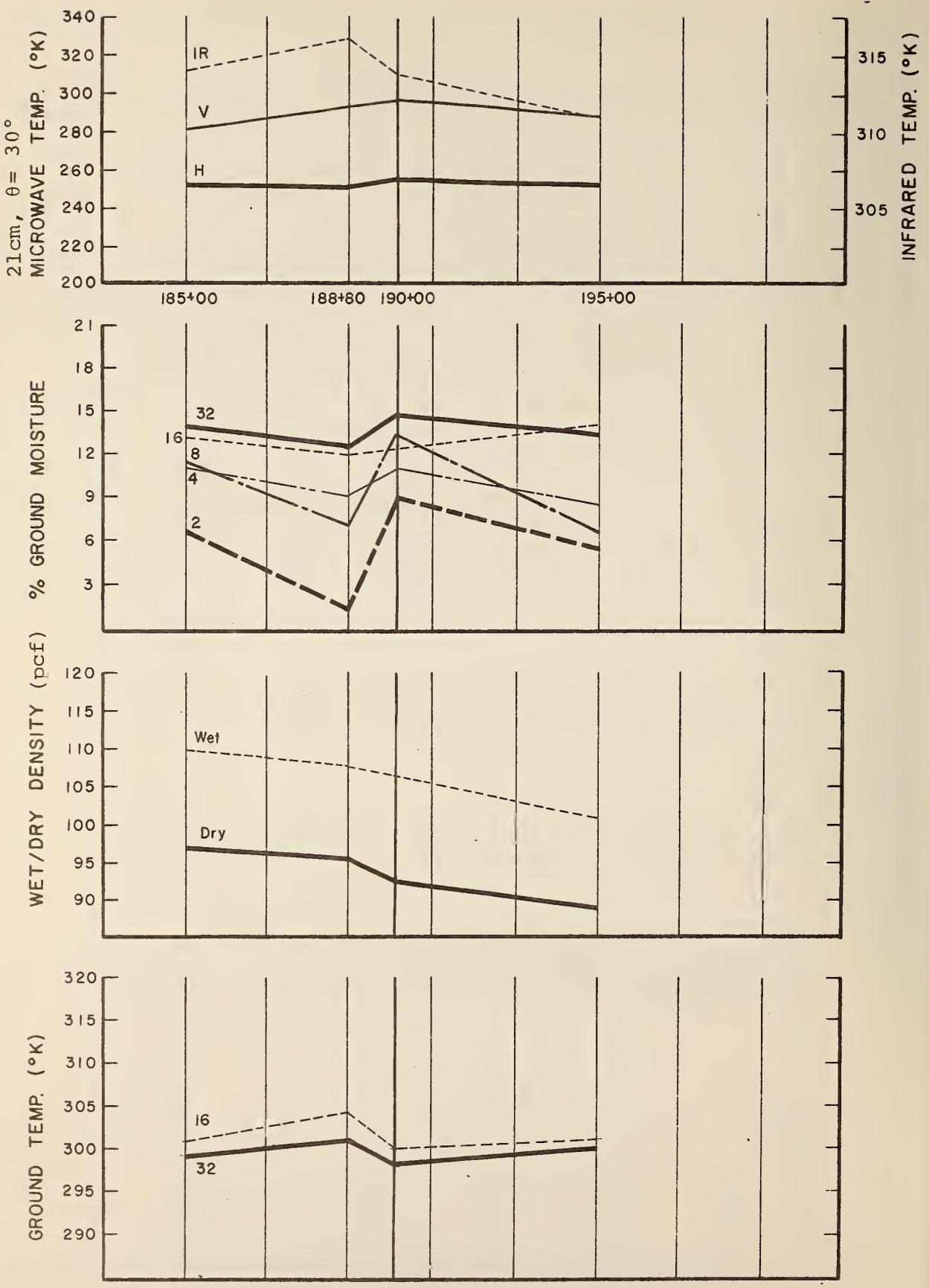

Figure 3.21 Correlation of Measurements Clay County D

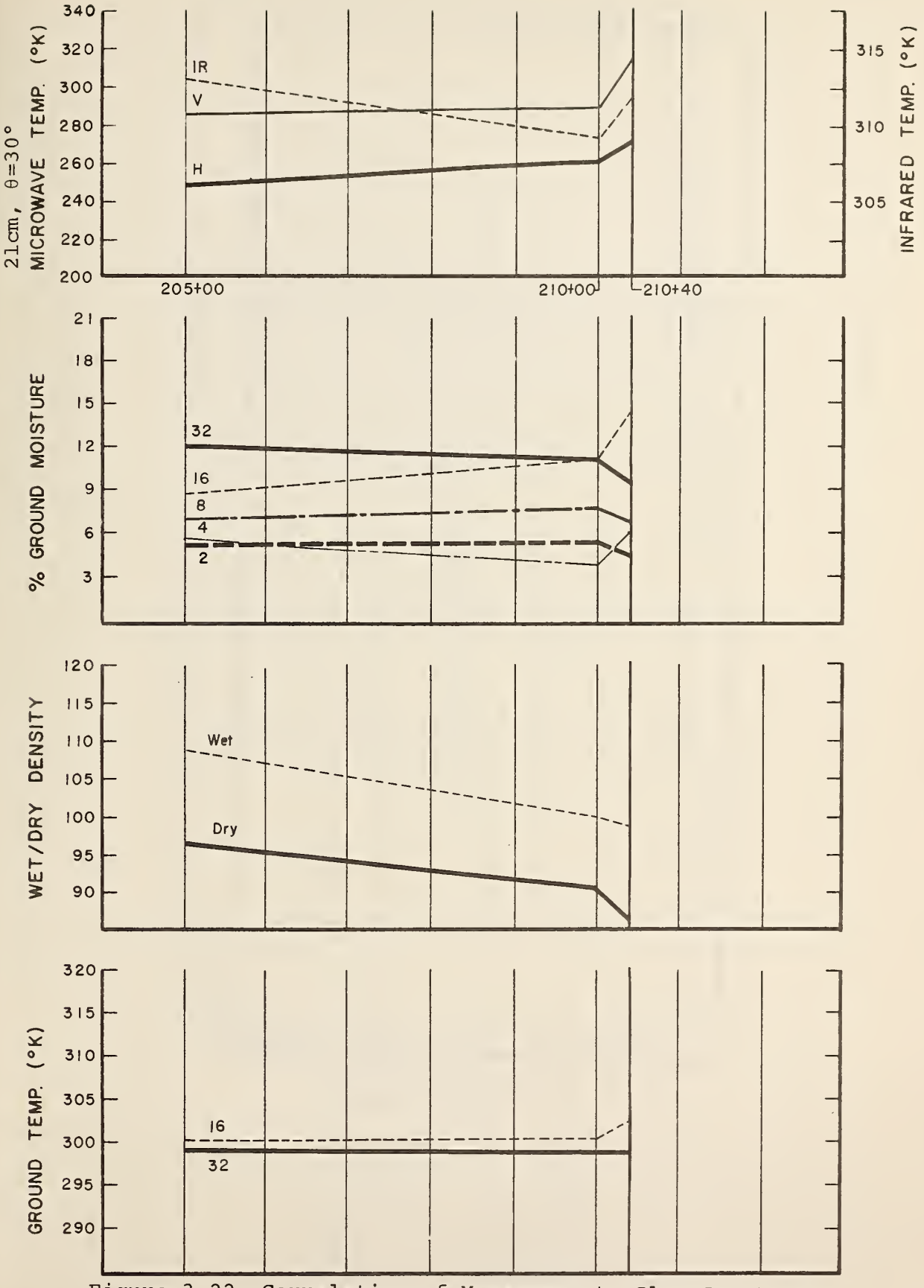

Figure 3.22 Correlation of Measurements Clay County D

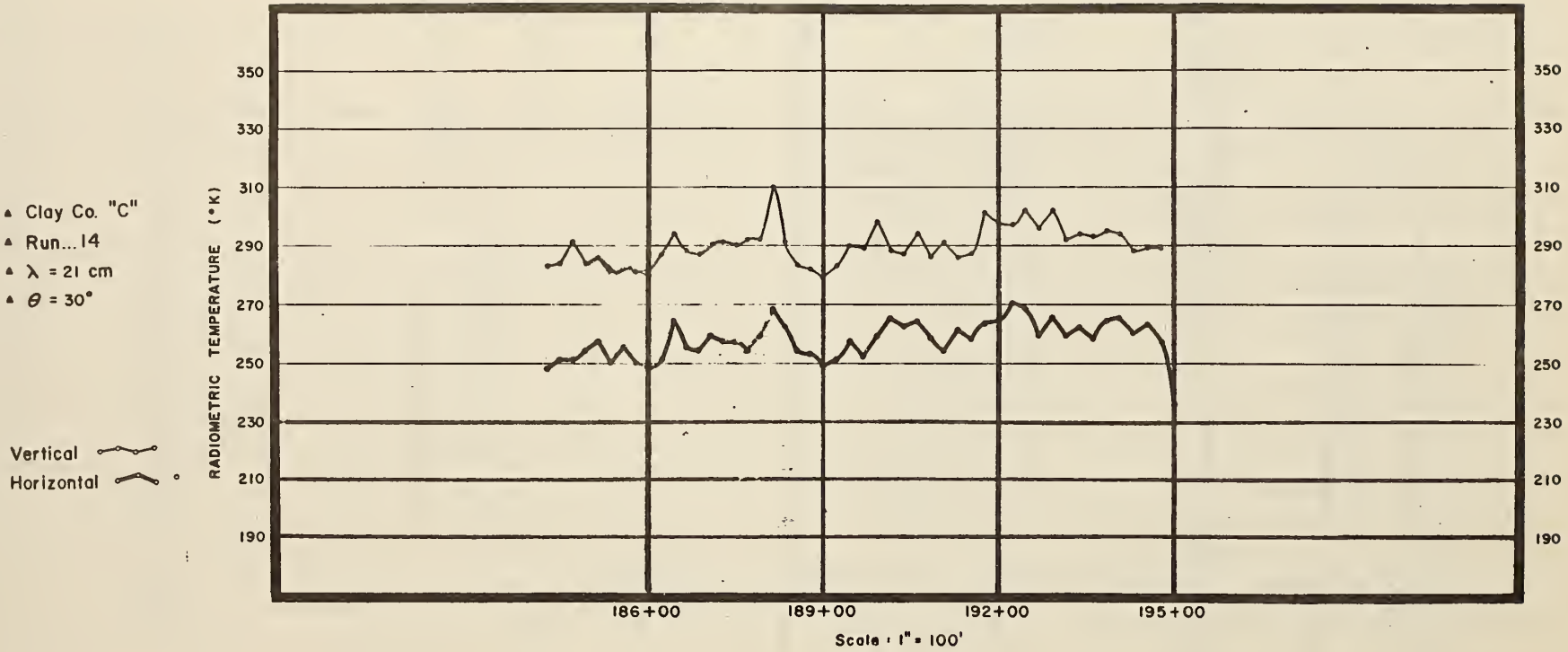

Figure 3.23 Microwave Profile - Clay County Line C

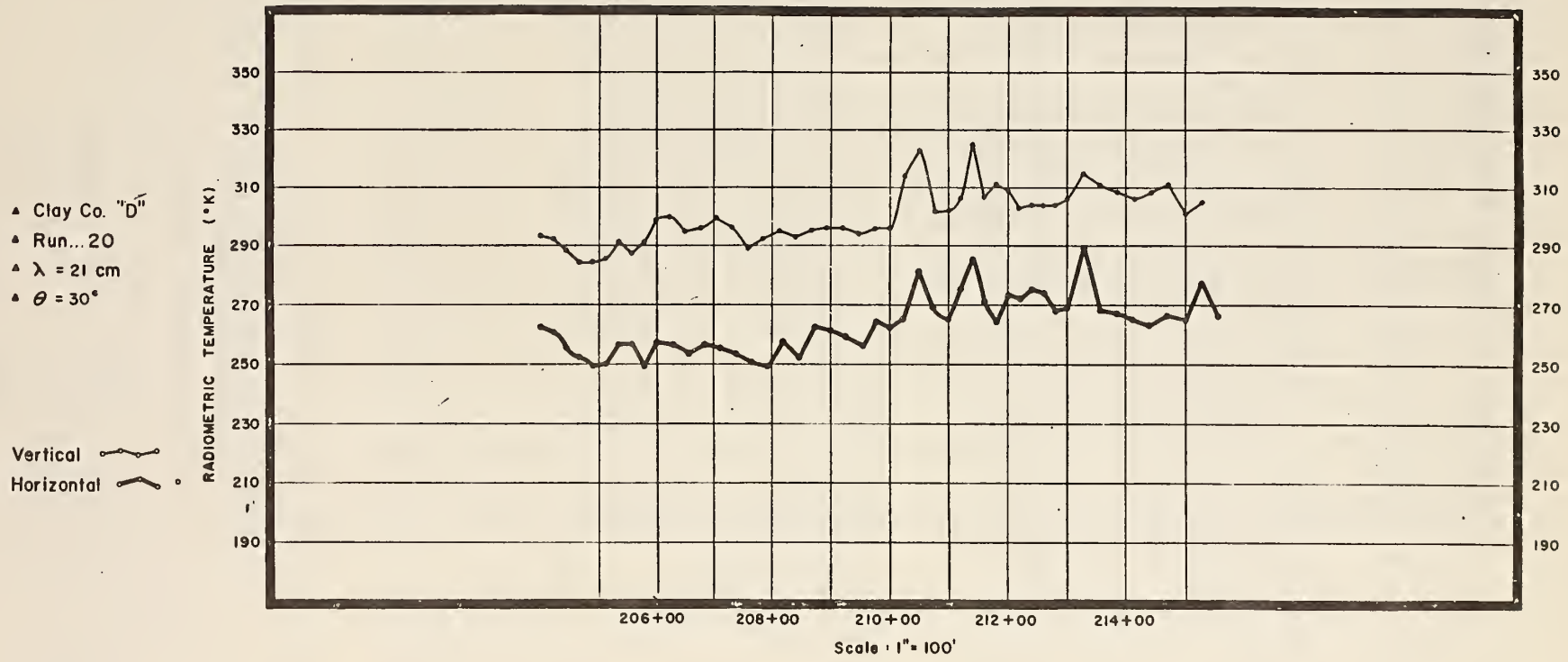

Figure 3.24 Microwave Profile - Clay County Line D

significantly large effect on microwave emissions. Similarly, Line D, where the increase in antenna temperatures exceeds that of Line C, no prominent downward trend in soil moisture is obvious.

Interestingly, a downward trend in wet and dry bulk density measurements occurs in both Clay County Lines suggesting a potential dependency of the L Band signal on that soil parameter. Like the Galena Line E example, this conclusion is based on relatively few stations and is not apparent on better documented lines.

In summary, the Clay County L Band radiometric data show a potential dependency on soil moisture in the upper few centimeters.

3.8 Kansas City Line A

Line A data in the L Band (30° look angle) at the Kansas City Site were collected between 15:01 and 15:25 under clear skies on August 19, 1971. Approximately 400 feet of data were collected over a sparsely vegetated surface. Data from five ground truth stations spaced 100 feet apart provides correlative moisture and temperature measurements, however, no bulk density values were collected. Table 3-7 summarizes the ground truth data.

No extraordinary perturbations occur along the traverse although low antenna temperatures characterize the zone between 1+25 and 2+75 and higher temperatures the remainder of the line.

The larger scale trend depicted in Figure 3.25 is only partially represented in the profile in Figure 3.26 which shows the plot of the horizontal and vertical polarizations of the L Band radiometric data. Nevertheless, correspondence between low antenna temperatures and high soil moisture generally holds. Point-to-point correlations however, do not necessarily show a strong relationship.

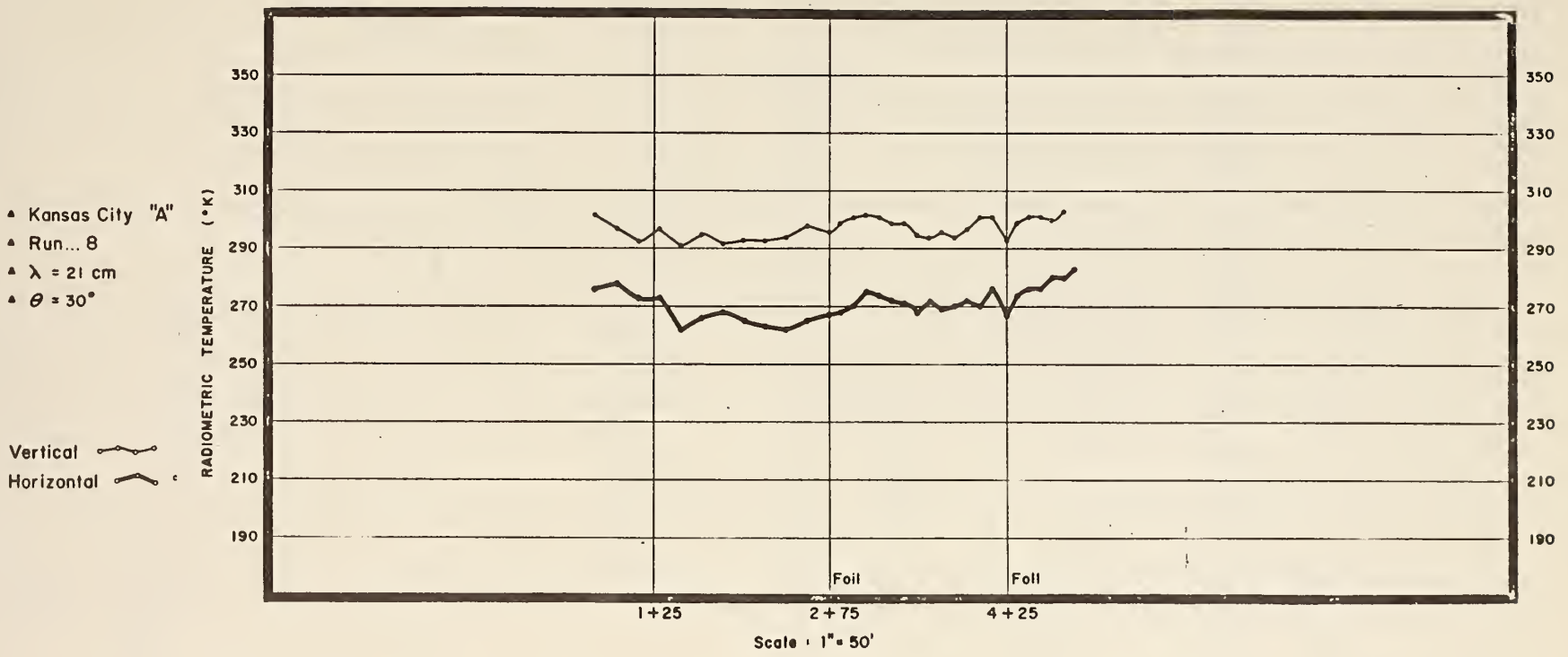

Figure 3.25 Microwave Profile - Kansas City Line A

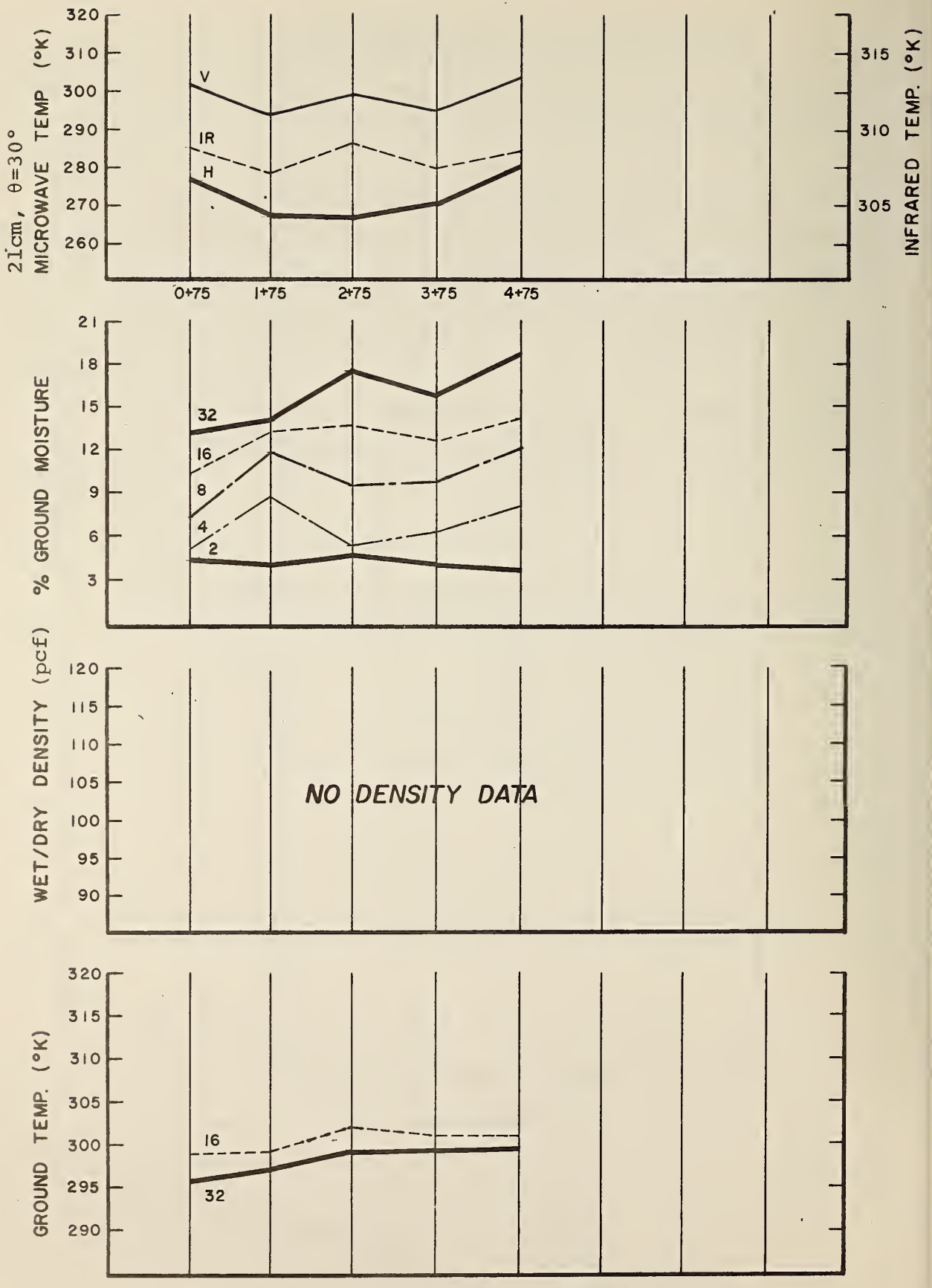

Figure 3.26 Correlation of Measurements

TABLE 3-7 GROUND TRUTH DATA KANSAS CITY SITE LINE A

Station	Dist. ℄ Truck	Sample Number	Depth (Cm.)	Percent Moisture	Average Temp.	Wet Density (pcf)	% Moisture @ 32 (Cm.)	Dry Density (pcf)
0+75	℄	A-66	2	4.0		No densities taken on Line A		
		B-66	4	5.1				
		C-66	8	7.6				
		D-66	16	10.3	25.8			
		E-66	32	12.9	23.5			
1+75	℄	A-67	2	3.7				
		B-67	4	8.9				
		C-67	8	11.8				
		D-67	16	13.1	26.2			
		E-67	32	13.9	24.5			
2+75	℄	A-68	2	4.3				
		B-68	4	5.8				
		C-68	8	9.3				
		D-68	16	13.5	29.0			
		E-68	32	17.8	26.1			
3+75	℄	A-69	2	3.7				
		B-69	4	6.3				
		C-69	8	9.5				
		D-69	16	12.4	28.1			
		E-69	32	15.8	26.2			
4+75	℄	A-70	2	3.5				
		B-70	4	8.2				
		C-70	8	12.0				
		D-70	16	13.9	28.6			
		E-70	32	18.6	26.5			
6+25	℄	A-73	2	4.1				
		B-73	4	7.0				
		C-73	8	10.9				
		D-73	16	18.2	29.2			
		E-73	32	22.0	26.7			

Note: Temperatures on this project are centigrade (not averaged).

Like the Galena sites, the upper soil strata appear relatively dry suggesting that the deeper soil strata provide a source of microwave emission. If this assumption holds then the ground temperatures at 16 and 32 centimeters have their effect on antenna temperatures. Soil temperatures at these depths however indicate relatively minor fluctuations and do vary inversely with soil moisture. Thus correspondence between microwave antenna temperatures and soil temperatures at 16 and 32 centimeters is poor. It is feasible that the upper strata, as in several Galena examples, rather than the deepest stations have the greatest effect on the microwave L Band signal.

Kansas City Lines A, B, and C run parallel to each other and each traverse is known to have crossed the boundary of a large subsurface void. The best estimate of the boundary location is near the midpoint of the profile. Assuming that the existence of a void affects soil conditions of the overburden and these conditions, in turn control microwave emissions, the expected radiometric response is a large scale trend of changing antenna temperatures.

Interestingly, such a large scale trend occurs on the Kansas Line A as noted. Presumably, because of dry ground conditions the Kansas City lines are good samples of the situation. The average antenna temperature to the left of Station 2+75 on Figure 3.26 is approximately 269 and to the right of the same station, approximately 274. Although available ground truth does not allow a definitive cause and effect relationship to be drawn, the contrasting microwave signal at this critical boundary must be acknowledged. Subsequent analysis on Line A should provide important insight to the subsurface void detection problem.

3.9 Kansas City Line B

The L Band signals in both polarizations at Line B show no large deviations from an average value. Perhaps the prime distinction of this line is the consistency in the signal and the small range of fluctuation (Figure 3.27), which is approximately 10°K.

Ground truth for this site is not available and therefore, no correlative analysis with ground parameters was possible. Field notes, however, do indicate that the vegetation at this site was unmowed whereas the same vegetation at Line C located slightly farther north was mowed thus yeilding the possiblity that effects of the vegetal canopy may be deduced.

In contrast with Line A, Line B shows no obvious response to the boundary of the subsurface void. Antenna temperatures average about 275 (horizontal polarization), which, based on Line A data, would indicate that the entire traverse was over the void. This however is not indicated on the map depicting the site location which shows that Line B presumably crosses the boundary of the subsurface void.

3.10 Kansas City Line C

Kansas City Line C data at L Band frequencies, 30° look angle were collected between 17:09 and 17:33 on August 19, 1971. The length of line is approximately 550 feet. Six ground truth stations provide soil moisture measurements and limited ground temperature and bulk density data which correlate in space with the microwave data. These data are given in Table 3-8.

The microvariations in soil parameters (Figures 3.28, 3.29) are similar to those noted at Line A in almost all respects. Like Lines A and B, the traverse of Line C presumably crosses the boundary of the subsurface void. Interestingly, a contrast in soil moisture distribution occurs between Line A and Line C.

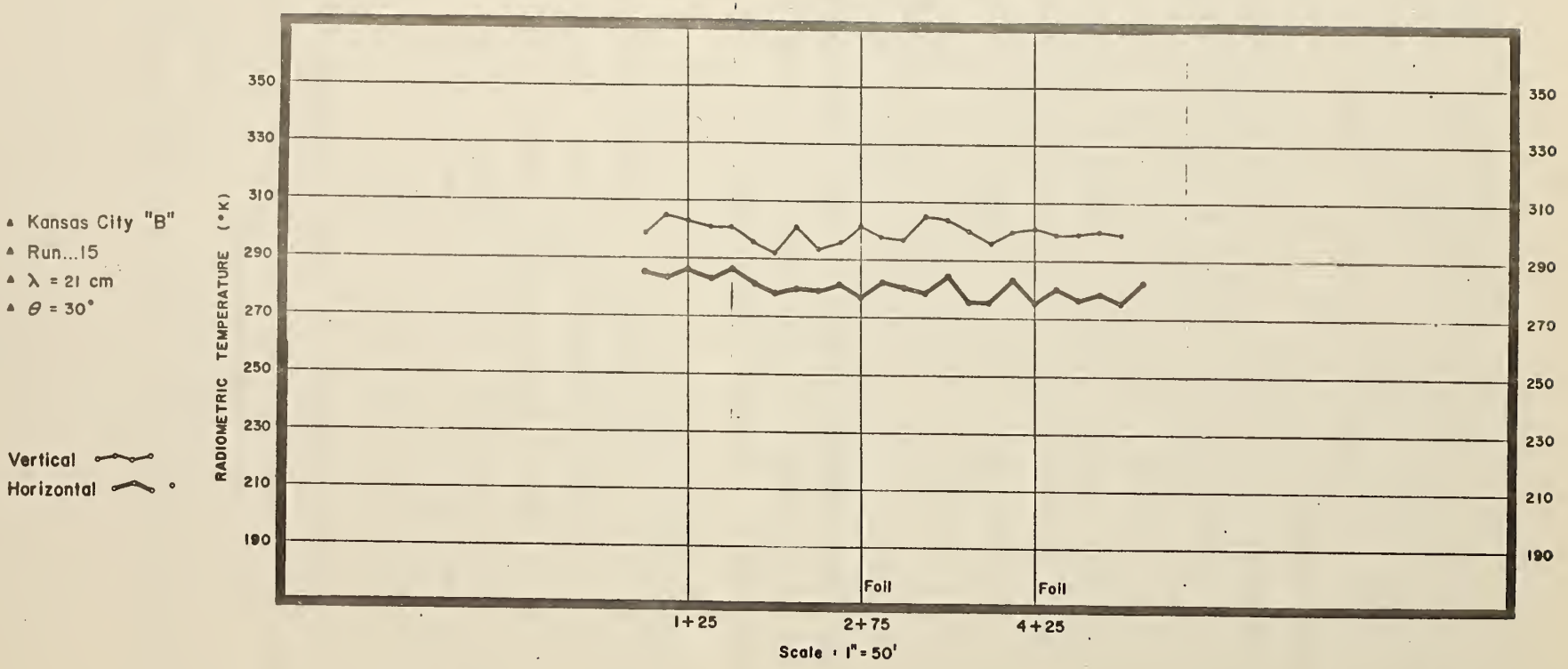

Figure 3.27 Microwave Profile - Kansas City Line B

TABLE 3-8 GROUND TRUTH DATA KANSAS CITY SITE LINE C

Station	Dist. ℄ Truck	Sample Number	Depth (Cm.)	Percent Moisture	Average Temp.	Wet Density (pcf)	% Moisture @ 32 (Cm.)	Dry Density (pcf)
0+75	℄	A-60	2	4.5		91.5	14.4	80.0
		B-60	4	5.0				
		C-60	8	6.3				
		D-60	16	11.1	25.8			
		E-60	32	14.4	23.5			
1+75	℄	A-61	2	4.9		91.0	12.6	80.8
		B-61	4	4.3				
		C-61	8	8.9				
		D-61	16	11.2	24.2			
		E-61	32	12.6	23.9			
2+75	℄	A-62	2	3.0		94.5	13.4	83.3
		B-62	4	6.5				
		C-62	8	6.9				
		D-62	16	10.4	24.4			
		E-62	32	13.4	23.0			
3+75	℄	A-63	2	3.4		99.25	11.6	88.9
		B-63	4	4.0				
		C-63	8	5.3				
		D-63	16	10.2	27.4			
		E-63	32	11.6	25.7			
4+75	℄	A-64	2	3.9				
		B-64	4	4.2				
		C-64	8	8.8				
		D-64	16	10.2	26.4			
		E-64	32	15.2	25.4			
5+75	℄	A-65	2	2.8				
		B-65	4	6.6				
		C-65	8	8.1				
		D-65	16	10.5	26.2			
		E-65	32	12.9	25.3			

TABLE 3-8 GROUND TRUTH DATA KANSAS CITY SITE LINE C
(Continued)

Station	Dist. ℄ Truck	Sample Number	Depth (Cm.)	Percent Moisture	Average Temp.	Wet Density (pcf)	% Moisture @ 32 (Cm.)	Dry Density (pcf)
6+25	℄	A-71	2	3.2				
		B-71	4	6.7				
		C-71	8	8.3				
		D-71	16	9.5	26.8			
		E-71	32	12.4	25.0			

NOTES: Temperatures on this project are centigrade (not averaged).

Densities on Line C were taken by Craig Falls, FHWA, at a depth of 9". A correction factor was computed and new readings were calculated for 12" depths.

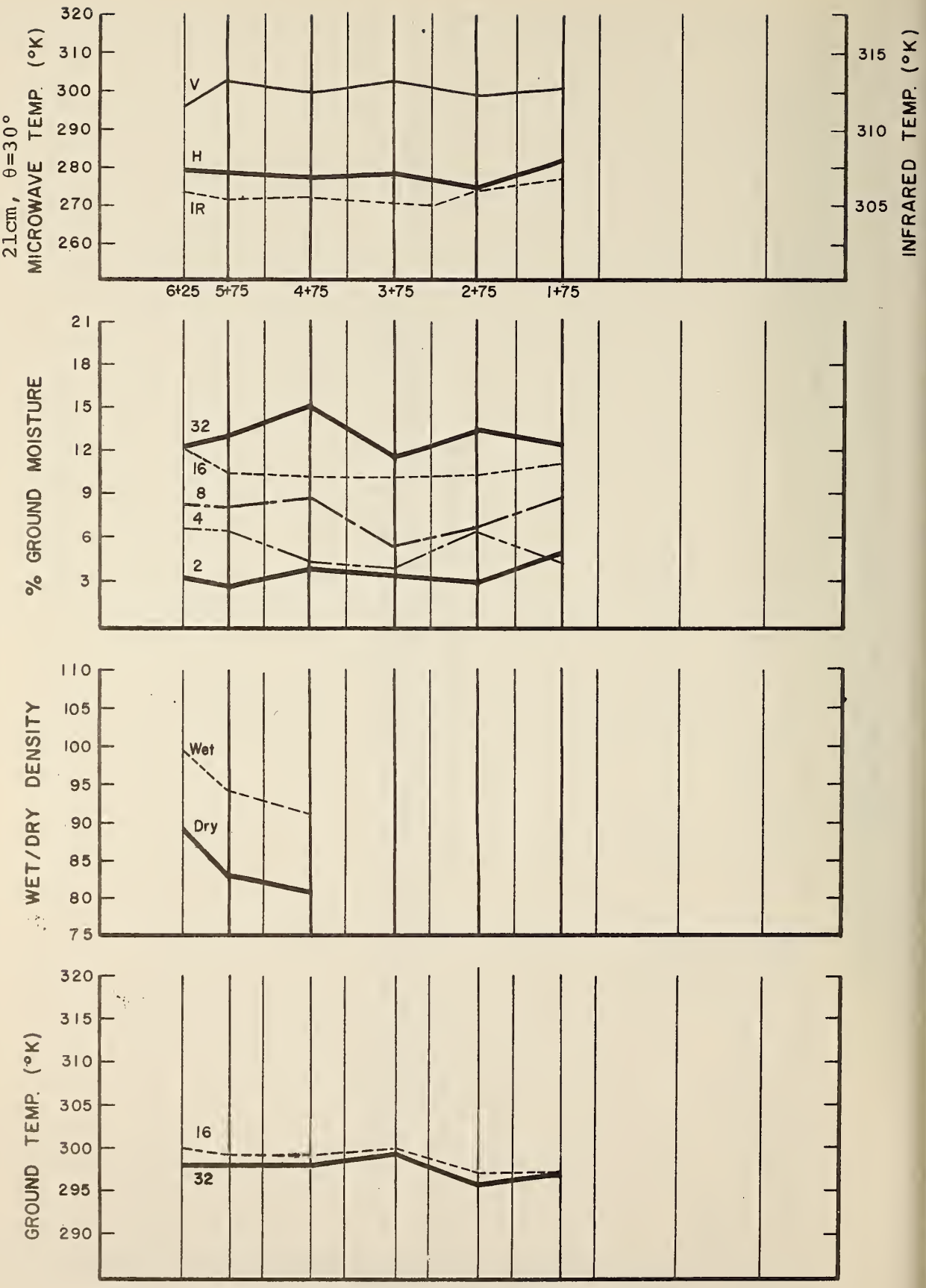

Figure 3.28 Correlation of Measurements Kansas City Line C

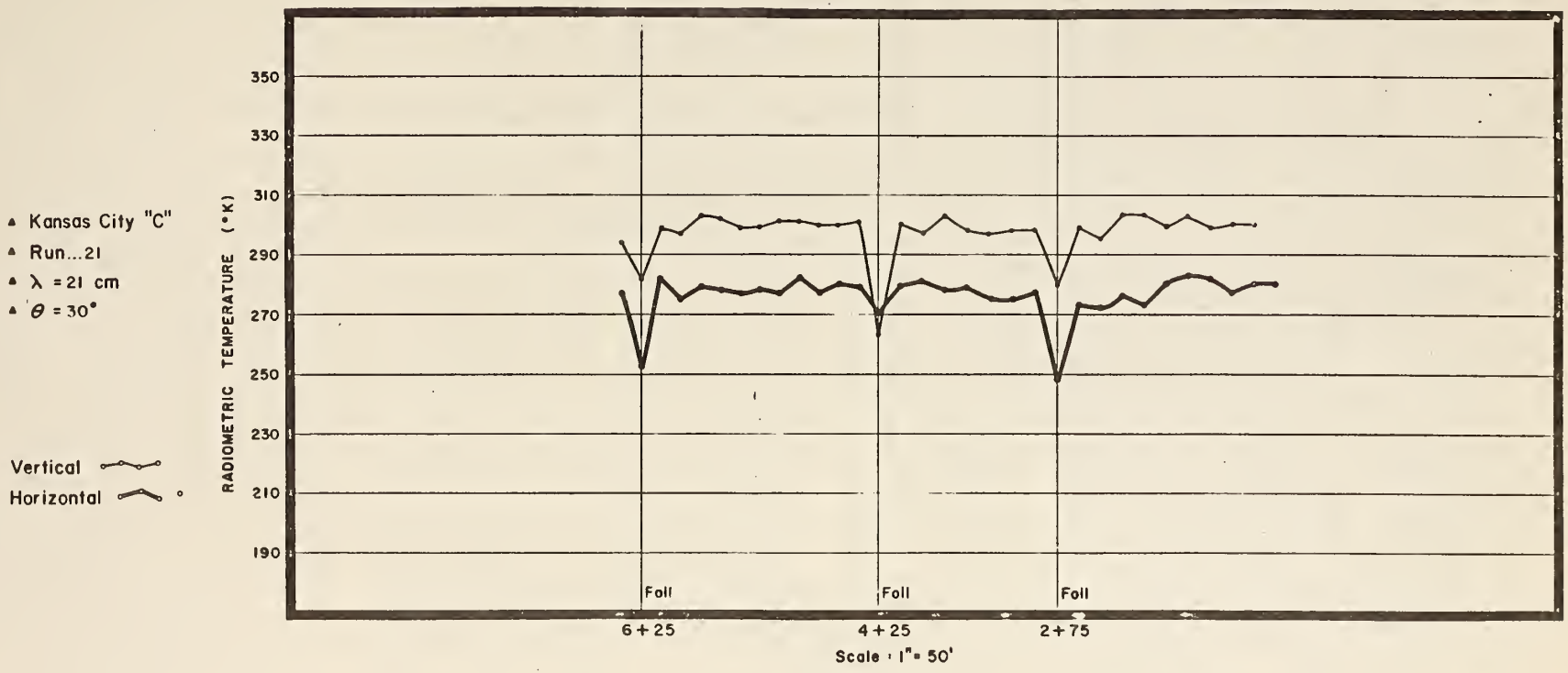

Figure 3.29 Microwave Profile - Kansas City Line C

Whereas line A soils increase in moisture across the traverse (notably above the subsurface void) Line C data are relatively stable at the various levels. The comparison of microwave data indicates an obvious lack of homogenitity between soil parameters in the two lines. Although the causes of this differential could not be determined here it is feasible that a structural geologic cause may be found.

The implication in making this comparison is that two sites which at the surface are equally representative of a "typical" condition over a subsurface void may provide contrasting results because of subsurface geologic differential. This is a commonly encountered characteristic of geophysical research.

Finally, in comparing Line C (mowed) to Line B (unmowed) no significant difference is seen indicating that the decrease in height of the vegetation did not have a major effect on the signal.

In summary, the data collected in the Kansas study program appears to provide most of the necessary elements to analyze the effects of subsurface voids on the microwave signal. While the assumption is correct that the L Band radiometer provides the most sensitive response to subsurface conditions, the results of the point-to-point correlations are not encouraging. However, other analytical techniques, which could be applied to the Kansas data may prove to be valuable in further evaluating the capability of microwave radiometers for the detection of subsurface voids.

4.0 COMPARATIVE ANALYSIS OF MICROWAVE DATA

Data collection in any microwave radiometric survey is governed by the physical parameters fo the earth's surface influencing microwave emissions, and instrument sensitivieies including sensor/ground geometry. The determination of the earth surface parameters which provided the objective of this study are generally beyond the control of the investigators, however, instrument sensitivities controlled largely by instrument wavelength, polarization, and look direction are determinable and based on definitive physical theory.

The physical theory describing microwave radiometric sensitivities usually integrates the effects of dielectric and conducting properties of the surface, surface roughness (measured in wavelength units) surface slopes, subsurface conditions, and vegetal cover. Because of the difficulty in measuring these combined, individual and interacting effects, verification of the effects of ground conditions on microwave temperatures in the current mathematical models depends heavily on the ground measurements of moisture and temperature which are easily measurable, and vegetal cover, surface roughness, and surface slope which may be estimated. The limited knowledge of dielectric properties and the inherent complexity in estimating soil conduction (electromagnetic and heat) properties integrated over three dimensional space precludes precise assessment of the physical theory.

As a result of current capabilities, investigators rely on empirical relationships to determine actual uses for the instruments. The Kansas data were acquired over a variety of natural conditions and in general possessed attributes predictable by microwave theory, however, when viewed in detail a large departure occurs between measured data and theoretical predictions. The reasons for the departure in measured microwave temperatures are not always apparent, however, they are expected and are fundamentally linked with the individual and interacting effects noted above. One standard approach of the microwave analyst is to address

the problem on a point-to-point basis (as done for the Scammon A and the Galena C sites in Section 3.0). General application of conclusions based on those data alone therefore do not necessarily follow.

The approach followed in the RESOURCES TECHNOLOGY CORPORATION analysis attempts to understand the Kansas data in a broad framework of reference. The data acquired are put into a statistical configuration and subjected to scrutiny as a mass. Although the insight to unique conditions are partially lost, an understanding of major trends emerges. Attention throughout the study was focused on the 21cm (L Band) radiometer which presumably provides the most useful data for subsurface conditions because of its penetration capability. Subsequent analysis of these data should consider the other radiometer frequencies and look angles for which data were collected. Once major trends are established and understood, detailed variations at individual sites then may be evaluated in terms of deviations from regional trends to provide the desired insight into the true potential of microwave radiometric surveys for the detection of subsurface voids.

The analysis of the effects induced on the microwave signal by microvariations in the physical characteristics of the terrain provides basic correlative information on the magnitude of the perturbation to be expected. However, because only one sample is available, temporal variance is not sensed. In order to acquire a better sample of typical natural variation in physical characteristics of the terrain, variation of a broad area, that is, macrovariation effects are analyzed. In this way empirical relationships between the various measured parameters are observed.

Section 3.0 describes the microvariation for each line. This section of the report presents an evaluation of the macrovariations in physical parameters of the soil (primarily moisture content and temperature) and their effect on the remotely sensed signals. Furthermore, the redundancies and statistical characteristics of the signals are described. Correlations, graphically

illustrated with two variable scatter diagrams, were made to show potential and known contigencies. These point-to-point correlations were developed in a regional context to evaluate any deviation from the typical regional conditions.

The microvariate analysis in Section 3.0 focused on data collected from each site but emphasized the Scammon A and Galena sites. These two sites were chosen since they 1) represent the extremes of the moisture-temperature spectrum experienced in the data and 2) they provided the most meaningful microwave data point.

The macrovariate analysis considers the microwave data collected from all sites by the 21cm radiometer at the 30° view angle. This approach maximizes the variation in geography and time by drawing data from each site measured during field operations and by utilizing runs occurring at different times during the day. This permits evaluation of the regional variability and trends in soil moisture and temperature fluctuations.

The disparity in the physical conditions shown in Section 3.0 of the wet Scammon soils and the dry Galena soils did not appear to significantly alter the conclusions drawn at either site. In both cases soil moisture and soil temperature distributions suggest an inverse relationship. Infrared temperatures appear to correspond weakly to variations in average moisture whereas microwave temperatures correspond best with average ground temperature distribution. Although the average microwave temperatures for both sites are very comparable (Scammon-V=295, H-263; Galena V-297, H-276), the Scammon site has a larger variance about the mean than that of the Galena site. Interestingly, ground temperatures between Scammon and Galena appear to vary in a similar manner.

4.1 Macrovariate Analysis of Physical Parameters

While an analysis of microvariations in physical parameters raises interesting questions concerning inter-relationships, no single site is characterized by the essential variety of environment to typify regional conditions in time. By redundant sampling

over broad areas and a variety of conditions, the ambiguities associated with ascribing a particular geologic cause to a microwave or infrared signal may be ascertained. Several types of data redundancy occur which include redundancy in time or space, signal received and experiment reiterations.

4.1.1 Temporal Redundancy

The temporal redundancy of prime importance to this analysis occurs between sites. Data were collected such that the same radiometer was employed at different times during different (or the same) days and as such makes duirnal variations a source of random variation in the overall program. Additionally, different radiometers were employed at the same time.

4.1.2 Spatial Redundancy

At least six runs were scheduled at each site, two for each of the three look angles. Although this permits a comparison of different frequencies at the same site, it also permits systematic analysis of the same frequency radiometer at the same site and perhaps cursory evaluation of the short term macrovariations.

4.1.3 Signal Redundancy

Although the scope of this effort did not include detailed analysis of temporal or spatial redundancies in the data, considerable attention was focused on the similarity in signals across polarizations and view angles. Figures 4.1, 4.2, 4.3 and 4.4 illustrate the relationship between vertical and horizontal polarizations across all angles for the Scammon A Site.

Vertical and horizontal polarizations in microwave studies typically provide the investigations with a discriminator of ground conditions. As a discriminator, investigators have used the difference in the antenna temperature (T_A) for each polarization within a sensor, and the difference in T_A for each polarization between sensors and as a function of a changing angle of incidence.

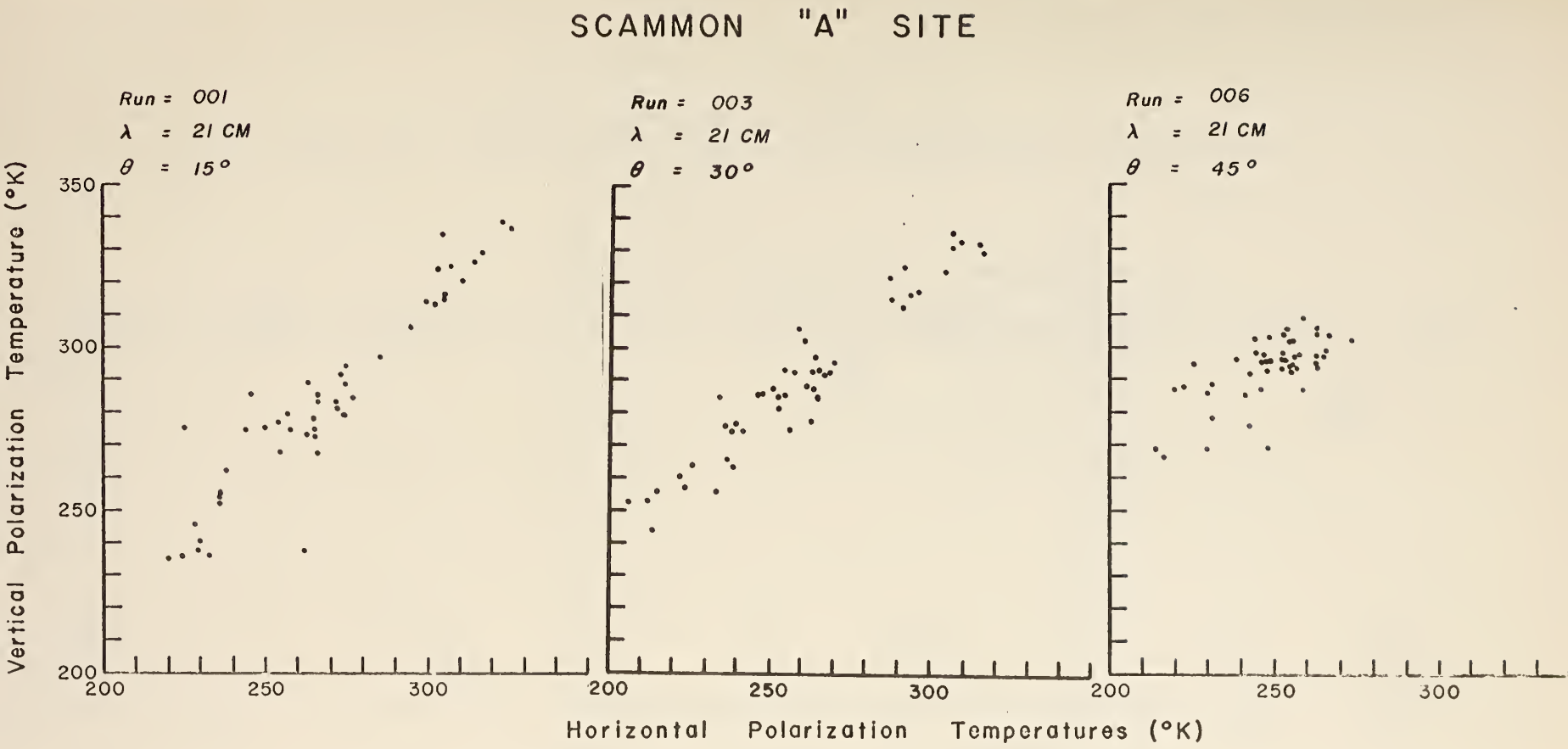

Figure 4.1 Correlation of Vertical and Horizontal Polarizations of 21cm Radiometer, Scammon Line A

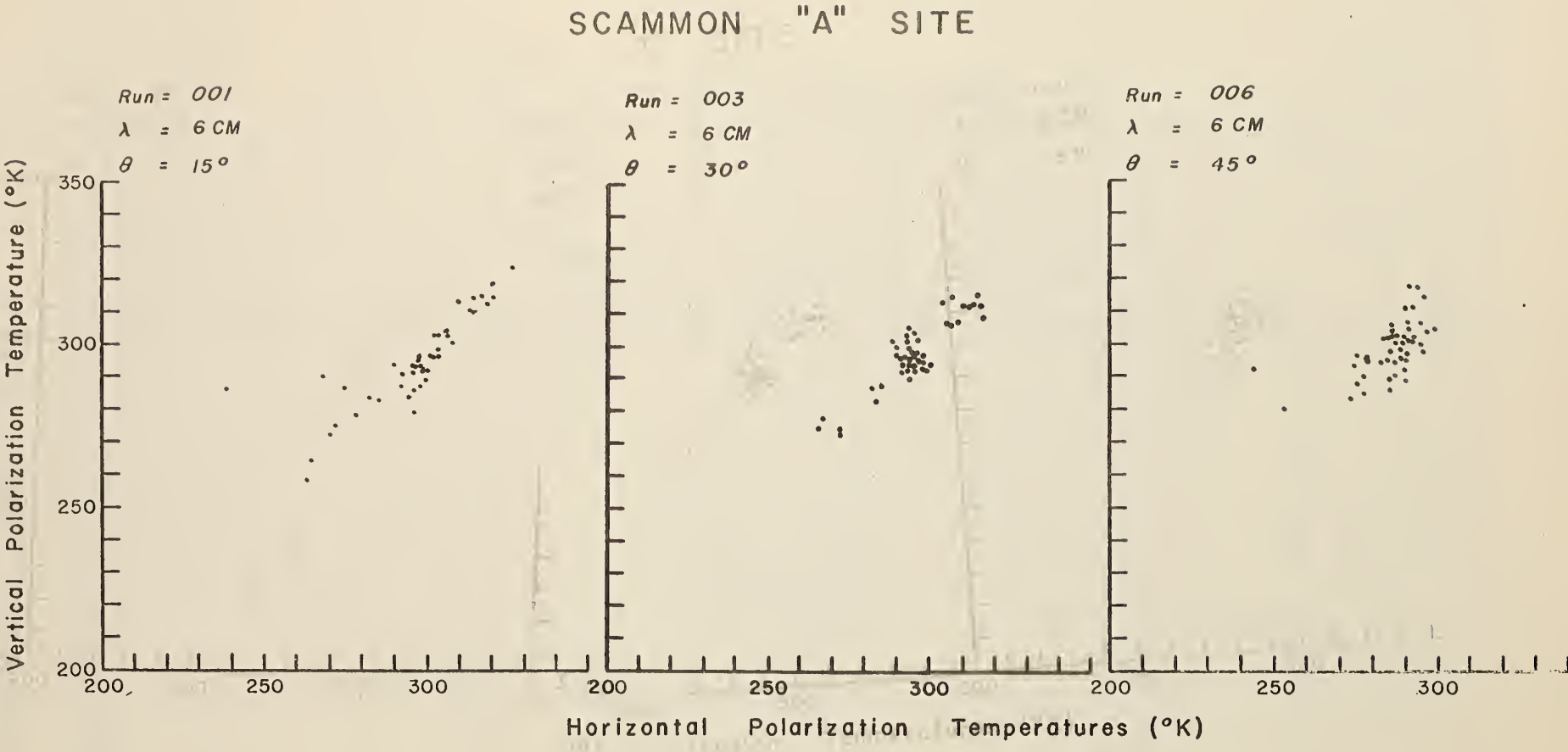

Figure 4.2 Correlation of Vertical and Horizontal Polarization of 6cm Radiometer, Scammon Line A

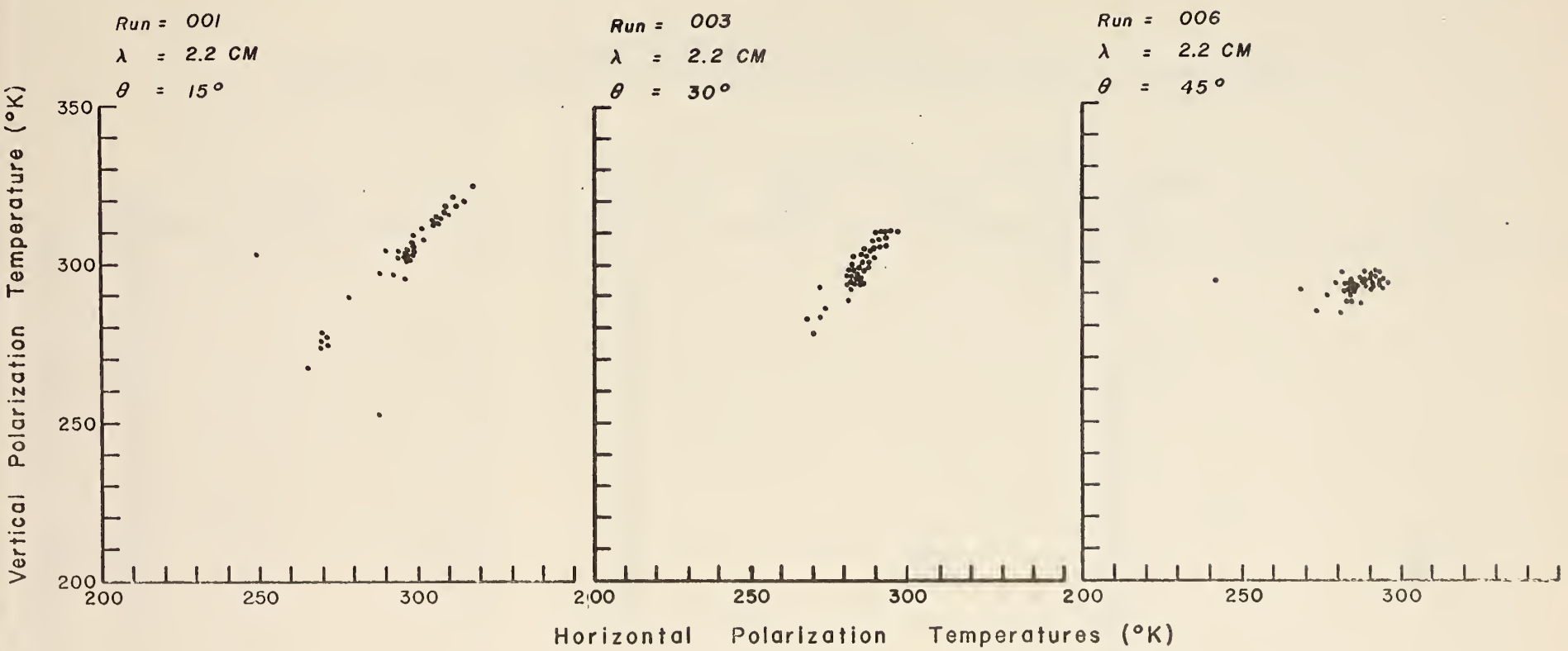

Figure 4.3 Correlation of Vertical and Horizontal Polarization of 2.2cm Radiometer, Scammon Line A

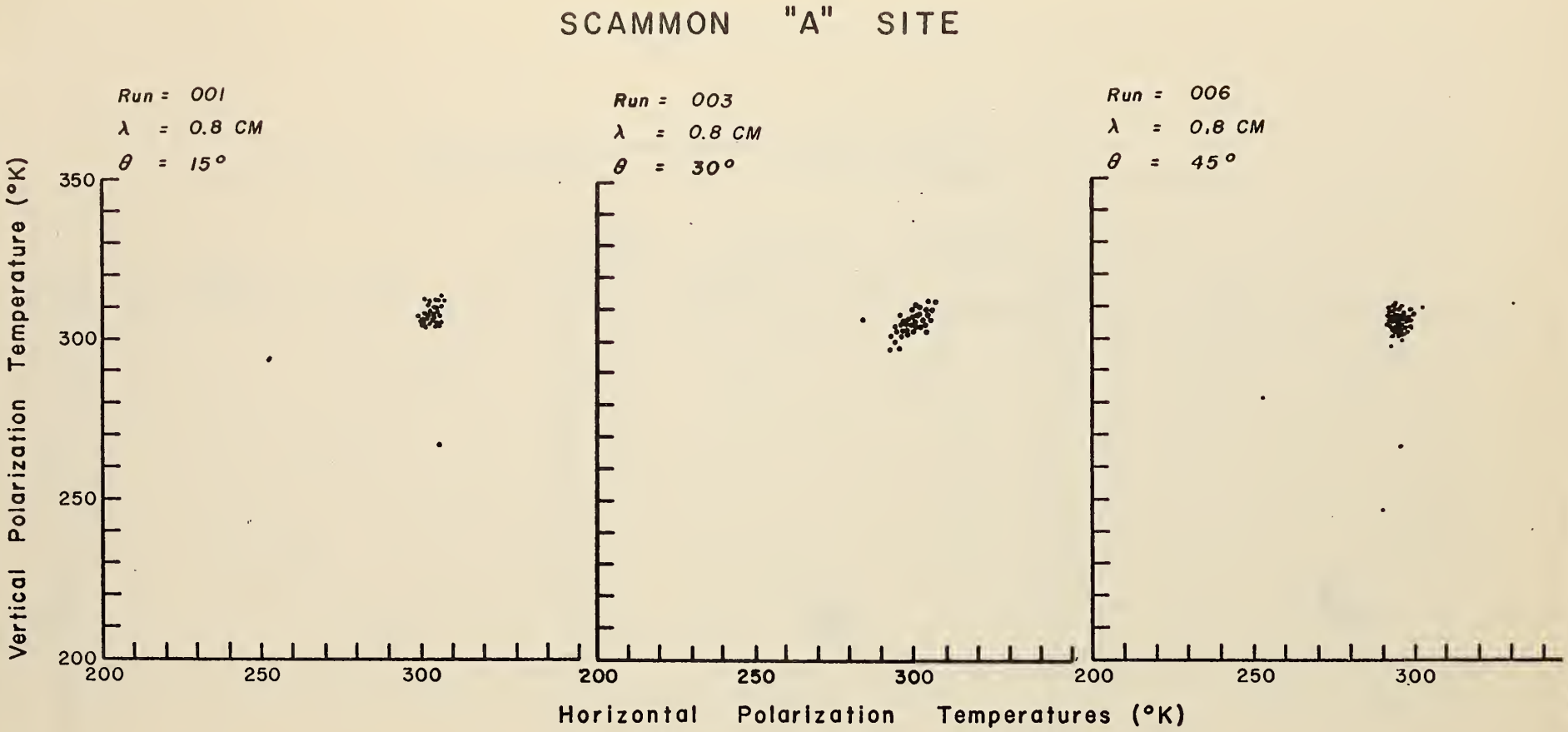

Figure 4.4 Correlation of Vertical and Horizontal Polarization of 0.8cm Radiometer, Scammon Line A

To empirically test the relationship between vertical and horizontal polarizations within a single sensor; that is, at one wavelength, scattergrams were produced for each sensor plotting vertical polarization as a function of horizontal polarization and visually evaluating the relationship (Figures 4.1 through 4.4). In nearly each case a strong positive linear relationship with little scatter about the regression line occurred as is exemplified in Figures 4.1 to 4.4 for three angles of incidence for each frequency. This relationship merely indicates that where horizontally polarized T_A rise, vertical polarized T_A rise, and that the difference between the two is relatively constant function. The question is not answered of whether or not the relatively small degree of fluctuation about a least squares regression is within or outside the level of random noise input. Further detailed analysis of that aspect appears in order.

Several other characteristics of the relationship should be noted. The range of variance of both V and H is similar within angles as indicated by the slope of the line, however, typically, as the angle of incidence increases from 15 to 45 degrees, the range of T_A variation along the Scammon line decreases. Consider Figure 4.1 where the range of temperature is approximately 110 T_A degrees for both polarizations and Figure 4.3 where the range is only 50 degrees. Of the 4 microwave wavelengths, both polarizations of the 45° angle, 0.8cm radiometer have the smallest ranges of only 10 T_A degrees for the entire length of line excluding the aluminum foil stations.

A nearly identical trend in V-H ranges occurs across sensors from the longer wavelength to the shorter wavelength sensors. As wavelength decreases from 21cm to 0.8cm the range of both vertical and horizontal polarizations decreases and shows almost no fluctuation at the shortest wavelength.

A comparison of the V-H relationship across all sensors (Figure 4.5) shows that nearly similar slopes occur for each sensor strongly implying similar distributions. Cursory observation of the scatter about the regression further implies relatively

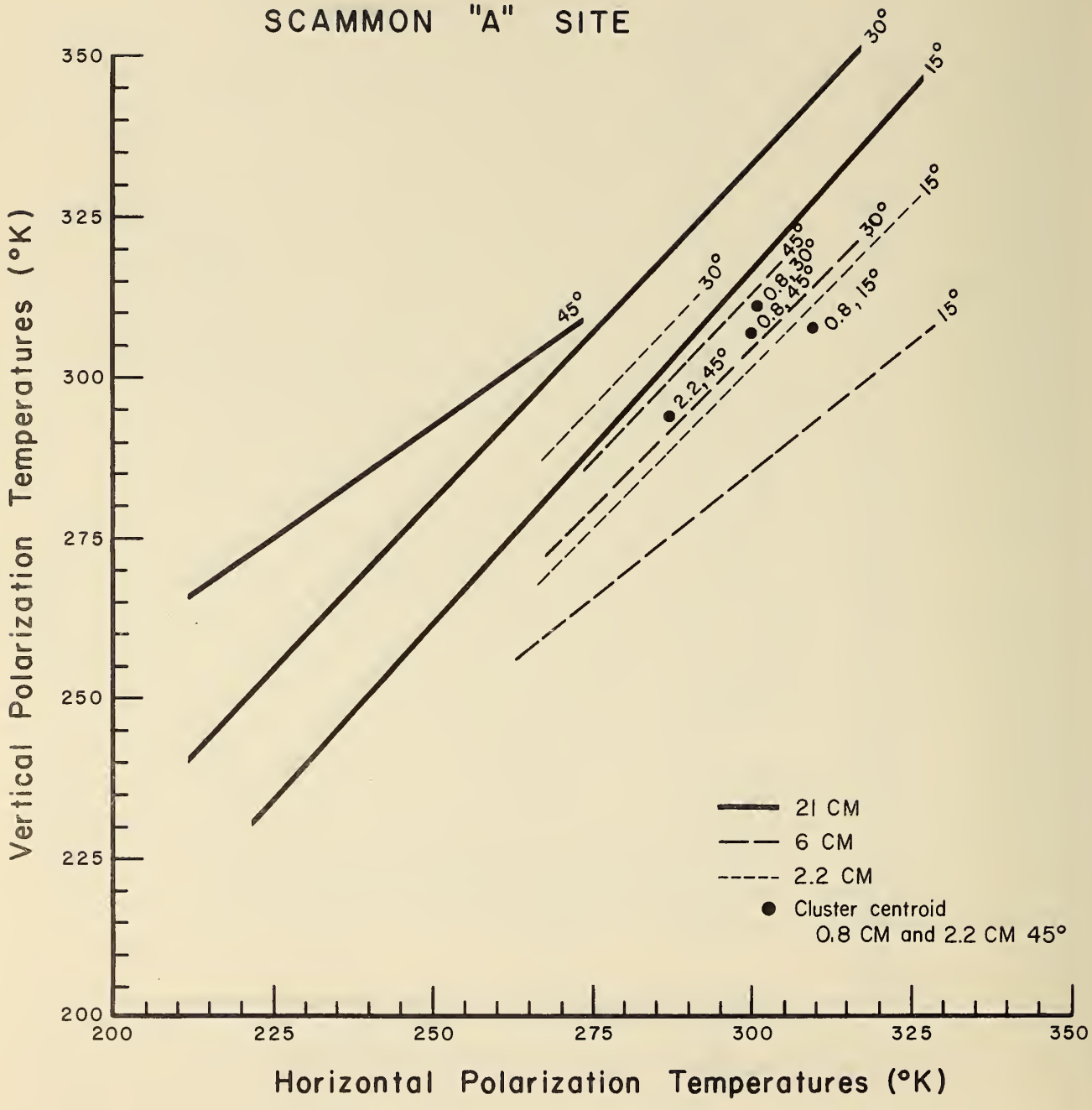

Figure 4.5 Comparison of Vertical and Horizontal Polarizations for All Scammon A Microwave Sensors (Runs 001, 003, and 006).

little variance (i.e. the line is a good approximation) in the V-H relationship in a general decrease in range of variance with increasing angle of incidence and decreasing wavelength. Despite the small variance about the regression line, the close proximity of the linear expression of the V-H relationship, suggest extensive redundancy in the long wavelength low angle data. Further, differences in vertical and horizontal polarization at any single frequency do not greatly differ and may not significantly contribute to detection of differences in ground conditions. Finally, as look angles increase, and wavelengths decrease, the range of variance in the signal decreases thus suggesting a decreasing sensitivity to variations in ground conditions.

4.1.4 Experimental Redundancy

Another important form of redundancy occurs in the form of reiteration of the entire experiment at a variety of sites. It is experimental redundancy which permits evaluation of the regional trends in the physical parameter. Although most sources of variation are considered random effects on the microwave signal, those sources which were measured on the ground may be analyzed for their systematic effects. In this way, a large sample of some 60 ground stations may be efficiently utilized.

4.2 Data Correlation

A correlation problem considers the joint variation of two measurements, neither of which is restricted by the experimenter. The relationship between both variables are observed as they occur in nature. Either variable may be considered independent. It is convenient to empirically study correlations between variables on scatter diagrams where two variables are plotted in a Cartesian coordinate planar system such as Figures 4.1 to 4.4. This is done to provide some visual evidence of whether the two variables are related. If the relationship is simple the plotted points tend to form an easily recognizable pattern such as a line. When the relationship is strong the pattern is distinct and points tend to overlap; when it is weak the points appear to spread out;

when there is no simple relationship or the relationship is poor, points appear to fall at random. In Figures 4.1 to 4.4 the relationship appears strong.

As an initial step in data correlation, the 21cm, 30° look angle data and ground truth data for each site were tabulated (Table 4-1). In an attempt to integrate all the ground truth in each category into a discrete index, an average of all levels for all points at a station was computed. Thus most moisture and temperature averages represent ten and twelve points, respectively; however, at several stations, less than the maximum number of points were available. Of the approximately 60 stations, 2 microwave measurements, both at the Scammon A site, were edited from the data as anomalous.

4.2.1 Correlation of Soil Moisture and Temperature

The analysis of microvariation at the Scammon and Galena sites suggested that an interrelationship exists between soil moisture and ground temperatures. Figure 4.6 illustrates the relationship for all sites each of which are designated by a unique symbol.

The scatter diagram indicates a moderately strong negative correlation, that is, an inverse relationship where there is approximately one percent decrease in ground moisture with a one degree centrigrade rise in ground temperature.

The scatter about the regression is large near the center of the graph suggesting that other variables such as soil type, topography and vegetal cover, or other factors considered in this study as random effects, have come into play. A second, more plausible explanation for the scatter lies in the data. Although the data from each site partially overlaps the data from other sites, each symbol tends to cluster in portions of the graph. In this sense the two attributes of moisture and temperature tend to segregate the sites. It should be noted that for purposes of this graph only two levels of ground temperature were available at the Clay

Table 4-1

Tabulation of M.W. Data by Station

SITE	ANTENNA TEMPERATURE		GROUND TRUTH DATA			SYMBOL	LINE	RUN	SAMPLE STATION
	Horizontal	Vertical	AV MOIS. (%)	AV TEMP. (°K or °C)	Infrared Temp. (°K)				
CLAY CO.	254	284	11.3	27.1	314.5	□	C	14	185 + 00
	254	292	8.6	30.0	316.8		C	14	188 + 80
	259	298	12.3	26.4	314.1		C	14	100 + 00
	257	289	9.8	27.6	311.3		C	14	105 + 00
	250	285	8.0	26.9	313.6		D	20	205 + 00
	262	296	8.6	27.4	310.0		D	20	210 + 00
	273	319	8.9	28.1	312.2		D	20	210 + 40
GALENA	273	296	5.3	34.3	310.1	○	A	1	12 + 00
	269	299	9.3	34.6	311.2		A	1	13 + 00
	277	295	3.9	36.8	311.1		A	1	14 + 00
	276	296	2.8	37.4	309.3		A	1	15 + 00
	275	297	2.8	38.5	309.3		A	1	16 + 00
	282	298	2.0	38.5	308.4		A	2	17 + 00
	257	272	2.8	36.8	309.4		A	2	18 + 00
	284	302	2.9	37.0	310.0		A	2	19 + 00
	285	307	2.3	37.2	312.9		A	2	20 + 00
	285	314	3.9	36.9	312.5		A	2	21 + 00
	271	303	8.0	35.1	314.7		D	11	19 + 50
	273	300	6.6	36.6	315.7		D	11	18 + 50
	256	297	4.6	37.7	315.4		D	11	17 + 50
	270	301	6.1	34.2	314.7		D	11	16 + 50
	251	284	6.0	29.6	312.1		D	11	15 + 50
	262	291	5.0	32.7	311.1		D	11	14 + 50
	269	300	9.6	33.4	318.8		D	11	13 + 50
	266	295	7.5	32.8	311.1		D	11	12 + 50
	267	295	7.5	34.8	314.5		D	11	11 + 50
	248	281	4.1				C'		12 + 30
	250	275	4.1				C'		12 + 50
	258	270	3.5				C'		14 + 30

(Table 4-1Continued)

Tabulation of M.W. Data by Station

SITE	ANTENNA TEMPERATURE		GROUND TRUTH DATA			SYMBOL	LINE	RUN	SAMPLE STATION
	Horizontal	Vertical	AV MOIS. (%)	AV TEMP. (°K or °C)	Infrared Temp. (°K)				
GALENA	272	298	5.7	35.3	312.8		E	3	10 + 50
	272	295	5.4	36.0	313.2		E	3	11 + 50
	283	304	4.4	37.4	309.1		E	3	12 + 50
	264	293	6.3	35.0	311.8		E	3	13 + 50
	268	292	9.8	33.8	311.9	•	A	3	146 + 50
	305	336	9.2	31.0	307.6		A	3	147 + 50
	278	301	8.6	31.8	310.7		A	3	148 + 50
	226	264	9.4	27.6	311.1		A	3	149 + 50
	240	277	12.7	30.1	315.7		A	3	150 + 50
	262	290	11.0	30.7	314.9		A	3	151 + 50
	260	302	6.6	33.9	314.3		A	3	152 + 50
	257	283	16.5	25.0	307.2		B	4	343 + 50
	252	284	14.2	25.6	307.6		B	4	344 + 50
	264	294	14.5	25.3	310.8		B	4	345 + 50
SCAMMON	263	293	9.0	29.0	313.6		B	4	346 + 50
	266	298	11.6	27.2	311.2		B	4	347 + 50
	261	291	12.4	26.7	312.6		B	4	348 + 50
	256	291	14.6	28.8	312.7		B	4	349 + 50
	254	292	11.8	29.5	312.2		B	4	350 + 50
	265	293	11.5	31.1	310.6		B	4	351 + 50
	258	290	11.2	33.3	310.6		B	4	352 + 50
			7.6	33.6			C		343 + 50
			10.6	33.6			C		344 + 50
			13.1	34.8			C		345 + 50
			11.5	34.0			C		346 + 50
			11.4	33.1			C		347 + 50
			14.8	30.2			C		348 + 50
			14.2	29.9			C		349 + 50
			9.6	29.7			C		350 + 50

(Table 4-1 Continued)

Tabulation of M.W. Data by Station

SITE	ANTENNA TEMPERATURE		GROUND TRUTH DATA			SYMBOL	LINE	RUN	SAMPLE STATION
	Horizontal	Vertical	AV MOIS. (%)	AV TEMP. (°K or °C)	Infrared Temp. (°K)				
KANSAS CITY	276	302	8.0	24.7	308.8	Δ	A	8	0 + 75
	267	294	10.3	35.4	307.4		A	8	1 + 75
	267	299	10.1	27.6	309.0		A	8	2 + 75
	270	295	9.5	27.2	307.6		A	8	3 + 75
	280	303	11.2	27.6	308.4		A	8	4 + 75
			12.4	28.0			A	8	6 + 75
			8.3	24.7			C	21	0 + 75
	282	301	8.4	24.1	307.2		C	21	1 + 75
	275	299	8.0	23.7	306.3		C	21	2 + 75
	278	303	6.9	26.6	307.8		C	21	3 + 75
	277	300	8.5	25.9	305.8		C	21	4 + 75
	279	303	8.2	25.8	305.6		C	21	5 + 75
	280	297	8.0	25.9	306.1		C	21	6 + 75

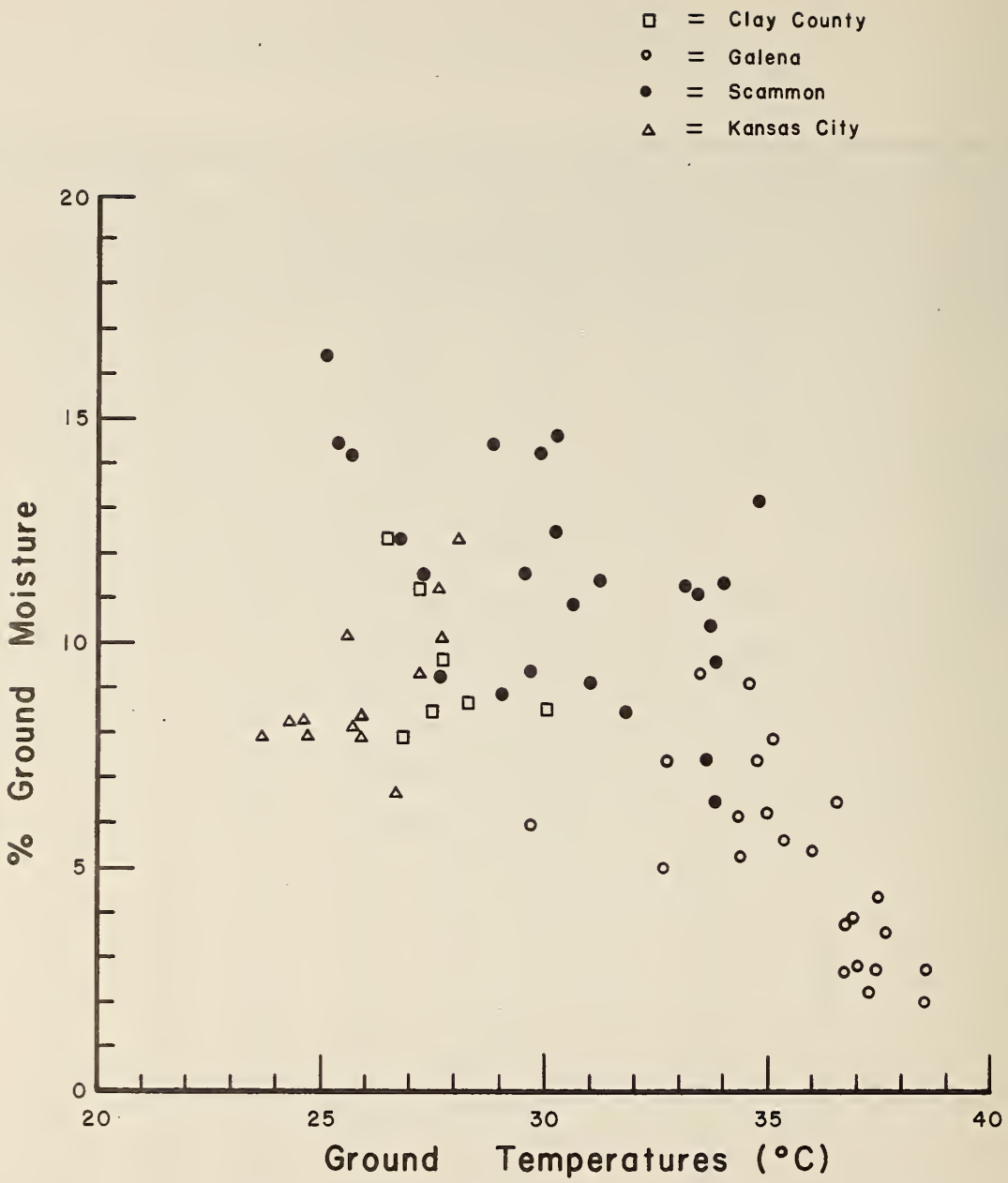

Figure 4.6 Correlation Between Average Ground Temperature and Average Ground Moisture

County and Kansas City sites. In both cases, these were temperatures collected at 16cm and 32cm depths, the lowest temperatures in the vertical profile. If the Clay County/Kansas City data were not included in the graph there would be considerably less scatter, or if they were adjusted on the basis of the Scammon/Galena regression, they would slide to the right and fit comfortably about the regression lone. The Scammon/Galena regression slopes at a slightly greater angle and the relationship becomes approximately 0.8 percent change in moisture for every one degree centigrade change in ground temperature.

4.2.2 Correlation of Microwave Response and Ground Moisture

Figure 4.7 is a scattergram of microwave temperature expressed as a function of average moisture for five levels at each site (unlike temperature-moisture measurements, which were collected for all levels). A regression line fit to this relationship indicates one degree antenna temperature drop for every three or four percent change in the average moisture. This relationship is not unlike that reported by other investigators for other geographic locations.

The scatter about the regression is large, however, indicating that random effects on the microwave signal are significant. For any particular level of ground moisture, it is reasonable to expect a variance ranging from approximately ± 7 to ± 18 percent about the estimated microwave antenna temperature.

The analysis of microvariations at Scammon and Galena suggested a possible relationship between infrared and percentage moisture. Although this relationship is indirectly related to the effects of ground moisture on ground temperature, the scatter diagrams in Figure 4.8 and Figure 4.9 do not show any relationship. Whereas Figure 4.8 attempts to compare infrared signals and average moisture from five levels, Figure 4.9 shows the relationship for the uppermost level, reasoning that infrared does not directly sense energy emitted from depth.

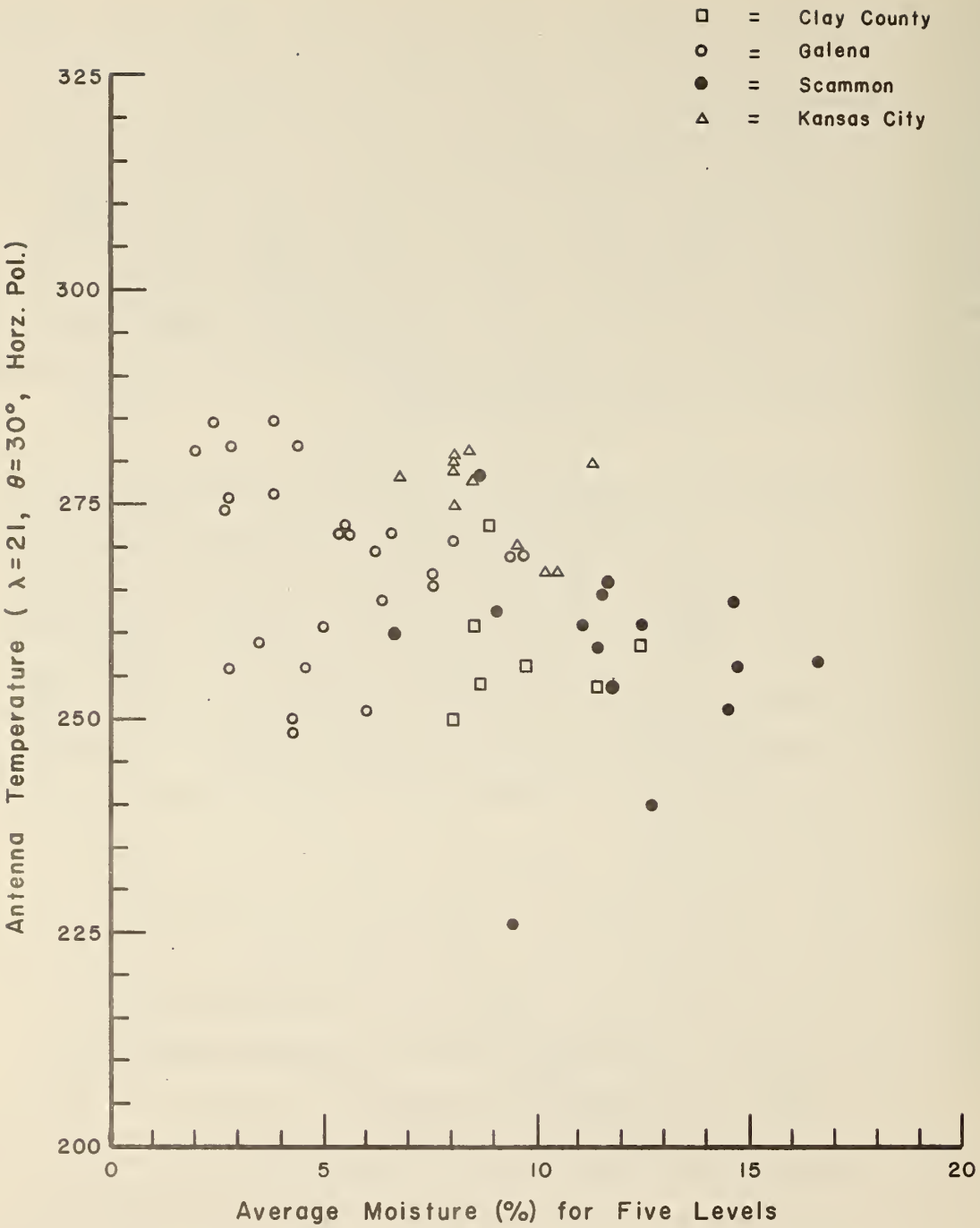

Figure 4.7 Correlation Between Average Ground Moisture for Five Levels and 21cm Microwave Antenna Temperatures.

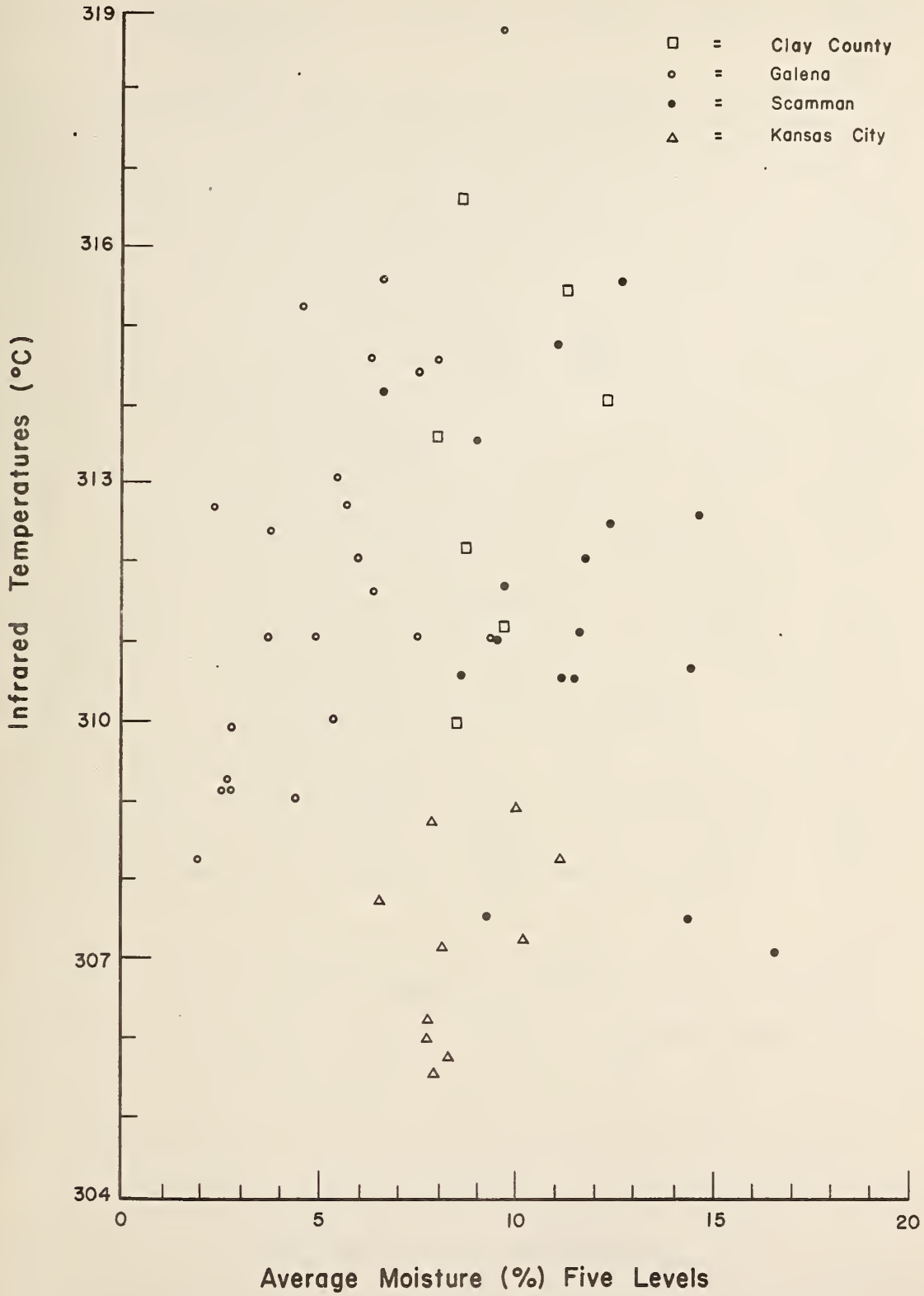

Figure 4.8 Correlation Between Average Ground Moisture for Five Levels and 8.0-14.0μ Infrared Radiometric Temperatures.

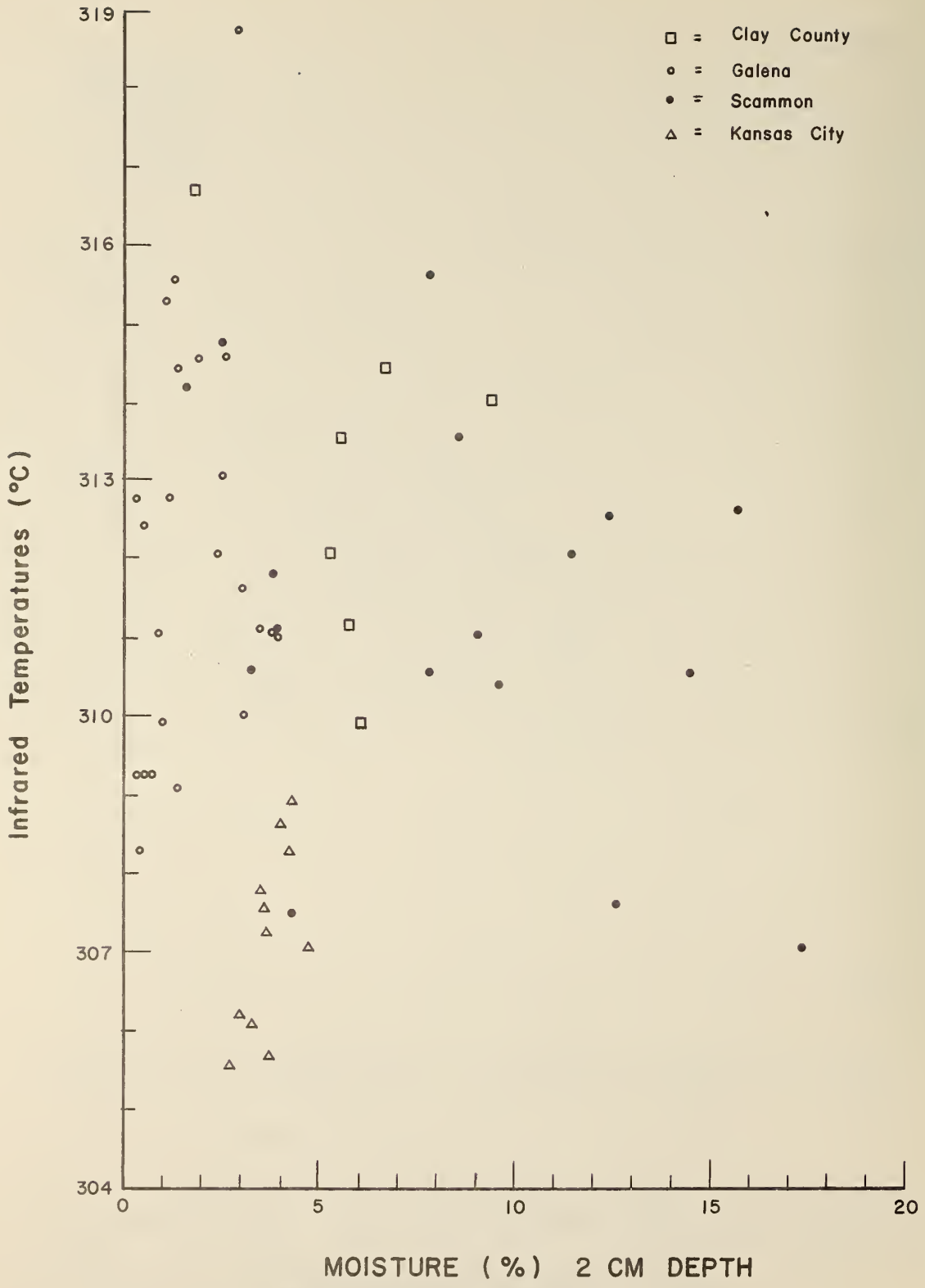

Figure 4.9 Correlation Between Average Moisture at 2cm Depth And 8.0-14.0μ Infrared Radiometric Temperatures.

4.2.3 Correlation of Remotely Sensed Signals and Ground Temperature

The apparently poor relationship between 21cm antenna temperature and average ground temperatures for five levels illustrated in Figure 4.10 is substantially improved when the two-level average for Clay County and Kansas City data are adjusted. The relationship would become considerably less scattered with all Clay County and Kansas City points falling between 20°C and 35°C. Based on the Galena/Scammon regression alone, a one degree centigrade increase in ground temperature induces about 1/3 degree centigrade increase in microwave antenna temperature. For any particular ground temperature one could expect a $\pm$ 7 to $\pm$ 12 degree variance in microwave temperature. Empirically this variance severely limits precise ground temperature predictability.

As was noted previously in this report, no simple relationship between infrared temperatures and ground temperatures is apparent. Because sensitivities of the infrared radiometer exceeds that of the microwave instrument, and infrared scale in Figure 4.11 is considerably elongated relative to the microwave scale in other figures in order to study the distribution of points. Two feasible explanations of the explanations of the unexpectedly poor correlation between ground temperatures and infrared temperatures occur in the data collection and reduction process.

In the first case, it is known that the infrared radiometer senses only the energy emitted from the surface of the earth, the averages in Figure 4.11 are ground temperatures averaged over 5 levels of depth to 32cm. Thus, similar scatter diagrams were constructed for surface and 2cm depths with equally poor correlations. These are not included in the report.

A second factor possibly inducing the poor correlation relates to the necessary time lag between collection of the infrared data and collection of the ground truth. In logistically difficult areas the lag may have been several hours. Thus, the ground truth and the measurements do not correlate precisely in

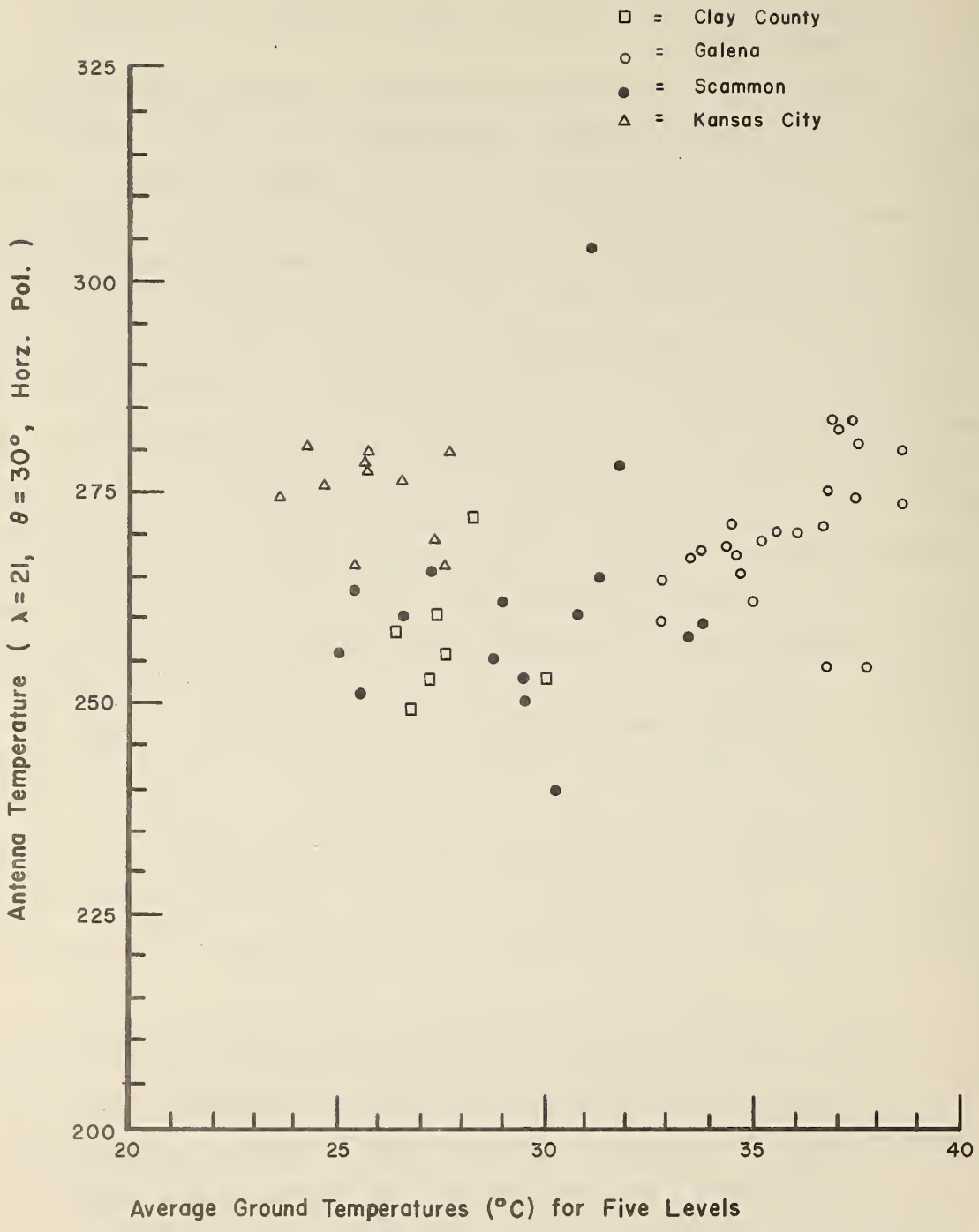

Figure 4.10 Correlation Between Average Ground Temperature for Five Levels and 21cm Microwave Antenna Temperatures

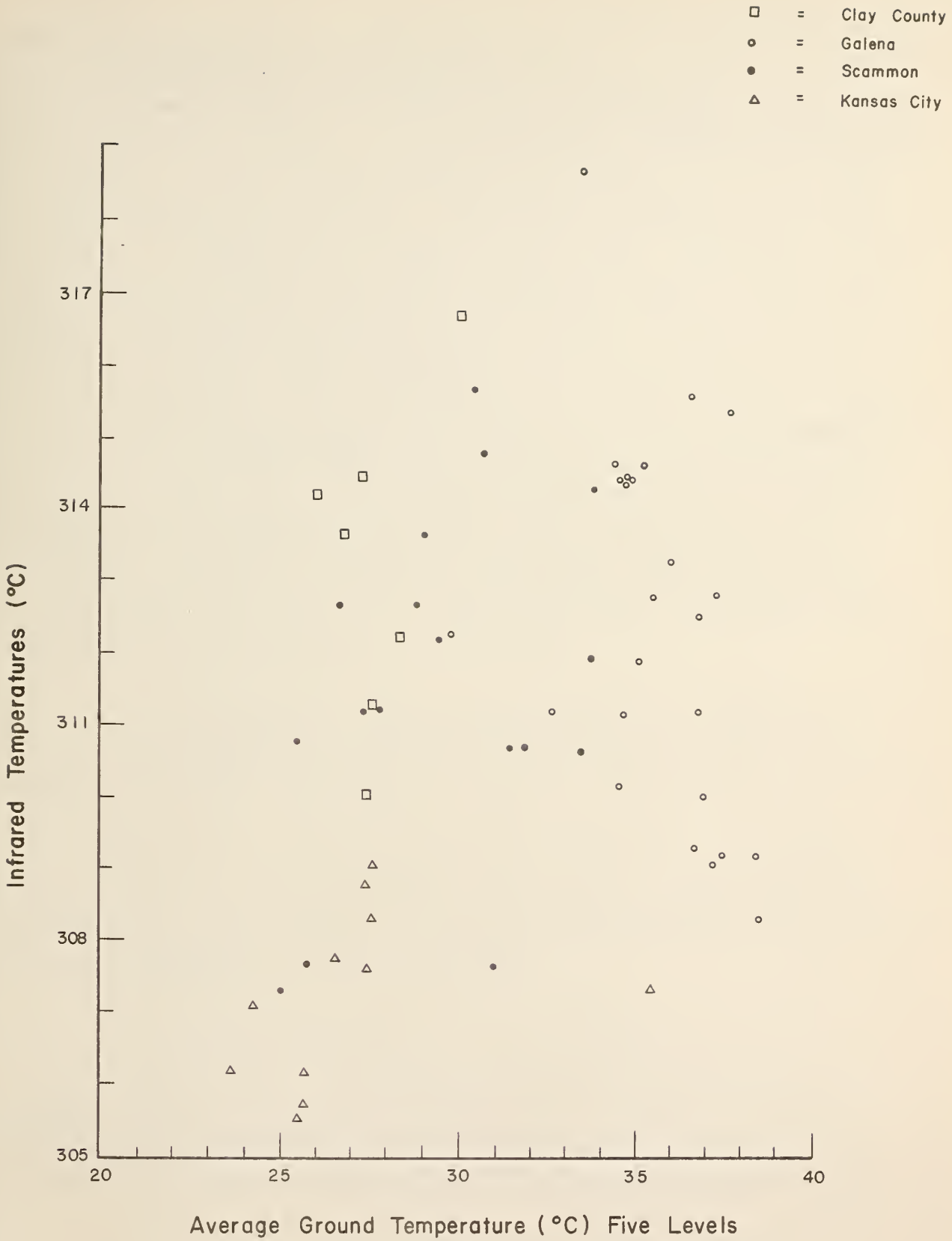

Figure 4.11 Correlation Between Average Ground Temperature For Five Levels and 8.0-14.0μ Infrared Radiometric Temperatures.

time, resulting in the poor correlation. Based on a large number of other studies, the relationship between the infrared and ground truth should have correlated in some exponential relationship better than the observed distribution.

5.0 CONCLUSIONS AND RECOMMENDATIONS

The application of microwave radiometry to surface mapping is comparatively new. A few surveys have been conducted for the purpose of investigating microwave responses to varying geologic phenomena, soil moisture, sea state and underground voids. The results of theoretical studies of such data tentatively have established that there is promise to the application of microwave radiometry to the determination of sea state and in mapping soil moisture. A recent single frequency aerial microwave survey of the underground cave areas in Kansas City, Kansas indicated that over that specific mine area a relatively low microwave temperature anomaly occurred. With the results of the latter survey in mind this present study was designed to determine if by making a multifrequency microwave radiometer survey using truck mounted instrument, underground voids and subsidence prone areas could be delineated. The study of the data from this survey has given rise to the following general conclusions:

1) No microwave anomalies could be directly attributable to the presence of subsurface void spaces based on the analysis of the data collected in this empirical study.

2) Variations in the recorded microwave temperature profiles could not individually be attributed to the effect of any single microwave radiation parameters such as ground temperature, soil moisture or density changes.

5.1 Detailed Conclusions

In arriving at the general conclusions noted above the data were studied for each line individually and then studied statistically by combining all of the data. The combination of data was accomplished to determine if obvious effects of single

ground truth parameters could be discovered. The specific relationships which were established by this analysis were:

1) Polarization effects (variation in the vertically polarized microwave temperatures (T_V) minus the horizontally polarized microwave temperature (T_H) were fairly constant for an individual wavelength and viewing angle. The difference in $T_V - T_H$ decreased as the wavelength decreased as the viewing angle increased.

2) A weak trend (with large deviations) demonstrated that a 1°K decrease in microwave temperature occurs for each 3.5% soil moisture increase. This relationship is drawn from a plot of all the microwave temperature data from the 21cm radiometer. The deviation of individual data points from a best fit trend line through the data is large and indicates that a simple predictive relationship between microwave temperature and soil moisture was not demonstrated.

3) An expected correlation of the PRT-5 infrared radiometer temperatures with the fourth power of ground temperature did not materialize.

4) Qualitative evaluation of the ground temperature and the L Band radiometer temperature showed a weak linear correlation.

5.2 Recommendations

The enormous amount of ground truth and microwave radiometer data collected during the course of this survey and a recognition of the numerous radiation parameters and their complex interrelationships indicate that a continuing study of the data could yield additional valuable results and should be pursued. It is entirely possible that deterministic and further empirical

manipulations of the data could uncover relationships in the microwave response which can be practically exploited for subsurface void detection.

Since only weak correlation of ground measurements and "apparent" microwave anomalies occurred at any of the sites studied, we do not believe that the acquisition of core hole data would be beneficial at this time. Such a program should only be undertaken following further analysis of the existing data.

As is true with most research studies of this nature it is always hoped by the investigators that an easy or positive solution to the objective be found. Such a solution was unfortunately not evident in this study in which passive microwave radiometric techniques do not appear to be currently applicable to void space detection. However, we do feel that the potential of such systems warrants further study to better define their characteristic outputs and responses.

Appendix A

MICROWAVE RADIOMETRY

A.1 PRINCIPLES

In the microwave portion of the electromagnetic spectrum and at temperatures commonly found near the earth's surface, the spectral intensity $I_\lambda(\theta)$ of the radiation emitted at wavelength λ in the direction of a nadir angle, θ, is proportional to the absolute temperature T and the emissivity of the surface:

$$I_\lambda(\theta) \propto \varepsilon(\theta)T \qquad \text{(A-1)}$$

The product $\varepsilon(\theta)T$ is commonly referred to as "emitted brightness temperature," T_B. Measurements are generally expressed in terms of that product and radiometers are calibrated with reference to a radiation source of known brightness temperature.

The brightness temperature of a surface observed by a radiometer at some height h above the surface is also affected by the atmosphere in several ways. First, the radiation leaving the surface contains a component which consists of reflected incoming radiation emitted by the atmosphere above the surface (plus a component due to the cosmic background). Secondly, on leaving the surface, the radiation is attenuated by the atmosphere in propagating to the radiometer. Finally, the atmosphere between the radiometer and the surface itself emits radiation which contributes to the received signal. These contributions to microwave radiometric measurements can range from a negligible amount for a clear, dry day at frequencies below 15 GHz, to very substantial values for humid, cloudy and/or rainy conditions at frequencies above 20 GHz. A more comprehensive treatment of techniques for removing atmospheric

contributions from microwave radiometric measurements is given in a report documenting data correction techniques for the NASA P3A radiometer system (Edgerton, 1970).

$$T_B'(\theta,h) = \left[\varepsilon(\theta)T + r(\theta)T_S\right] \tau(h) + \int_o^h T_A(h) \frac{\partial \tau}{\partial h} dh \qquad \text{(A-2)}$$

where T_S is the brightness temperature of the sky, T_A is the ambient temperature of the atmosphere, r is the reflectivity of the surface, τ if the transmissivity of the atmosphere, and θ is the viewing angle of the radiometer antenna.

The first term in Equation (A-2) relates to radiation from the surface; the second term relates to atmospheric radiation. Calm water has an emissivity of only about 0.4 (near $\theta=0$) and, therefore, always appears quite cold. Water clouds vary in transmissivity virtually from 0.0 to 1.0 depending on thickness, liquid water content and radiometric frequency. Ice cloud transmittance is always very close to 1.0. Thus, over water, thick water clouds may appear much warmer than the water surface. The emissivity of dry, natural surfaces such as soils, sediments and outcropping rocks, varies from about 0.8 to 0.95, depending on vegetation cover and angle.

Microwave brightness temperatures of natural materials are dependent upon a number of physical properties. These include moisture content, density, surface roughness (including microrelief, particle or fragment size and shape, vegetal cover, etc.), thermometric temperature, and stratigraphy (layerings, etc.). Compositional variations are of less importance in determining the microwave characteristics of material, except in circumstances where significant amounts of metallic or magnetic minerals are present. With the exception of the thermometric temperature and surface roughness dependence, these parameters are all associated with the dielectric properties of the material. Other factors which must be considered in determining the microwave

characteristics of natural materials include: observational frequency or wavelength, antenna polarization, and antenna viewing angle. Moisture content is one of the most influential variables contributing to brightness temperature variations, and must be taken into account when considering any potential geologic application.

Considering that radiation emitted by most surfaces is polarized, Equation (A-2) can be written for both horizontal and vertical components. Horizontal and vertical polarizations are defined such that the electrical vectors lie in planes parallel and perpendicular to the earth's surface, respectively.

$$T'_{B,H}(\theta,h) = \left[\varepsilon_H(\theta)T + r_H(\theta)T_S\right]\tau(h) + \int_o^h T_A \frac{\partial\tau}{\partial h}\, dh \qquad \text{(A-3)}$$

$$T'_{B,V}(\theta,h) = \left[\varepsilon_V(\theta)T + r_V(\theta)T_S\right]\tau(h) + \int_o^h T_A \frac{\partial\tau}{\partial h}\, dh \qquad \text{(A-4)}$$

Subscripts H and V denote horizontal and vertical polarization, respectively. Only ε and r depend on polarization in Equations (A-3) and (A-4). Thus, polarization strictly relates to characteristics of the material.

The difference between $T'_{B,V}$ and $T'_{B,H}$ varies strongly with nadir angle, θ. This difference is largest at the Brewster angle which, for most natural surfaces, occurs near =70°. $T'_{B,H}$ is usually less than $T'_{B,V}$. For smooth, nonlayered surfaces, $T'_{B,V}$ is equal to $T'_{B,H}$ at nadir where θ=0°. For any given nadir angle, the difference $T'_{B,V}-T'_{B,H}$ decreases with increasing surface roughness. Thus, the roughness of a surface is related to the difference between $T'_{B,V}$ and $T'_{B,H}$. This effect is illustrated in Figure A-1 which shows brightness temperatures at 0.81 cm observed with a ground based radiometer over various surfaces.

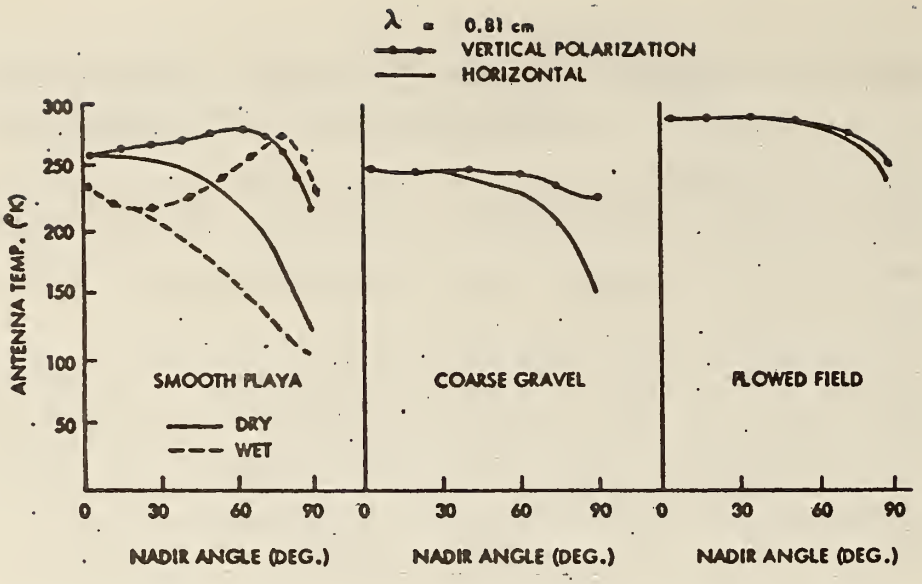

Figure A-1 Microwave Emission of Several Surfaces

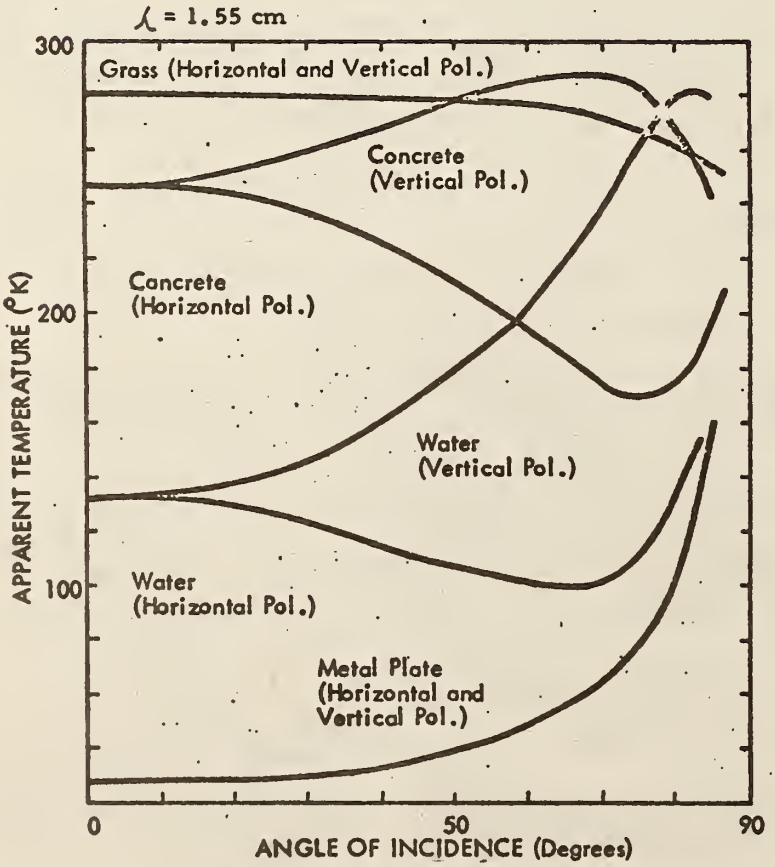

Figure A-2 Apparent Temperature of Several Surfaces as a Function of Viewing Angle

Figure A-2 illustrates some of the factors affecting the apparent radiometric temperature as discussed above. In these examples, the thermometric temperatures of the surfaces are assumed to be 290°K and the observational wavelength is chosen to be 1.55 cm. These theoretical curves also include the effect of reflected radiation from a standard atmosphere. Grass behaves as a rough surface at this wavelength and shows no difference in behavior between horizontal and vertical polarization. Its apparent temperature is almost equal to its thermometric temperature and there is very little change in its radiometeric behavior with angle. The behavior of a metallic plate is quite different from that of grass. The emissivity of metal, which is a good conductor, is almost zero and the temperature shown is very close to the unpolarized sky temperature. The examples of a smooth water surface and concrete show the effect of the dielectric constant on apparent temperatures of smooth surfaces. Water and concrete also show polarization effects which are typical of most dielectric materials as do sand and dirt. For a smooth surface, the vertically polarized temperature always has a maximum at the Brewster angle which is nearly equal to the thermometric temperature of the surface and is hotter than the corresponding horizontal temperature. The Brewster angle for a material is strongly dependent on the dielectric constant of the material and tends toward an angle of 90° for very large dielectric constants.

Unfortunately, measurement of the complex dielectric constant at microwave frequencies, particularly for substances with small loss tangents, is quite difficult. A number of measurements are collected in Table A-1. It will be seen that the complex dielectric constant K does not vary greatly, though it has a tendency to increase with density; (for certain silicate rocks, e.g., pumice, the relation $\sqrt{K} = 1+\rho/2$, where ρ is the density, holds quite well (Peake, 1969). This density relationship

Table A-1

Frequency in GHz	K		Density	Material
	ε_r	tan δ		
35	2.3	0.08		Red Granite
35	2.4	0.06		White Granite Crushed
35	1.7	0.012		White Pumice Crushed
35	1.6	0.02		Black Pumice Crushed
1.0	35	0.175	3.01	Chondritic Meteorite
14	4.6	0.006	1.81	Halite
14	3.8	0.012	1.56	Halite
14	3.3	0.009	1.42	Halite
10	4	0.1		Limonite (Coarse)
10	4	0.01		Limonite (Fine)
8.5	3.3	0.0055	1.11	Magnesite Hard Packed
8.5	2.45	0.002	1.22	Quartz Powder
0.1	10	0.02		Basalt (Hawaii) Oven Dry
0.1	10	0.08		Basalt (Hawaii) 0.36% Water
0.1	7 to 9	0.1		Granite (Quincy)
0.1	8.4	0.006 to .018	2.65	Limestone (Lucerne Valley)
0.1	5.5	0.001		Rhyolite
10	4.8	0.005	2.45	Basalt (Vesicular)
10	4.4	0.013	2.63	Biotitc Granite
10	5.1	0.081	2.35	Obsidian
10	4.8	0.009	2.74	Olivine Basalt
10	5.4	0.086	2.68	Scrpentine
10	5.0	0.027	1.62	Volcanic Ash
10	4.7	0.017	2.27	Altered Tuff
10	5.5	0.016	2.03	Tuff
10	4.7	0.01	2.3	Hornblende
10	3.0	0.012	0.78	Mono Pumice
14	2.9	0.011	1.63	Desert Sand
14	8.2 to8.6	0.004 to .02	2.65	Limestone (Lucerne Valley)
14	4.7 to 6	0.01 to 0.1	2.35	Asphalt
14	4.5 to5.2	0.02 to .06	2.1	Concrete
3	81	0.38		Maine Potato 80% Water

is illustrated with 21 cm data obtained near Mono Craters where all the rocks in the area are silicic volcanics of very similar composition. These rocks possess a range of densities and occur in a variety of forms (e.g., pumice, volcanic glass, etc.).

Emissivities were computed from radiometric measurements at an observational wavelength of 21 cm and compared with rock densities on Figure A-3. Densities shown are average values for three samples from each scan path. A significant feature of these data is the close correspondence between decreasing emissivities at low antenna viewing angles and increasing rock density. At higher antenna viewing angles, above 40°, the effects of surface roughness are more pronounced and the relationship is obscured. At the low viewing angles, a change in emissivity of 0.5 corresponds to a density change of 1.0. This amounts to a brightness temperature change of about 15°K. The loss tangent, on the other hand, can vary over several orders of magnitude. Penetration may vary from several meters for dry sand, to a few millimeters for wet soil in the centimeter wavelength range, Figure A-4.

Figure A-5 shows the dielectric constant for several soils as a function of moisture content. It is clear that the moisture content has a decisive influence on both the real part of K and the emissivity. This is the basis for the expectation that microwave imagery can provide a means for monitoring or mapping soil moisture.

The microwave emission characteristics of soils have been investigated with increasing interest during the past several years. These studies indicate that the vertical and horizontal distribution of soil moisture can be mapped over a broad class of terrain surfaces including rangeland, marshlands, agricultural and desert areas. Research activities have been focused on establishing basic relationships between microwave emission and the distribution of moisture. The effects of surface and

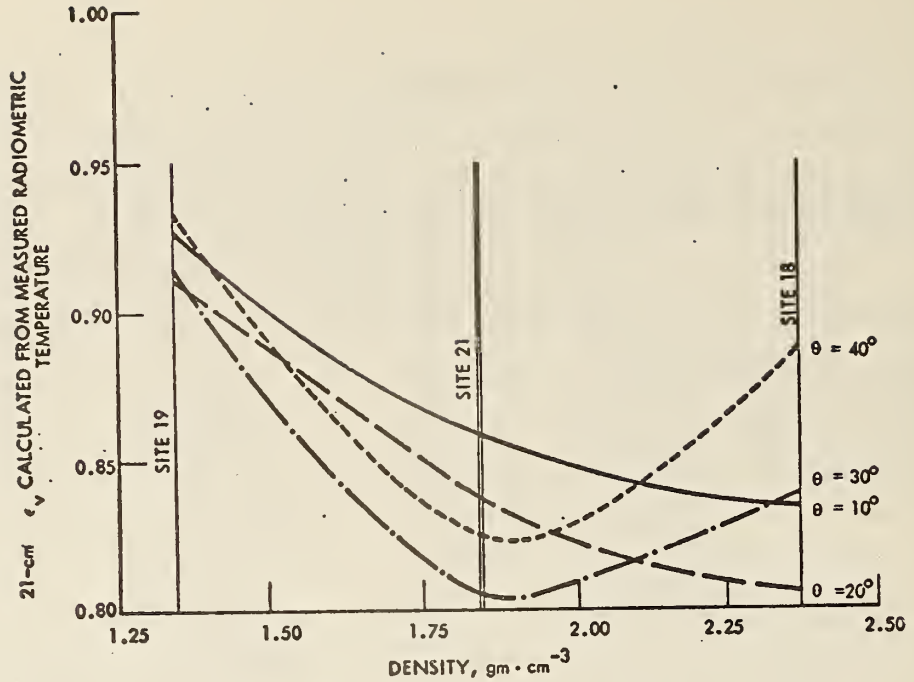

Figure A-3 21cm$_v$ as a Function of Density for Acidic Volcanic Rocks of the Mono Craters Area, California (Derived from Sites 18, 19 and 21) (Aerojet-General Independent Research)

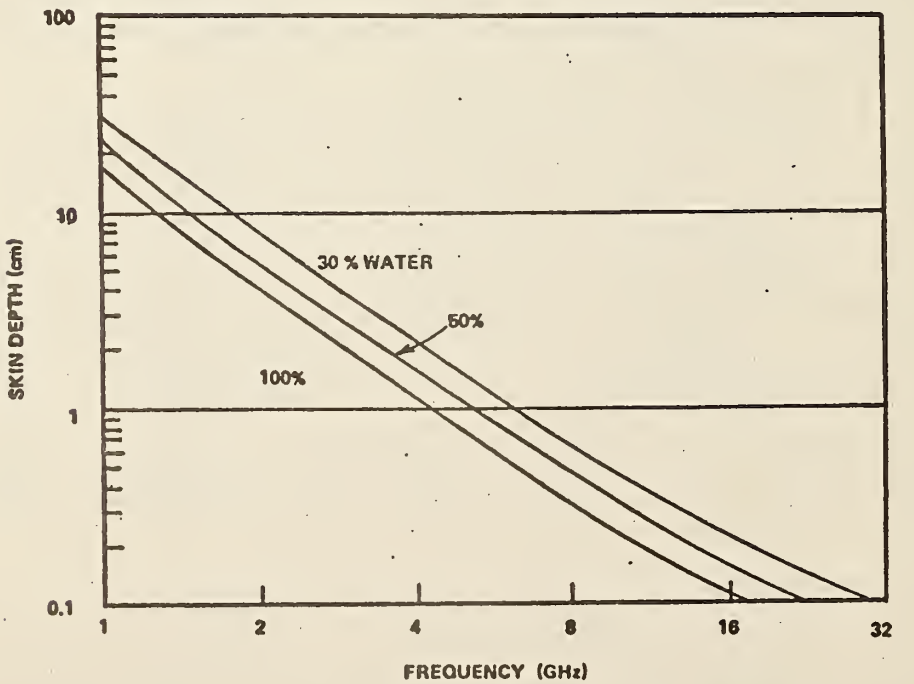

Figure A-4 Skindepth vs Frequency for Water (100% Curve) and for Media whose Dielectric Constant is 50 and 30% respectively of the Dielectric Constant of Water
(Aerojet-General Independent Research)

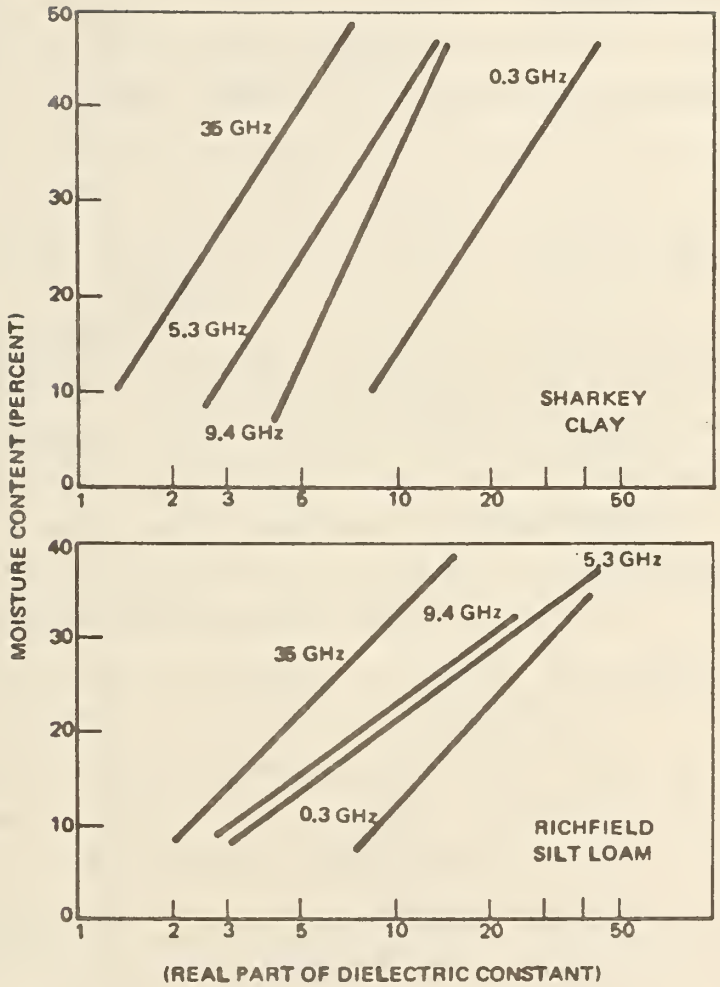

Figure A-5 Relative Dielectric Constant of Soils versus Moisture Content (after Lundien)

volume scattering, temperature gradients and soil density have also been considered. This work, including theoretical studies, laboratory and field measurements, demonstrates a basic relationship between microwave emission and soil moisture content. These basic investigations have recently been augmented with aircraft measurements. Although the extensive ground control data (vertical soil moisture and temperature profiles) needed to quantitatively demonstrate airborne mapping of soil moisture content were not available during the initial flights, the early results have been very encouraging. This portion of the report summarizes the results of the soil moisture studies.

Ground based experiments conducted on a field site at the U. S. Water Conservation Laboratory near Tempe, Arizona, encompassed microwave measurements of soil moisture content which can be compared directly with soil moisture profiles obtained by conventional coring techniques. Microwave brightness temperature measurements of the soil plot were taken at observational wavelengths of 0.81, 2.2, 6.0 and 21 cm (frequencies of 37, 13.4, 4.99 and 1.42 GHz, respectively) over a period of several weeks as the field was allowed to dry from a flooded condition to as low a moisture content as possible. In this experiment, statistically significant numbers of vertical moisture profiles were taken. Figure A-6 gives a comparison of moisture profiles determined from core sampling (solid lines with vertical bars corresponding to the range of moisture values noted during sampling) and moisture profiles determined from radiometric measurements (indicated by symbols). The moisture profiles are given as volume of water per unit area versus depth. The soil moisture content values were obtained by statistical core sampling techniques. The soil moisture data were linearly extrapolated beyond 32 cm. Wavelengths are given near the compiled results. Case 1 represents the saturated condition;

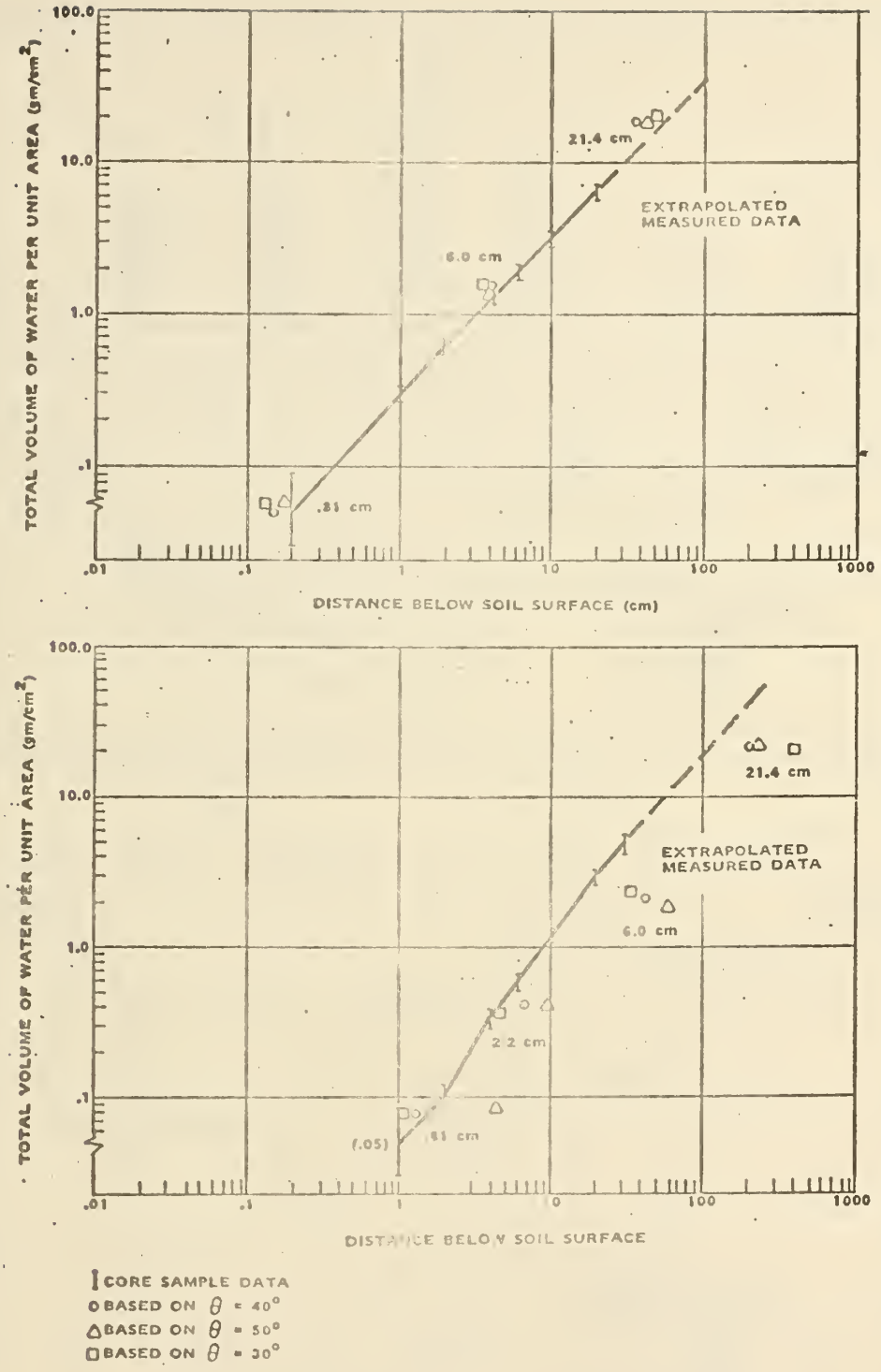

Figure A-6 Comparison of Soil Moisture Profiles Determined with Microwave Radiometry and Core Samples (Aerojet-General Independent Research)

radiometric data used for the calculations were obtained shortly after the field had been flooded and after all traces of surface water had disappeared. The data for Case 2 were obtained at the driest condition reached, some thirteen days after the Case 1 measurements.

Excellent agreement of measured and estimated moisture profiles were obtained for saturated and moderately moist soil conditions (8 to 30 percent). Similarly, agreement between measured and estimated moisture profiles at lower moisture contents is also good, although the values corresponding to 6.0 and 21.4 cm radiometric measurements are not in close correspondence. This arises from uncertainties in (1) the accuracy of extrapolated core moisture data and (2) estimating the depth of investigation (skin depth) of long wavelength radiation in dry (low loss) soils. Skin depths are determined by the dielectric properties of soils. Accurate dielectric constant data are not presental available at these wavelengths. This limitation will be removed when reliable dielectric values become available.

An example of microwave radiometric determination of soil moisture content under circumstances more realistically approaching operational conditions, was obtained during a multi-wavelength radiometric traverse across the San Andreas Fault Zone in an area east of the Salton Sea, near Salton Parkside, California. In this area, rising ground water occurs at intervals along the fault, increasing soil moisture content near the surface.

The microwave traverse was performed along a one-half mile segment of a power-line access road. Thermometric temperatureprofiles in the alluvium were taken before, during, and after the completion of the traverse line. Samples were taken from the surface, and at depth intervals of 0 to 7.5 cm, 7.5 to 15 cm, and 15 to 30 cm. The moisture data are compiled on Figure A-7. The largest moisture variations occurred in the 15 to 30

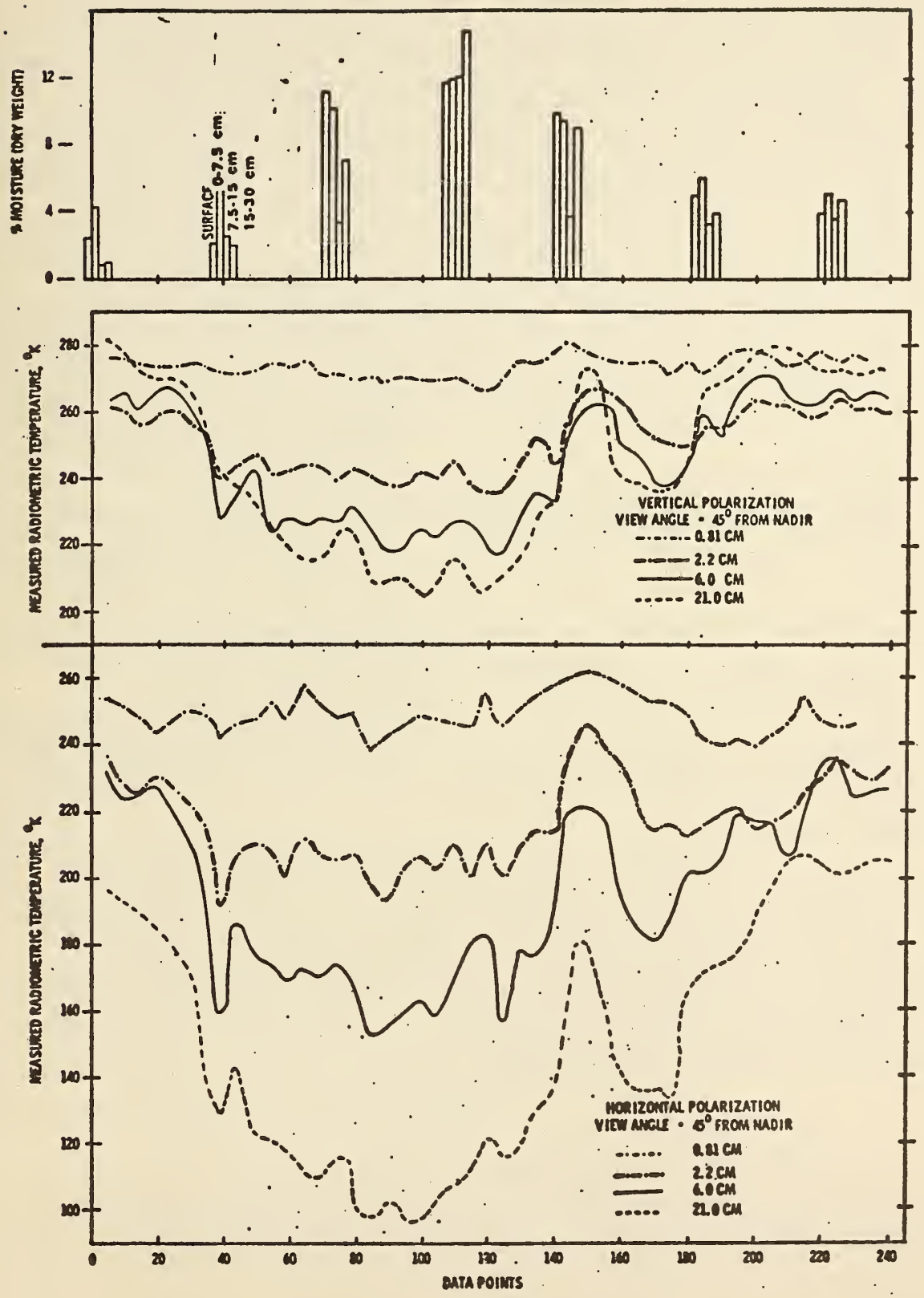

Figure A-7 Radiometric Traverse Across Trace of the San Andreas Fault, Salton Sea Area, Calif. (Aerojet-General Independent Research)

cm interval. The point-to-point variability of moisture content values at a particular depth along the traverse must be partly attributed to precipitation which occurred prior to the traverse. The 7.5 to 15, and 30 cm depth samples are probably most representative of the equilibrium conditions prevalent at this site. Microwave profile data taken at observational wavelengths of 0.81, 2.2, 6.0 and 21 cm for a view angle of 45° are shown in the lower portion of the figure. Note that the 0.81 cm temperatures are consistently warmer and less polarized than the corresponding longer wavelength temperatures, and that there is little correlation between moisture condition and microwave emission at 0.81 cm. Correlation is much better at longer wavelengths, where brightness temperatures decrease with increasing soil moisture conditions. In general, larger brightness temperature anomalies were observed as the observational wavelength increased. This is evident between data frames 130 and 150 where the horizontally polarized brightness temperature changes at wavelengths of 2.2, 6.0 and 21 cm are 36°K, 42°K and 64°K, respectively. The limited correlation with moisture observed at 0.81 cm is largely due to scattering associated with surface roughness. This effect was not evident in the 2.2 cm data.

For the present study it has been assumed that subsurface voids or partially subsided areas may be a controlling factor in the distribution of the near-surface soil moisture patterns. If this is true then mapping the surface soil moisture content will give an indication of the underground areas where subsidence may be expected.

A.2 Instrumentation

A microwave radiometer is designed to measure the thermal noise power delivered to it by the antenna. There are two basic configurations commonly used; the unmodulated or

straight power receiver, and the modulated or "Dicke" type receiver. In each type, the RF amplifier and/or the mixer-IF amplifier may be absent. The essential difference between the two types is that the first is simply a power meter whereas in the Dicke type the receiver is alternately switched to look first at the antenna and then at a load maintained at a stable reference temperature. The resulting signal is later detected in a synchronous detector driven in synchronism with the switch. Although the basic sensitivities of the two systems are comparable, the Dicke type is much less affected by gain fluctuations in the electronics, and is essential where relatively long integration times are required.

The following is a brief description of the radiometers, field laboratory and other instruments used in the experiments discussed in this report.

A.2.1 Microwave Radiometers

The microwave sensors are Dicke-type radiometers, operating at wavelengths of 21, 6, 2.2, and 0.81 cm. A functional block diagram of the 2.2 and 0.81 cm instruments is given in Figure A-8. The 21 and 6 cm radiometers differ slightly in that the 21 cm operates as a TRF (tuned radio frequency) receiver, rather than superheterodyne receiver and the 6 cm unit operates single sideband in order to maintain a narrow bandwidth.

The four radiometers are packaged on drawers, each of which fits into a thermally stable insulated box maintained at 55°C+0.1°. The boxes with radiometer drawer installed are completely RFI (radio frequency interference) shielded and contain associated dc power supplies.

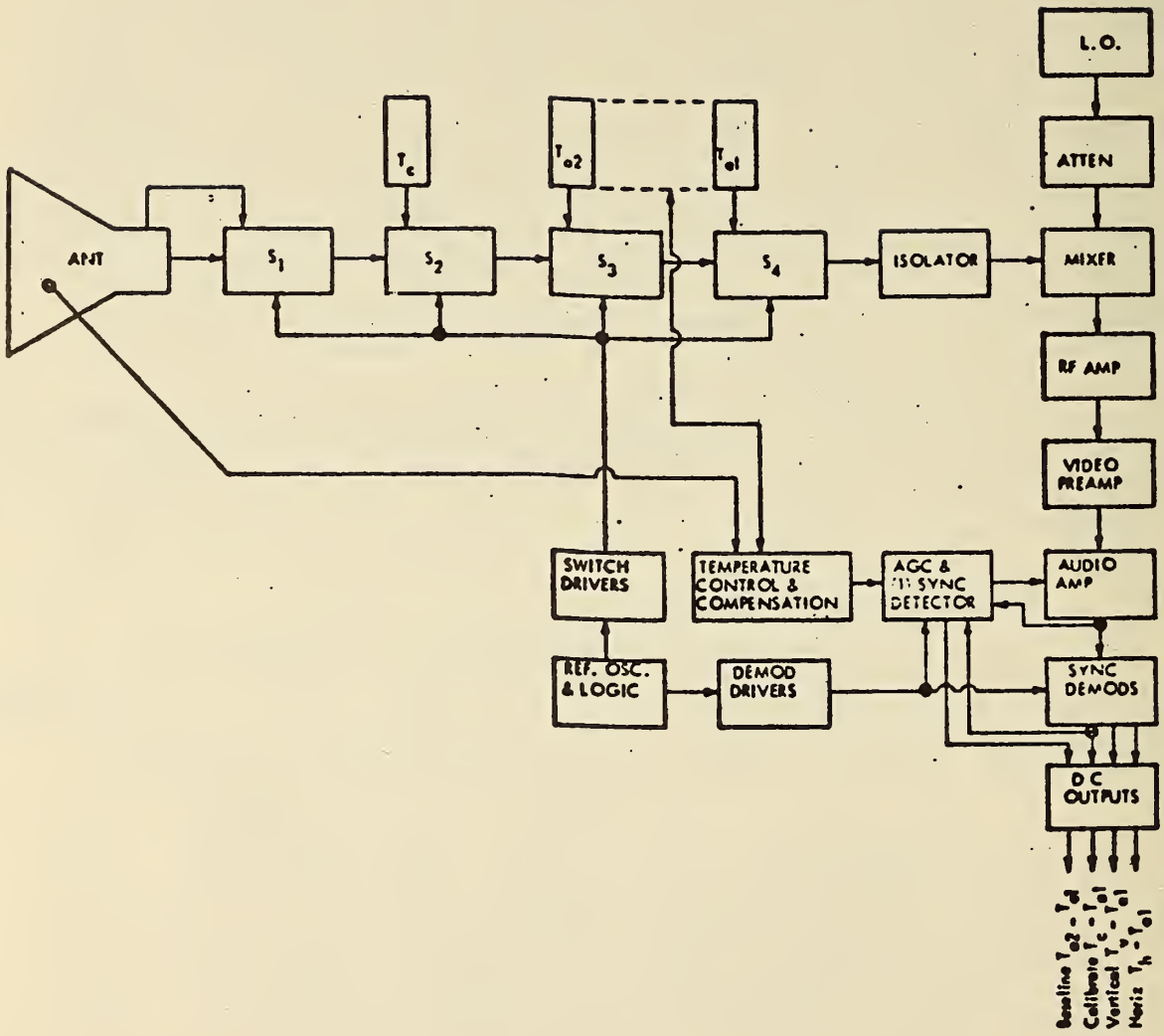

Figure A-8 Functional Block Diagram of 2.2 and 0.81cm Radiometers

The characteristics of these instruments are listed below:

Wavelength	21 cm	6 cm	2.2 cm	0.81 cm
Center Frequency	1.4 GHz	4.99 GHz	13.4 GHz	37 GHz
Bandwidth	28.4 MHz	6 MHz	300 MHz	300 MHz
Sensitivity 1 sec ΔT_{rms}	0.9°K/sec	2.0°K/sec	0.5°K/sec	0.5°K/sec
Antenna Beamwidth	15°	5°	5°	5°
Antenna	3-foot Phased Array	3-foot Phased Array	Lens Horn	Lens Horn
Accuracy	$\pm$2°K	$\pm$2°K	$\pm$1°K	$\pm$1°K

The integration periods for all of the radiometers can be varied from 0.01 to 10 seconds. The radiometers are packaged individually and may be operated separately or clustered. They are environmentally stable and can operate in temperatures from -40°C to +50°C. They feature semi-portability for airborne operation or transportation into remote areas. Continuous, simultaneous, direct reading (0 to 5 Vdc corresponds to 0 to 500°K) outputs of horizontal and vertical polarization, calibration reference, and baseline are available for immediate interpretation on a voltmeter and/or for recording on strip chart or magnetic tape. The instruments are self-calibrating.

A.2.2 Microwave Field Laboratory

The Microwave Field Laboratory consists of an International Model 1700 all-wheel drive truck with an 18-foot van body. The instruments are mounted on a hydraulically operated boom, 25 feet in length, controlled from a position near the cab of the truck. A remote control head is mounted on the end of the boom to allow the radiometer to be scanned in the elevation plane through an angle of 180°. The programming of this

head is controlled by a digital data acquisition system in the van. The end point of terrain scans is adjusted to coincide with the local gravity vector, scanning from nadir to zenith. Scan steps have been set at 5°, but other values, including non-equal steps, can be obtained as desired. The hydraulic boom is also extendible to permit versatility in types of measurements. The van houses the monitoring and recording equiment, as well as the meteorological, hydrological, and geophysical equipment for collecting supporting environmental data. Table A-2 lists some of this equipment. A 15 kW diesel generator is mounted in an enclosed compartment in the rear of the van, and supplies power for the equipment, as well as the heating and air conditioning system.

Table A-2

Infrared Radiometer with Various Filters
Closed Circuit TV
Wind Speed-Direction Indicator
Barograph
Hydrograph
Relative Humidity Meter
Thermistor Probes (various types)
Digital Thermometer
35-mm Camera
4x5 Camera
Hydrometer
Scales
Soils Sampling Devices (coring tools, augers, etc.)
Glass Thermometers
Drying Ovens
Optical Comparator
Microscope
Surveying Equipment

A.3 Data Reduction

The reduction of microwave brightness temperature from in site measurements recorded on digital magnetic tape may conveniently be divided into three tasks: (1) formatting process of the raw data tape which contains the radiometer data using a Varian 620i computer, (2) computing brightness temperature on the 620i computer and recording the resultant values on magnetic tape, and (3) printing these brightness temperatures on computer off-line printouts governed by an IBM 360/65 computer. The formatting procedures in (1) link the field van digital recording system with the 620i machine while the printing in (3) is done on off-line using a 360/65 computer for rapid processing of large amounts of data.

The radiometer gains and antenna loss factors are inputted and employed in the computations mentioned in (2). Generally speaking, the above processes (1), (2) and (3) allow a relatively rapid method of arriving at microwave brightness temperatures with a minimum amount of cost. A complete volume of data corresponding to a full day's measurement program with the laboratory field van may be processed within 24 hours. It should also be noted that supplementary information such as air temperature, pressure, location and numerous thermo-couple entries may be processed simultaneously with the microwave data.

Of the techniques used to calibrate microwave radiometers and to determine the power losses of antennas and waveguide configuration related to the radiometer, a combination of liquid nitrogen cooled loads and high-altitude measurements of the sky are presently considered to be the most accurate. Not only is the measured brightness temperature of the sky in the microwave spectrum significantly lower than the measured temperature of a matched load at ambient temperature, but the brightness temperature of the sky is known to a reasonably high accuracy provided atmospheric data (air temperature, pressure and relative humidity) is available. The error in the

calculated brightness temperature of the sky is usually less than $\pm 1°K$. The error in the temperature of the liquid nitrogen cooled load is usually less than ± 1 (or 2 degrees) and the error in the ambient temperature is usually less than $\pm 1°$. This section is concerned with presenting the major steps used to calibrate radiometers and to determine power losses of antennas and waveguide corrections and, hence, obtain absolute radiometric temperatures.

Data taken during the high-altitude calibration is summarized in Table A-3. Data is taken for each frequency and for each polarization.

Table A-3

DATA TAKEN DURING HIGH-ALTITUDE MEASUREMENTS		
	Voltage	Thermal Temp
Standard Gain Horn Measurement of Sky (zenith)	V_S	
Ambient Load Measurement	V_L	T_L
Liquid Nitrogen Cooled Load Measurement	V_C	
Usual Configuration of Antenna and Waveguide System Measurement of Sky (zenith)	V_A	T_A

In reality a temperature gradient exists along the ambient loads and along the antennas and waveguide sections. If the gradient becomes substantial (10° or more) the procedure of calibration discussed below must be altered to include the temperature gradient (Poe, 1970). Fortunately, however, in most measurements the temperature gradients can be neglected.

Using atmospheric data (air temperature, pressure, and relative humidity) for cloudless skies, calculation of the brightness temperature of the sky T_S can be made (Stogryn, 1968). (Atmospheric data should be given in sufficient detail for altitudes up to 30 or 40 kilometers.) The calculations are made for each frequency.

Since the power loss in the standard gain horns is usually negligible the output voltage V_m of the radiometers is related to the brightness temperature T_m incident on the standard gain horn by

$$T_m = \frac{V_m - T_S}{\left(\frac{V_L - V_S}{T_L - T_S}\right)} + T_S \qquad \text{(A-5)}$$

The radiometric temperature of the liquid nitrogen cold load together with the measured output voltage V_C is used to check the linearity of the radiometer and to arrive at an average gain of the radiometer.

The fractional total power loss α of an antenna and waveguide connector used in the normal or usual configuration with the radiometer is determined from

$$\alpha = \frac{T_{mS} - T_S}{T_A - T_S} \qquad \text{(A-6)}$$

where T_{mS} the radiometeric temperature calculated from (A-5) from the measured voltage of the sky V_A. In general, α varies with frequency and polarization.

Thus, if V volts are measured with the usual configuration of antenna, waveguide connection of the radiometer system, the absolute temperature T of the energy incident of the antenna is

$$T = \frac{1}{1-\alpha} \left[\frac{V - V_S}{\left(\frac{V_L - V_S}{T_L - T_S}\right)} + T_S - T_A \right] \qquad \text{(A-7)}$$

where T_A is the average thermal temperature of the antenna and waveguide system. Of course, there are equations such as (A-7) for each polarization and frequency.

Table A-4 is an example of the calibration method discussed above. The data corresponds to the vertical polarization at 94 GHz using high-altitude measurements taken at Edwards Air Force Base.

Table A-4

EXAMPLE OF CALIBRATION CALCULATIONS	
$V_S = 1391$ mv	(V is in millivolts and T is °K)
$V_L = 3157$ mv	$T_L = 282.6°K$
$V_A = 1757$ mv	$T_A = 276.6°K$
T_S (calculated from atmospheric data) = 36.5°K	
and $T = \frac{1}{1 - .2125}\left[\frac{V - 1391}{7.176} + 36.5 - .2125\ T_A\right]$	

GPO 866-641